THE ROLE OF SEXUAL DIMORPHISM IN CARTILAGE TISSUE REGENERATION

A Dissertation
Presented to
The Academic Faculty

By

Ramsey Christian Kinney

In Partial Fulfillment
of the Requirements for the Degree
Doctor of Philosophy in Biomedical Engineering

Georgia Institute of Technology
May 2008

THE ROLE OF SEXUAL DIMORPHISM IN CARTILAGE TISSUE REGENERATION

Approved by:

Dr. Barbara D. Boyan, Advisor
Department of Biomedical Engineering
Georgia Institute of Technology

Dr. Zvi Schwartz
Department of Biomedical Engineering
Georgia Institute of Technology

Dr. Anthanassios Sambanis
School of Chemical Engineering
Georgia Institute of Technology

Dr. Timothy M. Wick
Department of Biomedical Engineering
University of Alabama at Birmingham

Dr. Lawrence J. Bonassar
Department of Biomedical Engineering
Cornell University

Date Approved: October 9th, 2007

ACKNOWLEDGEMENTS

I would first like to thank my advisors, Dr. Barbara Boyan and Dr. Zvi Schwartz. At times they felt more like parents than advisors, feeling the need to give guidance on dating or etiquette as much as on science and research. Unlike many graduate students, I usually had no problem convincing my advisors to listen and agree with my ideas. The true challenge was getting them to agree with each other, even if they happen to be saying the same thing two different ways. However, I now understand this was partly because they both wanted the best for me in their own way.

I am also grateful to the other members of my thesis committee. Dr. Larry Bonassar for the expertise he provided on chondrocyte/alginate constructs, as well as making sure I understood the statistical consequences of my experiments; Dr. Anthanassios Sambanis for his persistent reminder to apply basic engineering principles when designing my experiments, as well as his wealth of experience in the area of tissue engineering; and Dr. Tim Wick for his continual support and encouragement even when his career took him away from Georgia Tech.

I would also like to thank my many collaborators, whom this project could never have been completed without. Dr. Martin Lotz for providing the human articular chondrocyte cell source; Dr. Don Ranly for providing his histological expertise, help with the IACUC procedures, and for being a calm amongst the Boyan-Schwartz storm; Dr. Jacqui McMillan for her friendship and surgical mentorship; and Dr. Brani Vidakovic for his assistance with the statistical analysis.

There are many administrators and staff I would like to acknowledge for their help and support through this long journey; Dr. Ajit Yoganathan and Dr. Steve Deweerth of the Biomedical Engineering Department as well as Sally Gerrish and Leita Young, and especially Beth Bullock for her never ending help in navigating the red-tape maze; Dr. Bob Nerem and the Georgia Tech/Emory Center for the Engineering of Living Tissues and the Petit Institute for Bioengineering and Biosciences for the opportunities they have provided me, as well as the technical staff including Steve Woodard, Johnafel Crowe, Tracey Couse, Dr. Laura O'Farrell, Cherry Forkey and Kelly Winn; Hong Yi at Emory for her assistance with the electron microscopy; Dr. Barbara Wauryzniak and AppTec for their processing of the *in vivo* histology; and Johnathan Glass, Diego Remolina, Steve Marzec and Jesus Mata-Acosta for their assistance with all my computer needs. I would also like to thank the MD/PhD program at Emory for their support and encouragement including Dr. Allan Levey, Dr. Kenny Offermann, Dr. Chuck Parkos and Dr. Marie Csete, as well as Mary Horton, Barbara Powley and Sabrina Mallet.

The Boyan Lab is a complex machine with many cogs and wheels that are required for it to work. First of all, I would like to thank the undergraduates that have been a critical part of my success including Meghan Gilroy, Shannon Sedai-Fatehi, Michael Chervonski, Carolyn Yeago and especially Angela Gill. I am also grateful to all the staff who have made the lab function over the years including Dr. Liping Wang, Dr. Rene Olivares-Navarrete, Seyed Safavynia, Reyhaan Chaudhri, Sharon Hyzy, Gary Seeba, John Dooley, Ronnie Allen, Johnathan Turner, Marc Duran, Maya Fisher and Jaime Lazin. I am also thankful to all the graduate students that have come and gone over the years, but I would like to specifically acknowledge my office mates Dr. Alice

Zhao, whom I spent many an afternoon discussing Chinese versus American culture and politics, and Bryan Bell, whom has been like a little brother in more ways than one.

Lastly, I would like to thank my close friend Dr. John “the Jovi” Redding, my parents Carole and Tom, my older brother T.K., and my girlfriend Lea for being there whenever I needed them.

This research was funded by the following sources: US PHS Grant DE05937, US PHS Grant DE08603, NSF Grant EEC-9731643, the Georgia Research Alliance, the Price Gilbert Jr. Foundation, the American Association for Dental Research, the Whitaker Foundation, the Musculoskeletal Transplant Foundation, and the Georgia Tech/Emory Center for the Engineering of Living Tissues

TABLE OF CONTENTS

LIST OF TABLES

LIST OF FIGURES

LIST OF SYMBOLS AND ABBREVIATIONS

ACI	autologous chondrocyte implantation
AMP	2-amino-2-methyl-1-propanol
ANOVA	analysis of variance
BMP	bone morphogenetic protein
BSA	bovine serum albumin
COMP	cartilage oligomeric protein
DAG	diacylglycerol
DBM	demineralized bone matrix
DEPC	diethylpyrocarbonate
DHT	5-hydroxytestosterone
DMEM	Dulbecco's modified Eagle's medium
DMMB	1,9-dimethylene blue
DMSO	dimethyl sulfoxide
E_2	17β-estradiol
E_2-BSA	BSA conjugated 17β-estradiol
EDTA	ethylene diamine tetraacetic acid
ER	estrogen receptor
FBS	fetal bovine serum
FGF	fibroblast growth factor
GAG	glycosaminoglycan
GAPDH	glyceraldehyde 3-phosphate dehydrogenase

HAC	human articular chondrocyte
HBSS	Hanks' balanced salt solution
HRT	hormone replacement therapy
IGF	insulin-like growth factor
Ihh	Indian hedgehog
IP_3	inositol 1,4,5-triphosphate
MAPK	mitogen-activated protein kinases
OVX	ovariectomized
OVX-E_2	ovariectomized with E_2 supplementation
PBS	phosphate buffered saline
PCR	polymerase chain reaction
PKC	protein kinase C
PLC	phospholipase C
*p*NPP	*p*-nitrophenyl phosphate
QS	qualitative scoring system
RC	rat costochondral resting zone growth plate chondrocytes
rER	rough endoplasmic reticulum
RIA	radioimmunoassay
RT	reverse transcription
RT-PCR	reverse transcription polymerase chain reaction
RGPC	rat growth plate chondrocyte
SDS	sodium dodecyl sulfate
SHAM	sham-operated

Shh	sonic hedgehog
SOX-9	SRY (sex determining region Y)-box containing gene 9
TCA	trichloracetic acid
TGF-β	transforming growth factor beta
TNF-α	tumor necrosis factor alpha

SUMMARY

Osteoarthritis is a degenerative joint disease characterized by progressive erosion of the articular cartilage. It is a debilitating disease that affects millions of people and costs billions of dollars in treatment and disability claims. Current treatment involves drug therapy to manage pain, reparative surgeries and eventually total joint replacement. The ultimate goal is to develop an *in vitro* tissue engineered cartilage graft or *in vivo* tissue regeneration protocol to heal the arthritic lesion before total joint arthroplasty is needed. However, the development of such therapies has proven to be difficult due to the complex biology of the chondrocyte. Epidemiological studies have established a relationship between osteoarthritis and menopause suggesting that estrogen may be important in the development of cartilage therapies. The overall goal of this research project was to advance the field of cartilage tissue regeneration by investigating the role of 17β-estradiol (E_2), an active estrogen metabolite, on the chondrocyte phenotype. The central hypothesis was that E_2 would play an important and sex-specific role in regulating chondrogenesis.

The central hypothesis was first tested by investigating the effects of E_2 on *in vitro* cultured human articular chondrocytes (HACs). The higher incidence of osteoarthritis in women suggests that there may be intrinsic sex-specific difference between male and female articular chondrocytes. E_2 has previously been shown to regulate rat growth plate chondrocytes through traditional nuclear receptor mechanisms, but only female cells exhibit rapid membrane-associated effects mediated through protein kinase C (PKC) alpha. HACs were obtained at the time of autopsy from three male and

three female donors between 16 and 39 years of age. Second passage cultures were treated with E_2 for 24 hours to assess the effects of the hormone on proliferation, matrix production, and differentiation. In addition, the chondrocytes were treated for 3, 9, 90 or 270 minutes and PKC specific activity was determined. All chondrocytes were positive for aggrecan and estrogen receptor alpha mRNAs but were negative for collagen type II mRNA indicating the HAC had lost a portion of their chondrocytic phenotype due to monolayer culture. Only cells from female donors responded to E_2 as evidenced by an increase in DNA synthesis, sulfate incorporation and alkaline phosphatase activity. E_2 caused a rapid membrane mediated increase in PKC activity in the female cells within 9 minutes that was maximal at 90 minutes. Treatment with the PKC inhibitor chelerythrine blocked these effects. These results provide the first definitive evidence that HACs exhibit an intrinsic sex-specific response to E_2 and suggest that sexual dimorphism may be an important variable for cartilage regeneration.

The next aim was to develop an animal model to examine the *in vivo* role of E_2 in skeletal tissue regeneration. Demineralized bone matrix (DBM) is an osteoinductive material that can stimulate cartilage and bone formation. The osteoinductivity of commercial human DBM is tested in male athymic rats and mice, but DBM performance in these animals may not reflect performance in female animals, or provide information on E_2's role in the process. To gain insight, human DBM was implanted bilaterally in the gastrocnemius of twenty-four athymic female mice and twenty-four athymic female rats. Eight animals in each group were sham-operated (SHAM), ovariectomized (OVX), or ovariectomized with E_2-replacement (OVX+E_2) via subcutaneous slow release capsules. Four animals from each group were euthanized at 35 days and four at 56 days. Uterine

weight and blood estrogen levels confirmed ovariectomy and E_2-replacement were successful. Histological sections of implanted tissues were evaluated qualitatively for absence or presence of DBM, ossicle formation and new bone or cartilage using a previously developed qualitative scoring system (QS). Histomorphometry was also used to obtain a quantitative assessment of the osteoinduction. OVX mice had a small but significant QS decrease at 35 days compared to SHAM mice, confirmed by quantitative measurement of ossicle, marrow space, and new bone areas. The QS in rats was not affected by OVX but histomorphometry showed decreased new bone in OVX rats, which was restored by E_2. The QS indicated that the number of new bone sites was not reduced by OVX in rats or mice at 56 days, but the relative amount of new bone versus marrow space was affected and differed with animal species. Residual DBM was less in OVX animals, indicating that DBM resorption was affected. Cartilage was present in rats but not mice, suggesting that endochondral ossification was slower, and indicating that bone graft studies in these species are not necessarily comparable. These results show the importance of E_2 in human DBM-induced endochondral osteogenesis.

We then wanted to test our animal model with a tissue engineered cartilage construct to study how E_2 could specifically affect *in vivo* chondrogenesis. The problem was approached by developing and characterizing a method for microencapsulating growth plate chondrocytes in alginate using high electrostatic potentials. Hydrogel encapsulation has been shown to redifferentiate *in vitro* expanded chondrocyte and stimulate chondrogenesis in mesenchymal stem cells. Rat costochondral resting zone growth plate chondrocytes (RCs) were microencapsulated at low ($6x10^6$ cells/ml) and high ($50x10^6$ cells/ml) cell density, producing microbeads less than 200 micrometers in

diameter. Encapsulated RCs demonstrated minimal proliferation with 98% viability at two weeks in low density cultures and 77% viability at high density, indicating potential mass transfer limitations. Gene expression by RT-PCR showed encapsulated RCs expressed mRNA for cartilage specific matrix proteins, but light and electron microscopy illustrated negligible matrix secretion. Low and high cell density beads were implanted intramuscularly into athymic mice. Histology of unencapsulated RC controls showed cartilage nodule formation. Low density microbeads implanted for 12 weeks remained viable but did not demonstrate chondrogenesis while high density microbeads provided evidence of hypertrophic chondrocytes indicating further endochondral differentiation of the encapsulated growth plate cells. This suggests that alginate microencapsulation could be restricting growth plate matrix formation but does not block endochondral differentiation.

After establishing a microencapsulation method with RCs, we then wanted to apply the technique to HACs and characterize their phenotype. HACs were microencapsulated at low ($6x10^6$ cells/ml) and high ($50x10^6$ cells/ml) cell density in alginate microbeads using the same method developed for RCs. Encapsulated HACs demonstrated minimal proliferation with approximately 90% viability at two weeks for both low and high density microbeads, indicating a different response to mass transfer limitations compared to RCs. Light and electron microscopy illustrated metabolically active cells with pericellular matrix deposition. Gene expression by RT-PCR showed encapsulated HACs continued to express the cartilage-specific matrix proteins aggrecan and COMP during two weeks of *in vitro* culture, but still did not express collagen type II. Encapsulation was shown to increase levels of the transcription factor SOX-9, which is

required for chondrogenesis. The microbeads were then treated with TGF-β1 in an attempt to redifferentiate the cells, but the growth factor had no effect on aggrecan, collagen type II, or SOX-9 expression. The development of a tissue engineered construct that was capable of forming phenotypical cartilage was not successful with either RCs or HACs. More optimization of the alginate microencapsulation is needed before it can be used to test the effects of E_2 on *in vivo* implanted tissue constructs.

In summary, this work has demonstrated that E_2 plays a significant role in orthopaedic tissue engineering and regenerative medicine. We have shown that E_2 has an important sex-specific function in regulating the phenotype of HACs. Moreover, the osteoinductive properties of DBM are inhibited in an estrogen deficient environment. We were unable to produce a tissue engineered cartilage implant to determine what role E_2 could have on chondrogenesis. However, our results suggest that the successful production of tissue engineered constructs will likely depend on knowing and manipulating the actions of sex hormones to ensure chondrocytes in culture form physiological cartilage. Finally, this work shows it is important to take into account the type of patient and pathology. The postmenopausal *in vivo* environment may be inadequate for chondrogenesis and must be considered when designing cartilage grafts.

CHAPTER 1

Specific Aims

Millions of people in the U.S. are diagnosed and treated for osteoarthritis each year. It is a debilitating disease that costs billions of dollars in treatment and disability claims. Current treatment involves drug therapy to manage pain, reparative surgeries and ultimately total joint replacement. Attempts to repair the cartilage have variable results that are not curative and artificial implants usually fail due to wear and loosening after 10-20 years. With the ever increasing longevity in developed nations, a patient may require two or three implant revision surgeries over their lifetime. Unfortunately morbidity and mortality increase significantly with each subsequent procedure. The ultimate goal is to develop an *in vitro* tissue engineered cartilage graft or *in vivo* tissue regeneration protocol to heal the arthritic lesion before total joint arthroplasty is needed. However, the development of such therapies has proven to be difficult due to the complex biology of the chondrocyte. Epidemiological studies have established a relationship between osteoarthritis and menopause suggesting that estrogen may be important in the development of cartilage therapies.

The ***overall goal*** of this research project was to advance the field of cartilage tissue regeneration by investigating the role of 17β-estradiol (E_2), an active estrogen metabolite, on the phenotype of chondrocytes. ***Specific Aim 1*** focused on establishing and characterizing a primary human articular chondrocyte (HAC) cell source, and then examining the response of the chondrocytes in culture to E_2. ***Specific Aim 2*** involved

establishing an ovariectomized animal model to investigate the effects of E_2 on *in vivo* orthopaedic tissue implants. ***Specific Aim 3*** entailed developing and characterizing a microencapsulation method for *in vitro* culture and *in vivo* delivery of chondrocytes to study the effects of E_2 on chondrogenesis. The ***central hypothesis*** was that E_2 plays an important and sex-specific role in regulating chondrocyte phenotype and chondrogenesis.

SPECIFIC AIM 1: To determine the response of human articular chondrocytes to 17β-estradiol.

The effect of E_2 on HACs has not been previously studied. It is known that articular chondrocytes from both sexes express the cytoplasmic receptors for E_2, but post-menopausal women have a higher prevalence of osteoarthritis than men of the same age. This suggests a sex-specific role for E_2 in female chondrocytes that is not found in male cells. The ***objective*** of this specific aim was to use the information provided by the rat costochondral growth plate chondrocyte (RC) cell model to investigate the sex-specific effects of E_2 on HACs in culture. The phenotype of the HAC cell source was characterized by gene expression and the effects of E_2 on proliferation, differentiation and matrix synthesis were examined. A possible E_2 signaling mechanism was determined by using various cellular signaling activators and inhibitors. The ***working hypothesize*** was that E_2 would cause a sex-specific response in female chondrocytes mediated through a rapid increase in protein kinase C (PKC) activity that promoted a more differentiated state.

SPECIFIC AIM 2: To develop an *in vivo* model for investigating the effects of 17β-estradiol on orthopaedic tissue implants.

The *in vivo* hormone environment is essential to the physiologic function of orthopaedic tissues and is therefore important for any tissue engineered implant. Demineralized bone matrix (DBM) is an osteoinductive material that has been shown to form bone and cartilage when implanted in mesenchymal tissues that would otherwise not form skeletal tissues. The ***objective*** of this specific aim was to use ovariectomy to simulate a post-menopausal environment in athymic rodents and analyze the effects of E_2 deficiency on DBM induced endochondral ossification. The success of the ovariectomy was analyzed by measuring serum estrogen levels and uteri weight. Histomorphometric analysis was used to quantify the effects of ovariectomy on skeletal tissue formation. The ***working hypothesize*** was that *in vivo* estrogen deficiency would impair DBM induced cartilage and bone formation, indicating an important role for estrogen status in orthopaedic regenerative medicine.

SPECIFIC AIM 3: To develop, optimize and characterize an *in vivo* cell delivery system for the investigation of 17β-estradiol on cartilage implants.

Monolayer culture results in changes in mechanical stresses on articular chondrocytes and causes their dedifferentiation towards a fibroblast-like phenotype. Encapsulation in alginate has been shown to reverse this process and promote expression of chondrocytic phenotype. The ***objective*** of this specific aim was to develop a method to microencapsulate chondrocytes in alginate and optimize the system to maximize cell viability and chondrocytic phenotype. The effects of E_2 could then be investigated by

implanting the alginate microbeads into the animal model developed in Specific Aim 2. The ***working hypothesis*** was that three-dimensional encapsulation would promote a chondrocytic phenotype and redifferentiated chondrocytes.

SIGNIFICANCE

The current biochemical knowledge of articular chondrocytes, especially in humans, has so far been inadequate for the development of cartilage regeneration therapies. Understanding the basic mechanisms of hormone regulation in articular cartilage will assist the development of novel therapies for the osteoarthritis and other orthopaedic diseases. The successful production of a tissue engineered cartilage replacement will also depend on knowing and manipulating the actions of hormones to ensure chondrocytes in culture form physiological cartilage. The ability to produce a tissue engineered cartilage replacement will not be possible until we determine how all the independent variables function together to produce cartilage. It is also important to take into account the type of patient and pathology. The postmenopausal *in vivo* environment may be inadequate for chondrogenesis and must be considered when designing cartilage grafts. The correct chemical mediators are essential for cartilage homeostasis and may need to be supplemented even after implantation of the graft to ensure continued success. This study directly addressed these challenges by uncovering the basic biology of the human articular chondrocyte and applying this knowledge to improve cartilage regeneration strategies.

CHAPTER 2

Background and Literature Review

CARTILAGE, CHONDROGENESIS, AND DEGENERATIVE JOINT DISEASE

Cartilage is a connective tissue of predominantly mesodermal origin that provides mechanical support and structural form to many areas of the musculoskeletal system. Cartilage differs from most other tissues due to the fact it does not contain vascular, nervous or lymphatic structures. It is composed of a single cell type referred to as the chondrocyte and a complex extracellular matrix consisting mostly of collagen and proteoglycans.

Within the developing embryo, chondrogenic cells arise mostly from the mesoderm with some structures of the face and neck being neural crest in origin [1]. Interaction between the mesenchyme and epithelial layers via reciprocal induction, as well as cell-cell and cell-matrix interactions, leads to cell condensations and differentiation of mesenchymal stem cells into chondroblasts and osteoblasts (bone forming cells). Chondrogenesis is marked by the expression of several cartilage-specific molecules, the most important being the transcription factor SOX-9 activated via the *Wnt*, sonic hedgehog (*Shh*), and indian hedgehog (*Ihh*) signaling pathways [2-4]. The *COL2A1* promoter region is activated when SOX-9 is bound resulting in up-regulation of collagen type II, a cartilage-specific matrix protein. Synthesis of aggrecan, a cartilage-specific proteoglycan, and other collagens like type IX and type XI are also increased in the presence of SOX-9. Other important molecules involved in chondrogenesis include the

TGF-β family, bone morphogenetic proteins, fibroblast growth factors, and insulin-like growth factors.

Chondrocytes are round in morphology and vary greatly in size based on the type of cartilage, zone, and state of differentiation [4, 5]. In general, they range from 10-20 micrometers in diameter with a single round nucleus. The chondrocytes represent 5-10% of the total cartilage tissue volume but are solely responsible for production and maintenance of the extracellular matrix. A well developed Golgi apparatus reflects this primary role. Chondrocytes respond to an array of chemical mediators including hormones, growth factors and cytokines, as well as mechanical and possibly electrical stimuli.

The extracellular matrix of cartilage is composed mainly of water (60-87%), collagens (10-30%), and proteoglycans (3-10%) [6]. The matrix can be categorized into three distinct regions: the pericellular, territorial, and interterritorial regions [4, 5, 7]. Each region has a different composition of collagens, proteoglycans and other matrix components. The pericellular region completely surrounds the chondrocyte forming a lacuna and is primarily defined by the presence of collagen type VI [8]. It is rich in proteoglycans and noncollagenous protein like fibronectin and is thought to function as a transducer of biochemical and biomechanical signals between the chondrocytes and extracellular matrix. The territorial region encompasses the pericellular matrix and is composed of a thin collagen fiber network that is theorized to provide extra structural protection for the chondrocytes from mechanical deformation. The interterritorial region is the largest component of the cartilage matrix and consists of all the secreted material

between the territorial matrices. It contains most of the proteoglycans as well as large covalently linked collagen complexes.

Collagen complexes form a type of endoskeleton or scaffold that provides cartilage with tensile strength [5, 7]. There are at least 15 distinct collagen types found within cartilage that contribute to over 50% of the dry weight of the tissue. All collagens are composed of a characteristic triple-helix structure that makes up a majority of the molecule's length. The major cartilage collagen is collagen type II, which accounts for 90-95% of the total in most cartilage tissues. Other collagens found in cartilage include types I, IV, V, VI, IX, X and XI. The large collagen complexes found in the cartilage matrix are mostly composed of covalently linked collagen types II, IX and XI. Collagen fibers also act to anchor and immobilize proteoglycans in the cartilage matrix.

Proteoglycans are complex macromolecules that allow cartilage to resist compressive loads [4, 5]. They consist of a protein core with covalently bound glycosaminoglycans. These repeating disaccharide chains are heavily sulfated and become ionized at physiologic pH producing a negatively charged matrix that is capable of attracting and holding a significant quantity of water. This osmotic resistance provides the support needed to oppose compression. The major glycosaminoglycans found in cartilage are chondroitin sulfate, keratan sulfate and dermatan sulfate. The largest and most abundant core protein isoform in cartilage is called aggrecan. Several other smaller proteoglycans with different core proteins are also found in cartilage including biglycan and decorin. The core proteins of the proteoglycan are then bound to a hyaluronic acid backbone via link proteins. Hyaluronic acid is a glycosaminoglycans but it is not

sulfated. The hyaluronic acid is subsequently linked to the collagen scaffold, anchoring the proteoglycans in the extracellular matrix.

There are also other extracellular matrix components found in minor amounts within cartilage [5]. Cartilage oligomeric matrix protein (COMP) is found mostly in the pericellular and territorial regions and thought to be involved in cartilage differentiation and pathogenesis [9, 10]. Other noncollagenous matrix molecules are also found in small amounts including fibronectin, thrombospondin, and tenascin.

There are three types of cartilage tissue: hyaline, fibrous, and elastic [11]. Hyaline cartilage is mostly found in the synovial joints to reduce friction as well as to cushion and absorb stress. Articular cartilage can be divided into four zones: superficial, transitional, deep, and calcified [5, 7, 12]. The superficial or tangential zone forms the articulating contact surface. It has a greater density of cells compared to the other zones which are elongated parallel to the surface. The matrix contains the highest concentration of water but with decreased proteoglycan content, and the collagen fiber network is aligned parallel to the surface similar to the chondrocytes. The transitional or middle zone has a greater concentration of proteoglycans compared to the superficial zone. In addition, the chondrocytes are more spherical with an increased density of synthetic organelles indicating a greater role in matrix production. The collagen endoskeleton has no particular alignment as it transitions between the superficial to deep zones. The chondrocytes in the deep zone tend to align in perpendicular columns. The deep zone has the lowest water concentration and greatest concentration of matrix molecules which align perpendicular to the surface. The calcified zone marks the transition from cartilage to subchondral bone and is characterized by the presence of collagen type X. The

chondrocytes appear smaller with decreased presence of synthetic organelles. Certain structural components of the thorax, head and neck are also formed of hyaline cartilage including the costae, trachea, larynx and the end of the nose.

The epiphysial or growth plates of the long bones consist of a special type of hyaline cartilage involved in endochondral ossification. Chondrocytes of the growth plate are separated into specific zones corresponding to their phenotype and level of differentiation [13]. The resting or reserve zone consists of typical hyaline cartilage with small chondrocytes and nominal mitotic activity. The chondrocytes differentiate in response to the appropriate biological signals and enter the growth zone which consists of a proliferative and hypertrophic zone. The cells of the proliferating zone undergo many successive mitotic divisions and align in long columns surrounded by a proteoglycan rich matrix. The chondrocytes stop dividing and begin to increase in size. This hypertrophic zone is characterized by the expression of collagen type X [7]. Finally, the zone of calcification designates the area where the cartilaginous matrix begins to calcify and the chondrocytes undergo apoptosis to make way for osteogenic cells.

Fibrous cartilage is found in areas subjected to higher stress compared to hyaline cartilage [11, 13]. Meniscal tissue and the intervertebral discs are examples of fibrous cartilage. These structures contain more collagen type I than hyaline cartilage giving them mechanical properties more akin to ligaments and tendons. Elastic cartilage has a matrix high in elastin molecules [11, 13]. This allows the tissue to deform and return to its original shape. Examples include the auricular cartilage around the ear, the epiglottis and the eustachian tubes that connect the inner ear to the sinuses.

Osteoarthritis is a degenerative joint disease characterized by biochemical and molecular changes within the tissue that result in progressive erosion of the articular cartilage [14]. For more than 90% of the cases there is no apparent etiology or initial cause for the disease and there appears to be a direct relationship to aging. This form of the disease is known as primary osteoarthritis. When the disease occurs in younger patients with a specific cause like traumatic injury or systemic metabolic disorders like obesity, then it is referred to as secondary osteoarthritis. Approximately 80% to 90% of the population is afflicted with degenerative joint disease by the age of 65. Age-dependent changes in extracellular matrix components result in decreased mechanical strength and resiliency of the cartilage tissue. Although the relationship to age and traumatic injury has often led to the oversimplification of the disease as a function of "wear and tear", research has shown there to be a complex cellular pathogenesis. Chondrocytes in osteoarthritic cartilage produce several cytokines including IL-1 and TNF-α that inhibit the production of extracellular matrix while also stimulating the release of metalloproteinases that degrade the matrix. These cytokines are also pro-inflammatory which causes an influx of inflammatory cells into osteoarthritic joints. It is still unknown what causes the chondrocytes to release the cytokines and trigger the degradation and inflammatory cascade.

There are numerous surgical procedures aimed at repairing or regenerating osteoarthritic lesions [15, 16]. The most common procedure for small defects is a microfracture technique that drills into the subchondral bone to elicit bleeding that brings progenitor cells and regenerative factors to the lesion. However, the tissue formed is a scar-like fibrocartilage that is mechanically inadequate and usually results in the lesions

reappearing. Autologous periosteal and perichondrial grafting has also been used to provide progenitor cells to the lesion site. These methods are limited by the size of graft that can be obtained while limiting donor site morbidity, but were capable of forming cartilage like tissue in small lesions. Nevertheless, the grafts eventually fail in most cases due to poor integration of the new tissue with the surrounding cartilage and subchondral bone leading to delamination and dislodging of the tissue.

Osteochondral transplantation, or mosaicplasty, has been used to repair large cartilage defects [15]. Plugs of healthy cartilage with subchondral bone are harvested from the joints of either cadavers (allografts) or a non-load bearing area of the patient (autograft) and inserted into the arthritic defect. The implanted hyaline cartilage/bone plugs are initially more stable than the fibrocartilage formed by previous methods. However, donor site morbidity can be severe with autografts resulting in progressive lesions while disease transfer and rejection are constant issues with any allograft.

Autologous chondrocyte implantation (ACI) involves harvesting a small amount of the patient's articular cartilage, isolating the chondrocytes, expanding the cells a hundred fold and them implanting them into the lesion [15, 16]. Although donor site morbidity is reduced due to the need for a smaller biopsy, the method is significantly more expensive, requiring an extra surgery as well as the costs of the cell culture which can take weeks or months. In addition, chondrocytes undergo a process known as "dedifferentiation" when expanded in monolayer resulting in a more fibroblastic-like phenotype with a decreased synthesis of collagen type II and increase in collagen type I synthesis. The procedure has been shown to form hyaline-like repair tissue, but adverse effects including graft failures occurs in a majority of patients. Optimization of the ACI

procedure as well as longer terms studies are required before the cost-benefit analysis can be thoroughly addressed.

Eventually attempts to repair or regenerate osteoarthritic joints with the above procedures are exhausted while the disease continues to progress. The severe pain and morbidity of bone to bone contact can be managed with pain medications for only so long before a total joint replacement is required. The artificial implants are usually made of chromium or titanium with polymer pads at the site of articulation and are very successful at restoring function to the joint [17]. However, the implants can fail due to wear and loosening after 10-20 years depending on the joint and require two or three revision surgeries over the lifetime of the patient. Unfortunately morbidity and mortality increase significantly with each subsequent procedure. The ultimate goal is the development of a treatment that can stop the catabolic cytokine cascade and heal the arthritic lesion before total joint arthroplasty is needed.

CARTILAGE TISSUE ENGINEERING AND REGENERATIVE MEDICINE

Injured or destroyed articular cartilage has limited regenerative capability [15]. This is due to the low proliferation rate of chondrocytes combined with the avascularity of cartilage limiting the flow of progenitor cells and regenerative factors into the site of injury. Moreover, damaged chondrocytes release enzymes called metalloproteinases that further degrade the cartilage matrix and propagate the injury. When the injury is severe enough to involve the subchondral bone and result in blood flow to the injured cartilage, the repair tissue is a scar-like fibrocartilage that is incapable of handling the compressive mechanical loading and eventually deteriorates. For these reasons and the fact that it is a

relatively simple tissue, cartilage has been a major focus of tissue engineering and regenerative medicine strategies.

Tissue engineering refers to the process of creating tissue *in vitro* for implantation into the body. Regenerative medicine is focused more on how to stimulate *in vivo* regeneration of tissue. Both these approaches have pros and cons when it comes to repairing cartilage injuries [15]. Growth of a tissue implant outside of the body allows greater control of the environment. Measurements of the cartilages characteristics can be taken and the parameters tailored for the desired tissue properties. However, *in vitro* tissue does not benefit from the complex *in vivo* biochemical and mechanical environment, which has so far been impossible to replicate precisely. Moreover, integration of the tissue engineered implants with native tissue has show variable success. Attempts to regenerate cartilage *in vivo* can overcome the issues of integration, but there are other problems to be addressed. Similar to other load bearing tissues like bone and muscle, cartilage is constantly under the influence of mechanical forces. *De novo* cartilage tissue can easily be dislodged or degraded before it has time to fully form and integrate. The *in vivo* environment can also be hostile to regeneration due to the release of pro-inflammatory and pro-degradative molecules and factors like interleukins and metalloproteinases. It is currently unclear which approach is superior, but future techniques for cartilage repair will likely utilize aspects of both methods.

Tissue engineering or regenerative medicine strategies rely on one or a combination of three components: cells, scaffolds, and the environment [15, 16]. A range of cell sources from differentiated adult cells to totipotent embryonic stem cells have been investigated for applications in cartilage repair. Each cell source has its own advantages

and disadvantages. For example, an autologous differentiated adult chondrocyte cell source already expresses the desired cartilage specific cellular processes, but they are difficult to harvest in sufficient quantities due to donor site morbidity. An allogeneic chondrocyte source from a cadaver bypasses the problem of donor site morbidity but then raises further immunological obstacles. Moreover, differentiated chondrocytes are difficult to expand in monolayer culture due to slow proliferation rates and because they undergo a process known as "dedifferentiation" in which they take on a more fibroblastic type phenotype with decreased expression of collagen type II and increased expression of collagen type I. Stem cells have the ability to undergo repeated mitotic division without altering their phenotype and therefore have been investigated as a solution to the problem of *in vitro* expansion. Most of the studies with stem cells have focused on adult mesenchymal stem cells due to the inherent legal and ethical question surrounding the use embryonic stem cells. Adult mesenchymal stem cells have the benefit of being an autologous cell source that can potentially be harvested from a variety of tissues of mesodermal origin including bone marrow stroma, muscle, and adipose tissue. However, since they are undifferentiated pluripotent cells they must be stimulated either *in vitro* or *in vivo* with the appropriate chondrogenic environment to become chondrocytes. Several studies have demonstrated that supplementation with growth factors like TGF-β, BMP, and IGF-1 can promote a chondrocytic phenotype, but the stability of the differentiation is unknown.

Artificial scaffolds have been used in tissue engineering to provide a structure on which cells are seeded, as well as in regenerative medicine as a way of recruiting cells and providing mechanical support to enhance tissue regeneration [15, 16]. Numerous types

of synthetic and biological materials have been examined including polymers, hydrogels, proteins, and extracted processed tissue. The ideal material for tissue formation or regeneration needs to be biocompatible with respect to the seeded cells or surrounding tissue. In addition, the materials must be bioresorbable and biodegradable to allow their eventual replacement with functional tissue. Porous polymers scaffolds of lactic and glycolic acid have been commonly used for cartilage tissue engineering as well as purified porous sponges of various collagens. Hydrogels of gelatin or polysaccharides are also popular in cartilage tissue engineering as they more closely mimic the water rich matrix of native tissue. However, hydrogels provide minimal mechanical support once implanted and therefore can jeopardize the success of the implant in load bearing applications without proper rehabilitation protocols. Extracted decellularized extracellular matrixes from various tissues like bone or intestinal submucosa are rich with growth factors and signaling molecules that are capable of recruiting and stimulating differentiation of adult stem cells at the site of injury. These differentiated cells can then produce their own matrix and regenerate the tissue. But similar to hydrogels, the decellularized matrix is not mechanically supportive.

The final component to be considered when designing a tissue repair strategy is the environment [16]. This includes biological, chemical, mechanical, and in some cases electrical stimulation of the cells, scaffolds, or site of repair. The addition of growth factors to the culture media of *in vitro* tissue constructs or to the site of intended *in vivo* tissue regeneration can enhance tissue formation. Moreover, other bioactive molecules can inhibit undesired pathological processes like inflammation and scar formation. Most cells require specific matrix interactions for proper phenotypical expression. Therefore,

the addition of tissue specific matrix molecules can be beneficial. In addition, the body is a dynamic environment and most tissues, especially those of the musculoskeletal system, are subject to an array of mechanical shears and stresses. Attempts to mimic these forces *in vitro* have been shown to be advantageous. The use of magnetic fields to produce electric fields as well as the direct application of electric current has also been investigated for nervous, muscular, and bone. Given the myriad of options, the real challenge is deciding which environment is required to achieve the desired outcome.

ESTROGEN AND SEXUAL DIMORPHISM IN ORTHOPAEDICS

Estrogens are steroid hormones most often associated with female development and reproduction. Like all steroid hormones, estrogens are derived from cholesterol and contain the characteristic four ring structure [18]. They are directly synthesized from androgens via loss of the C-19 methyl group and formation of an aromatic A-ring. There are three estrogens found in normal human physiology: estrone, estriol, and 17β-estradiol [19]. The most active form is 17β-estradiol (E_2) being 12 times more active than estrone and 80 times more active than estriol. The ovaries secrete predominantly E_2 and it is the most prevalent estrogen found in females.

Steroid hormones classically exert their effects by binding to intracellular receptors found in the cytoplasm of the cell [20]. The lipophilic molecules can easily pass through the plasma membrane and form hormone-receptor complexes. These activated complexes then translocate to the nucleus where they bind to DNA and stimulate transcription of the appropriate genes. This process is referred to as a genomic response and can take minutes, hours, or even days because of the time required for new protein

synthesis. There have been two cytoplasmic receptors identified for estrogens, estrogen receptor α (ERα) and estrogen receptor β (ERβ). Recently, it has also been demonstrated that steroid hormones have membrane bound receptors that initiate a cell response via secondary messenger signaling cascades [21]. This membrane response is rapid, occurring in seconds to minutes. It is currently unclear how the genomic and membrane responses may interact to dictate the cellular response to the hormone.

Estrogens have many important roles in both male and female physiology [19]. They are obviously pivotal in the formation of the female reproductive tract and external female genitalia during embryogenesis. Moreover, the menstrual cycle, pregnancy, and lactation are all tightly regulated by a careful balance between estrogens and progestins. They have several general metabolic effects in both male and females, although much less than that of androgens, which include changes in insulin levels, fat deposition, protein anabolism, and electrolyte balance. One of the most important effects of estrogen is on skeletal growth and development. Estrogens are responsible for the initiation of puberty and closure of the growth plate in both males and females [22]. In fact, females and males deficient or insensitive to estrogens from mutations in the aromatase enzyme or estrogen receptors have been shown to grow significantly taller due to delayed epiphysial union [23, 24]. Moreover, there has been significant literature that stresses the importance of sex hormones in the pathogenesis of several musculoskeletal diseases including osteoporosis and osteoarthritis [25, 26].

Cecil and Archer were the first to suggest a relationship between estrogen and osteoarthritis in 1925 when they described a menopause-associated arthritis [27]. Since their observations, epidemiological studies have shown both the prevalence and severity

of the disease to be a function of the patient's genetic sex [28-30]. Men exhibit a higher prevalence of osteoarthritis before the age of 50, while women have a higher prevalence after the age of 50. Moreover, postmenopausal women are more likely to have a general form of the disease that affects multiple joints with greater severity.

The presence of receptors for E_2 in chondrocytes supports these clinical observations that articular cartilage is an estrogen sensitive tissue. Articular cartilage estrogen receptors were first discovered in 1982 using radioactive binding assays in rabbits [31] and dogs [32]. The presence of estrogen receptors have since been confirmed in human articular cartilage by mRNA expression [33] and *in situ* hybridization [34], and have also been found using *in vitro* cultures of human articular chondrocytes [34] and rat growth plate chondrocytes [35].

Despite the epidemiologic observations and the establishment of estrogen receptors in cartilage, the specific physiologic effects of estrogen on chondrocytes are still unknown. Human clinical studies using hormone replacement therapy (HRT) have given varying and often conflicting results [36-38]. There has not been a consistent correlation between serum E_2 levels and the development or progression of osteoarthritis. Animal models have likewise shown differing results depending on the model used. Meniscectomy-induced osteoarthritis in rabbits has been shown to worsen with E_2 treatment [39] and improve with addition of an anti-estrogen, tamoxifen [40]. Intra-articular injection of E_2 into the knee joints of ovariectomized rabbits has also been reported as chondrodestructive [41]. However, E_2 treatment in ovariectomized sheep [42] and cynomolgus monkeys [43] resulted in less severe osteoarthritis compared to controls.

The molecular and biochemical mechanisms underlying the effects of estrogen in articular cartilage have not been thoroughly studied in any species. On the other hand, the effects of sex hormones on growth plate cartilage have been well characterized in the rat costochondral model. Female chondrocytes from both the resting and growth zone of the rat growth plate demonstrated a decrease in proliferation and an increase in alkaline phosphatase activity when treated with E_2 in monolayer cultures [44]. This indicates that E_2 promotes differentiation of the growth plate chondrocytes towards a mineralizing phenotype. Treatment with E_2 also resulted in increased deposition of both collagen and proteoglycan. These effects were not seen in male cells or with the inactive isoform 17α-estradiol.

Further studies suggest that these sex-specific effects of E_2 occur through a rapid membrane-associated mechanism (Figure 2.1). Treatment with E_2 resulted in a dose-dependent and time-dependent elevation of protein kinase C (PKC) [45] activity that was mediated through G-proteins and phospholipase C (PLC) [46]. A similar increase in PKC activity was observed when E_2 was conjugated with bovine serum albumin (BSA) to prevent diffusion through the plasma membrane [47], thereby inhibiting interaction with cytosolic estrogen receptors and eliminating possible genomic effects. Tamoxifen has also been shown to inhibit E_2 activation of PKC in growth plate chondrocytes [48]. Additional studies indicated that this PKC signaling cascade eventually results in phosphorylation of the mitogen-activated protein kinases (MAPKs), ERK 1/2 and p38 [49]. MAPKs are then capable of eliciting genomic responses and altering gene expression.

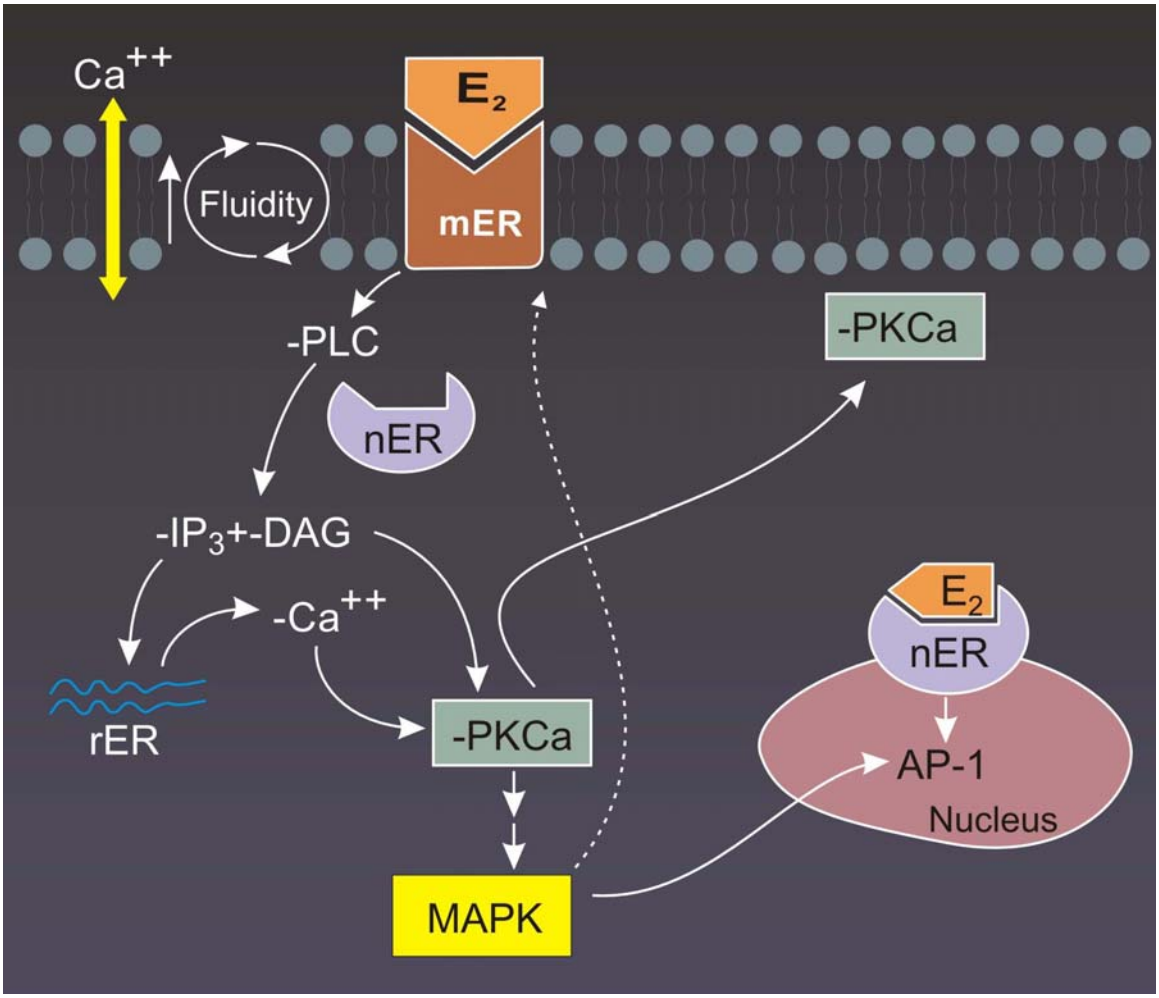

Figure 2.1: 17β-estradiol membrane mediated signaling cascade in growth plate chondrocytes

E_2 binds to a membrane receptor (mER) and stimulates phospholipase C (PLC) activity. PLC acts upon phospholipids to release inositol 1,4,5-triphosphate (IP_3) and diacylglycerol (DAG). IP_3 causes Ca^{2+} release from the rough endoplasmic reticulum (rER). DAG and Ca^{2+} act together to activate protein kinase C alpha (PKCα), which then acts upon mitogen-activated protein kinases (MAPKs) to alter gene expression.

HYDROGEL ENCAPSULATION OF CHONDROCYTES

Articular chondrocytes undergo a process known as dedifferentiation when cultured *in vitro* as monolayers. The lack of a three-dimensional matrix results in the chondrocytes expressing a fibroblast-like phenotype and the subsequent decrease in cartilage-specific processes. Chondrocyte dedifferentiation was first described in embryonic chick chondrocytes as changes in collagen synthesis [50] and was more recently confirmed to occur rapidly with the first few passages in human articular chondrocytes [51].

The dedifferentiation process is believed to be the result of actin stress fibers that form during attachment and spreading of the cells to a two dimensional surface [52-55]. Benya and Shaffer were the first to demonstrate that encapsulating chondrocytes in a three dimensional matrix to maintain their rounded morphology could reverse the dedifferentiation process [56]. They showed rabbit articular chondrocytes regained expression of collagen type II and aggrecan when cultured *in vitro* within agarose gels. However, agarose proved to be a non-ideal substrate due to the difficulty extracting the cells and extracellular components from the constructs.

Alginate was first used to encapsulate chondrocytes in 1989 by Guo and colleagues [57]. It was chosen as a potential matrix due to its inherent physical and chemical properties [58]. Alginates are a family of linear polysaccharides extracted from various species of brown seaweed. They are a block copolymer of β-D-mannuronate and α-L-guluronate linked via a 1-4 covalent bond. The ratio of monomers and the block pattern is highly variable and dependent on what species the alginate is isolated from. The guluronate residues rapidly cross link in the presence of divalent cations like Ca^{2+} to form a solid gel and entrap the chondrocytes. A chelating agent like sodium citrate can

then be added to break down the alginate matrix and release the cells and extracellular components.

The mechanical and material properties of the alginate gel are directly related to the molecular size and guluronate content [58]. Longer blocks of guluronate result in more cross-linking and therefore a stiffer gel. Increased cross-linking also results in a more chemically stable gel with longer degradation times due to a higher concentration of monovalent cations being required to disrupt the gel. The average molecular weight of the alginate also correlates to degradation rate as additional hydrolysis is needed to break the interconnected network. Moreover, alginates rich in guluronate create a larger and more defined pore structure and directly effect mass transfer within the gel.

Alginate encapsulation has been shown by several research groups to effectively reestablish a chondrocytic phenotype in a variety of dedifferentiated *in vitro* chondrocytes cultures including bovine [59, 60], rabbit [61, 62], and human [59, 63-65] articular chondrocytes. Three-dimensional encapsulation within alginate has also shown to promote chondrogenesis in chick mesenchymal cells [62] and fetal rat nasal fibrocartilage [66]. The current hypothesis is encapsulation of chondrocytes changes the mechanical stresses on the cell to those seen *in vivo* and promotes the expression of cartilage specific matrix molecules.

Several methods have been developed for seeding cells into alginate matrixes including injection molding to form constructs of a specific shape [67] as well as extrusion [68] or emulsification [69] techniques to form beads or capsules. The most common method used is extrusion which involves extruding an alginate-cell suspension through a needle

to form droplets that fall into a gelation solution containing divalent cations. The guluronate residues of the alginate then cross-link to form a solid gel and entrap the cells.

The bead size is a function of the gravitational and capillary surface forces acting upon the extruded droplet [70]. The gravitational force (F_g) acts to pull the droplet away from the end of the needle and is given by:

$$F_g = \frac{4}{3}\pi r^3 \rho g$$

where r is the radius of the droplet, ρ is the density of the alginate solution, and g is the acceleration due to gravity. The capillary surface force (F_γ) acts to hold the droplet to the needle tip and is given by:

$$F_\gamma = 2\pi r_i \gamma$$

where r_i is the inner radius of the needle and γ is the surface tension of the alginate solution. Equating the two forces allows an expression for the bead radius to be solved:

$$r = \left(\frac{3}{2}\frac{r_i \gamma}{\rho g}\right)^{1/3}$$

which demonstrates bead radius is a function of the needle size, surface tension, density, and gravity. The alginates beads produced by the extrusion method are typically 2-4 mm in diameter with needle radius being the dominant factor. Alginate solutions with viscosities capable of a reasonable flow rate are typically only 1%-4% giving them a comparable surface tension and density to that of water. Therefore, these parameters cannot typically be adjusted to significantly affect bead size.

A common problem among larger tissue engineered constructs is the development of necrotic cores due to mass transfer limitations [71-73]. Smaller beads could overcome this problem and may also allow minimally invasive injectable therapies. Several

methods have been developed to disrupt the capillary surface force and reduce the size of the alginate beads. The most frequent methods used with the extrusion method involve mechanical disruption with air flow [74] or the application of an electrostatic potential [70, 75]. The beads produced with an electrostatic potential are up to one thousand times smaller in volume compared to beads produced by gravitational force alone. Moreover, application of electrostatic forces is more effective than mechanical disruption, generating beads up to one hundred times smaller in volume.

The electrostatic force (F_e) acts along with the gravitational force (F_g) to counteract the capillary surface force (F_γ) and reduce droplet size [70]. The force exerted by the external electric field between the needle and gelation solution is given by:

$$F_e = 4\pi\varepsilon_o \left(\frac{V}{\mathrm{Ln}\left(\frac{4H}{r_i}\right)} \right)^2$$

where ε_o is the permittivity of air, r_i is the inner radius of the needle, and H is the distance from the needle to the solution. Once again, an expression for the bead radius can be solved by equating the capillary force to the disrupting forces:

$$r = \left(\left[\frac{3}{2\rho g} \right] \left[r_i \gamma - 2\varepsilon_o \left(\frac{V}{\mathrm{Ln}\left(\frac{4H}{r_i}\right)} \right)^2 \right] \right)^{1/3}$$

which demonstrates that bead size under the effect of an applied electrostatic potential is a function of the surface tension, density, needle radius, permittivity, voltage, drop

height, and gravity. The voltage and height can be easily adjusted to achieve a wide range of bead diameters for the desired application.

Alginate microencapsulation and environmental factors have the potential to interact additively or synergistically to promote tissue formation. Most groups have investigated how alginate encapsulated chondrocytes respond to traditional cartilage growth factors like IGF-1 or TGF-β [76]. No research has been done on how sex hormones like estrogen may affect alginate encapsulated chondrocytes. However, one study has shown that alginate encapsulation elicited an increase in PKCα activity and that this enzyme activity was correlated with increase expression and synthesis of collagen type II [62]. This is the same PKC isoform activated in rat costochondral growth plate chondrocytes when treated with E_2 [45]. This suggests a potential interaction between E_2 and three-dimensional encapsulation on *in vitro* chondrocyte cultures (Figure 2.2).

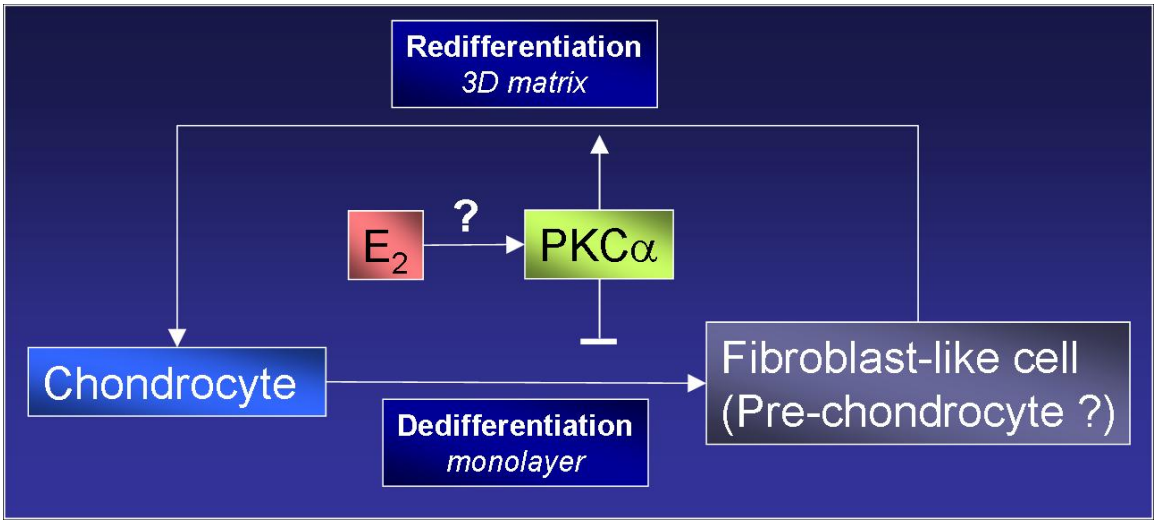

Figure 2.2: Potential interaction between estrogen and three-dimensional suspension for maintaining chondrocyte phenotype

Chondrocytes undergo a process known as dedifferentiation when cultured in monolayer. Three-dimensional suspension in hydrogels can redifferentiate the chondrocytes back to a normal phenotype, and is in part regulated by protein kinas C alpha (PKCα) activity. This is the same PKC isoform activated by 17β-estradiol (E_2), thereby suggesting a possible interaction between the hormone and three-dimensional encapsulation.

CHAPTER 3

Human Articular Chondrocytes Exhibit Sexual Dimorphism in Their Responses to 17β-Estradiol

INTRODUCTION

Epidemiological studies show sex-specific differences in both prevalence and severity of osteoarthritis [27-30]. Men exhibit higher prevalence of osteoarthritis before age 50, while women have a higher prevalence after age 50. In addition, postmenopausal women are more likely to have a general form of the disease that affects multiple joints with greater severity. This epidemiologic and pathologic gap between the sexes continues to increase with advancing age. Attempts to correlate biomechanical differences between males and females with the incidence and prevalence of osteoarthritis have failed to identify a causative factor, suggesting that there may be innate differences at the cellular level that contribute to disease severity.

One possibility is that sensitivity to estrogen plays a role. The presence of estrogen receptors (ER) alpha and beta in chondrocytes supports clinical observations that articular cartilage is an estrogen-sensitive tissue [31-34]. The parameters by which estrogen modulates chondrocyte behavior are not well understood, however. Human clinical studies using hormone replacement therapy have failed to show a consistent correlation between serum estrogen levels and development or progression of osteoarthritis [36-38]. Animal models have likewise shown differing results depending on the model [39-43].

Studies examining effects of the active estrogen metabolite, 17β-estradiol (E_2), on growth plates of mice and rats in organ culture indicate that responses to the hormone differ in a sex-dependent manner [77], suggesting that the sexual dimorphism is at the cellular level. ERα and ERβ are present in rat growth plate chondrocytes (RGPC) [48], but female cells possess more high affinity receptors than male cells [35]. In addition, there are marked differences in physiological responses of male and female RGPC cells to E_2 [44]. Female cells demonstrated decreased proliferation and increased alkaline phosphatase activity, indicating that E_2 promotes differentiation. E_2 also affected extracellular matrix production, resulting in increased synthesis of both collagen and proteoglycan. These effects were not seen in male cells or with 17α-estradiol.

Stereospecificity of the response to estrogen suggests a receptor-mediated mechanism. E_2 treatment increases membrane fluidity and phospholipid metabolism in female cells [78], and also results in rapid elevation of protein kinase C (PKC) activity [45]. The increase in PKC is mediated through G-proteins and phospholipase C (PLC) [46]. A similar increase in PKC activity was observed when E_2 was conjugated with bovine serum albumin (E_2-BSA) to prevent diffusion through the plasma membrane [47], thereby inhibiting interaction with cytosolic ERs. Whereas tamoxifen blocks E_2 activation of PKC in RGPC cells, neither the ER agonist diethylstilbestrol nor the ER antagonist ICI 182780 has an effect [48], suggesting that E_2 regulates chondrocytes through mechanisms other than those traditionally associated with nuclear receptors. E_2 also activates PKC in human colon cancer cells from females only [79], and activates PKC in female rat distal colon by an ICI 182780-insensitive mechanism [80].

Our goal was to determine if sexual dimorphism in response to estrogen is a feature of human articular chondrocytes (HAC). Cells from multiple donors were examined to verify that differences in response were due to genetic sex and not normal human variation**.** We first characterized the HAC to ensure they were phenotypically chondrocytes, and then examined their response to E_2 by measuring changes in proliferation, differentiation and matrix deposition. Finally, we investigated the potential role of PKC signaling in E_2 stimulation of HAC.

MATERIALS AND METHODS

Human Articular Chondrocyte Isolation and Cell Culture

Articular cartilage was isolated from the femoral condyles and tibial plateaus of human donors made available due to autopsy. Donors had no known history of joint disease and histological analysis was performed at the time of isolation to confirm the absence of any pathologies. The articular cartilage was cut into small pieces and washed twice for 20 minutes with Hanks' balanced salt solution (HBSS) containing 1% penicillin and streptomycin. The washed cartilage was digested for 1 hour with 0.25% trypsin-1 mM ethylene diamine tetraacetic acid (EDTA), followed by treatment with 0.2% collagenase for 3 hours. All enzymes were prepared in HBSS. The digested suspension was passed though a 40 μm mesh sieve and centrifuged at 2000 rpm for 10 minutes. The supernatant was removed and the chondrocytes were resuspended in full media containing 88% Dulbecco's modified Eagle's medium (DMEM), 10% fetal bovine serum (FBS), 1% penicillin/streptomycin, and 1% L-ascorbic acid [81].

Isolated primary HAC were plated on T75 flasks, grown to confluence, and harvested using 0.25% trypsin-1 mM EDTA. The cell suspension was centrifuged at 2000 rpm for 10 minutes, the supernatant removed, and the cells resuspended in cold DMEM, 20% FBS, 1% penicillin/streptomycin, and 5% dimethyl sulfoxide (DMSO). The chondrocytes were then frozen at –80^{o}C and shipped overnight from La Jolla, CA to Atlanta, GA. The chondrocytes were thawed, centrifuged, resuspended in full media and plated on T75 flasks. These cultures were grown to confluence and passaged one time as above. Thus second passage HAC cells were used for all experiments. Confluent second passage cultures were also used to assess expression of chondrocyte phenotypic markers. It was necessary to expand the cells in culture in order to obtain sufficient numbers for each set of assays.

Characterization of Cell Source

Articular chondrocytes dedifferentiate when expanded in monolayer cell culture [56, 82]. Therefore, reverse transcription polymerase chain reaction (RT-PCR) was used to assess the phenotype of the second passage HAC by measuring the mRNA expression of aggrecan, collagen type I, collagen type II, and collagen type X. Total RNA was extracted from the chondrocyte cultures with Trizol reagent. Lipophilic contaminants were removed by adding chloroform and centrifuging for 25 minutes at 4700 rpm. The aqueous phase was then washed with isopropyl alcohol to precipitate the RNA, and centrifuged for 20 minutes at 4700 rpm to form a pellet. The pellet was washed with cold 70% ethanol and centrifuged for 15 minutes at 4700 rpm. The supernatant was removed and the pellet allowed to air dry. The RNA was then dissolved in diethylpyrocarbonate

(DEPC) treated water and the purity and quantity was determined by UV spectrophotometry.

The total RNA sample from each donor was reverse transcribed using the First-strand cDNA Synthesis Kit (Amersham-Biosciences, Piscataway, NJ) and the specific anti-sense primer for each mRNA of interest. The cDNA was amplified using the Fisher PCR kit (Fisher Scientific International, Hampton, NH) and the specific sense and anti-sense primers. PCR conditions for each cycle included a 30 second denaturation at 94 ^{o}C, a 60 second annealing at 50-65 ^{o}C depending on the primer used, and a 30 second extension at 72 ^{o}C. The PCR-amplified products were run on 5% polyacrylamide gels using a buffer consisting of 0.9 M Trizma® base (tris[hydroxymethyl]aminomethane), 0.9 M boric acid, and 20 mM EDTA. Primary human fibroblast RNA was used as the positive control for collagen type I, and RNA extracted from rat growth plate cartilage was used as the positive control for collagen type X. The negative control for the extracellular matrix components was human lymphocyte RNA. RT-PCR for ERα was performed as above except RNA from human ovarian tissue was used as a positive control. RT-PCR primer information is summarized in Table 3.1.

Cell Proliferation

DNA synthesis via [^{3}H]-thymidine incorporation was used to estimate cell proliferation in response to E_2 [83]. Second passage HAC were grown to subconfluence in 96-well plates, and made quiescent for 48 hours by incubating with media containing 1% FBS. The cells were then treated with 10^{-11} to 10^{-7} M E_2 in 1% FBS media for 24 hours. Four hours prior to harvest, 0.05 μCi of [^{3}H]-thymidine was added to each well, giving a

Table 3.1: RT-PCR Primers for Second Passage Human Articular Chondrocytes

	Sense Primer	Anti-Sense Primer	Anneal Temp.	Product
Aggrecan	5′- TGA GGA GGG CTG GAA CAA GTA CC-3′	5′-GGA GGT GGT AAT TGC AGG GAA CA-3′	65 °C	349 bp
Collagen 1	5′-GTC AGG CTG GTG TGA TGG GA-3′	5′-AAC CTC TCT CGC CTC TTG CT-3′	60 °C	318 bp
Collagen 2	5′-CTG CTC GTC GCC GCT GTC CTT-3′	5′-AAG GGT CCC AGG TTC TCC ATC-3′	58 °C	429 bp
Collagen 10	5′-AGT CCT GGA CTC CAA CGA-3′	5′-TGG AAG ACC CCT CTC AC-3′	55 °C	357 bp
ERα	5′-AAG GAG ACT CGC TAC TGT-3′	5′-TCA AAG ATC TCC ACC ATG CC-3′	57 °C	740 bp

final concentration of 0.25 μCi/ml. At harvest, the cells were washed twice with 200 μl phosphate buffered saline (PBS), and then fixed by washing three times in 5% trichloracetic acid (TCA). The samples were then allowed to air dry and 100 μl 1% sodium dodecyl sulfate (SDS) was added to each well. The samples were incubated overnight at 4 ^{o}C, scraped, transferred to scintillation vials filled with 10 ml of Ready-gel (Beckman Coulter, Fullerton, CA) and counted for 1 minute. Each sample was normalized by the total protein content per well, as the assay precludes cell counting or measurement of DNA content.

Alkaline Phosphatase Specific Activity

Cells from each donor were grown to confluence in 24-well plates and treated with 10^{-11} to 10^{-7} M E_2 24 hours prior to harvest. At harvest, cells were washed twice with 500 μl PBS. An additional 500 μl of PBS was added, and the cell layer was scraped and transferred to 12x75mm test tubes. Another 500 μl of PBS was added to the test tubes, and samples were centrifuged for 20 minutes at 3200 rpm. The supernatant was decanted, another 500 μl of PBS added, and centrifugation was repeated. The supernatant was decanted again, and the pellet was suspended in 500 μl of a 5% Triton X solution. Samples were subjected to 3 cycles of freeze/thaw treatment in a methanol/dry ice bath to break up the cell layer pellet and 50 μl of each sample was aliquoted into a 96-well plate in duplicate.

A buffer solution consisting of 2-amino-2-methyl-1-propanol (AMP), *p*-nitrophenyl phosphate (*p*NPP), and $MgCl_2$ was mixed in a 1:1:1 (v/v/v) ratio. Fifty microliters of the buffer solution was added to each well in the 96-well sample plates, and the plates were incubated at 37 °C. Samples were incubated until they were a pale yellow

color within the range of the standard curve but not longer than 3 hours [84]. After removing the plates, 100 μl of NaOH was added to stop the reaction, and the plates were read in a Bio-Rad microplate reader (Bio-Rad Laboratories, Hercules, CA) at 405 nm. Each sample was normalized by the total protein content per well to determine specific activity.

Proteoglycan Production

[^{35}S]-Sulfate incorporation was used to measure proteoglycan production [85] in response to E_2. HAC were grown to confluence in 24-well plates and treated with 10^{-11} to 10^{-7} M E_2 for 24 hours. Four hours prior to harvest, 5 μCi of [^{35}S]-sulfate was added to each sample, giving a final concentration of 9 μCi/ml. At harvest, cells were washed once with PBS, 250 μl of 0.25 M NaOH was added, and the cells were scraped and transferred to 12x75mm tubes. Additional NaOH was added and the cell scraping repeated. Samples were vortexed and 50 μl removed for protein determination. Two hundred and fifty microliters of 0.15 M NaCl was added, and the samples were put in approximately 5-cm pieces of prepared 0.25 mm thick, 12-14KD molecular weight cut-off, dialysis tubing. The tubing was prepared in a solution of 100 mM $NaHCO_3$ and 10 mM Na_2EDTA. It was incubated at 60 °C for 2 hours in a shaking water bath. The incubation was repeated for another 2 hours with warm, fresh solution. The solution was replaced with 2 L of warm, ultrapure water, and incubated for 1 hour. Water replacement and incubation were repeated until the water became clear. The tubing and water were cooled to 4 °C and the water was replaced with 10% methanol. Tubing with the samples was placed in a 4 L beaker with dialysis solution (0.15M NaCl, 20mM Na_2SO_4, 20mM Na_2PO_4, pH 7.4) and incubated at 4 °C for 24 hours. The solution was replaced every 8

hours until the radioactivity was similar to baseline. Sample tubes were transferred into scintillation vials filled with 10ml of Ready-gel and counted for 1 minute. Each sample was normalized by the total protein content per well.

Protein Kinase C Activity

HACs from each donor were grown to confluence in 24-well plates and treated with 10^{-11} to 10^{-7} M of E_2 for 3, 9, 90, and 270 minutes. To isolate the membrane response, cells were also treated with 10^{-11} to 10^{-7} M E_2 conjugated to bovine serum albumin (E_2-BSA) for 90 minutes. E_2-BSA can not freely pass through the plasma membrane and therefore does not bind cytoplasmic receptors. At harvest, the cells were washed twice with 500 μl PBS, and 300 μl of RIPA buffer was added to lyse the cells. The PKC activity of each sample was measured using the Biotrak Protein Kinase C enzyme Assay Kit and procedure from Amersham Biosciences. The system is based upon the PKC catalyzed transfer of [^{32}P]-PO_4 from [^{32}P]-γ-ATP to a peptide specific for PKC. The reaction mixture consisted of 3 mM calcium acetate, 0.075 mg/ml Lα-phosphatidyl-L-serine, 6 μg/ml phorbol 12-myristate 13-acetate, 150 μM PKC specific peptide, and 7.5 mM dithiothreitol in a 50mM Tris/HCl buffer containing 0.05% (w/v) azide at pH 7.5. Twenty-five microliters of the mixture was added to 25 μl of each sample. γ-ATP Phosphorous-32 was mixed with a 1.2 mM ATP, 30 mM Hepes, 72 mM magnesium chloride solution at pH 7.4 and a total count of 450,000 ± 20,000 cpm per 5 μl was obtained. Five microliters of radioactive ATP buffer was added to each sample. The samples were centrifuged and incubated at 37 °C for 15 minutes. After incubation, 10 μl of the stop reagent containing 300 mM *ortho*-phosphoric acid and carmosine red was added and the samples were centrifuged again. The samples were mixed, and 35 μl

was transferred to the peptide binding papers provided in the kit. The papers dried for 5 minutes and were then washed twice in 75 mM *ortho*-phosphoric acid solution with agitation for 5 minutes. The paper disks were transferred into scintillation vials filled with 10 ml of Ready-gel and counted for 1 minute each. The total pmols phosphate (P) transferred per minute were calculated as follows: P = (T*1000)/(I*R), where I is the incubation time. The specific activity (R) of 1.2 mM Mg [^{32}P]ATP is equal to the total count (450,000 ± 20,000 cpm) per 5µl divided by the number of moles of ATP ($6x10^{-9}$) per 5 µl. The total phosphate (T) transferred to peptides and endogenous proteins is equal to the sample cpm minus the blank cpm. The blank cpm was measured using both cell lysate free reactions with reaction buffer to determine the background, and with cell lysate containing samples without reaction buffer to measure phosphorylation of endogenous proteins. Both blanks were significantly lower than the samples, but were equal to each other, indicating that there was minimal phosphorylation of endogenous proteins. Each sample was then normalized by the total protein content per well.

Macro Protein Assay

All samples were normalized by total protein content using the Pierce Macro BCA Protein Assay Reagent kit (Pierce Biotechnology, Rockford, IL). Reagents A and B were mixed in a 50:1 ratio to make the working reagent. Twenty-five microliters of each sample was aliquoted in duplicate to 96-well plates, and 200 µl of the working reagent was added to the sample plates. They were incubated at 37 °C for 30 minutes and read in the BioRad Microplate reader at 570 nm.

PKC Inhibition

To test whether the effects of E_2 on female HAC were mediated by PKC, confluent cultures were treated with 10^{-8} M E_2 in the presence and absence of 0.1, 1, or 10 μM chelerythrine. Chelerythrine has been shown to specifically inhibit PKC at concentrations less than 10 μM in several cell systems [86-88]. We previously showed that the effects of E_2 on RGPC are blocked by chelerythrine as well as by other PKC inhibitors including staurosporine and H-7 [89]. Following treatment, [^{35}S]-sulfate incorporation was measured as described above.

RESULTS

Characterization of Phenotype

Expansion of HAC for two passages in monolayer culture resulted in partial loss of phenotypic expression. The chondrocytes retained their ability to express aggrecan core protein mRNA (Figure 3.1), but lost expression of collagen type II mRNA. The cells showed an increase in collagen type I mRNA expression (Figure 3.1), but did not show any expression of collagen type X indicating the cells were not differentiating towards a hypertrophic phenotype. Despite loss of collagen type II expression, second passage cells were chosen in order to use the same six donors for all experiments, thereby reducing potential variability between donors. The mRNA expression for the above matrix components was not dependent on donor sex indicating that loss of collagen type II expression was not regulated in a sex-specific manner.

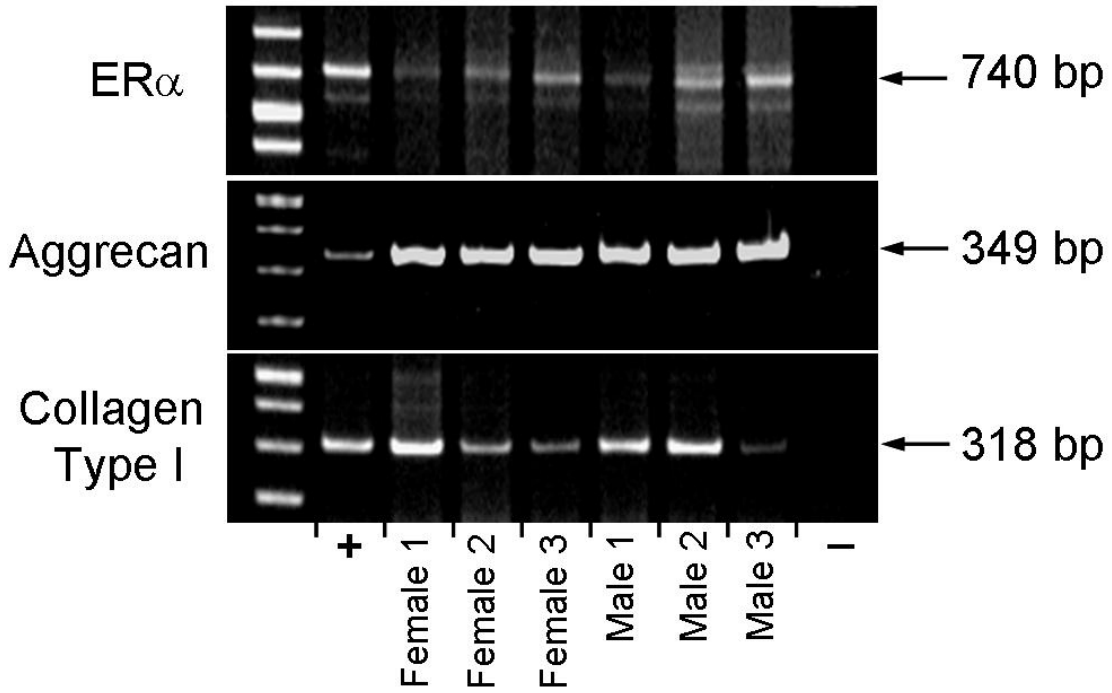

Figure 3.1: Characterization of second passage human articular chondrocytes

The phenotype of the human chondrocytes (HACs) was assessed by measuring the mRNA expression of aggrecan, collagen type I, collagen type II, collagen type X, and ERα. Both female and male cells showed expression of mRNA for aggrecan, collagen type I, and ERα. There was no detectable expression of collagen type II or collagen type X. The results indicate that second passage HACs are partially dedifferentiated towards a fibroblastic phenotype. However, the dedifferentiation is not sex-specific and the expression of ERα is retained in both male and female cells as well.

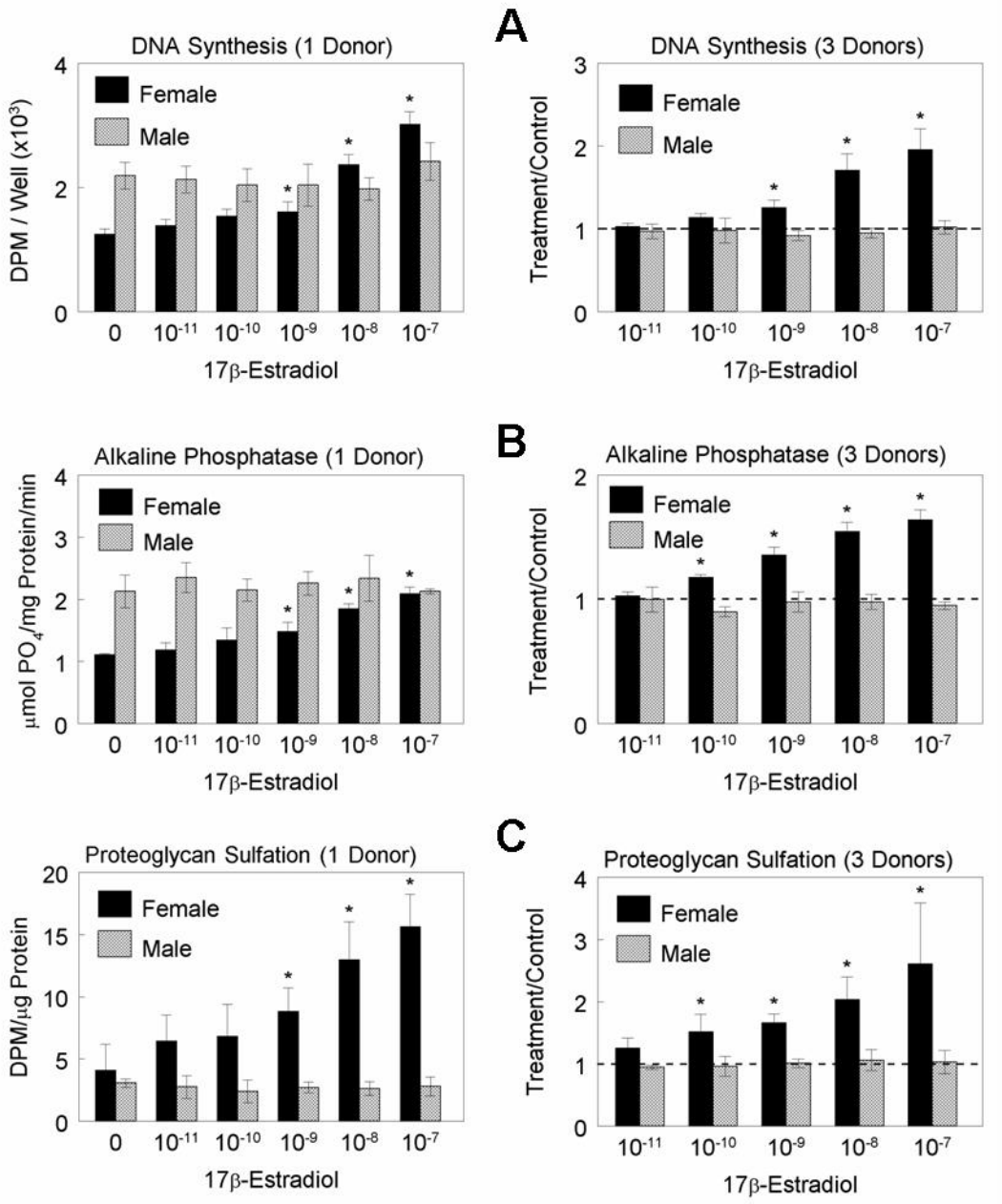

Figure 3.2: Effect of 17β-estradiol on proliferation, differentiation, and matrix synthesis

Second passage human articular chondrocytes (HACs) were cultured in monolayers and treated with 10^{-11} to 10^{-7} M 17β-estradiol (E_2) for 24 hours. **(A)** [^{3}H]-Thymidine incorporation was used to measure DNA synthesis. Female chondrocytes showed a significant increase in proliferation compared to control at 10^{-9} to 10^{-7} M E_2. Male chondrocytes did not show a response to E_2. **(B)** Alkaline phosphatase activity was used to indicate changes in chondrocyte differentiation. Female chondrocytes showed a significant increase in alkaline phosphatase activity compared to control at 10^{-10} to 10^{-7} M E_2. Male chondrocytes did not show a response. **(C)** Matrix synthesis was quantified

(Figure 3.2 continued) using [^{35}S]-SO_4 incorporation to measure proteoglycan production. Female chondrocytes showed a significant response compared to control at 10^{-10} to 10^{-7} M E_2. Male chondrocytes once again did not show a response to E_2. Values are the mean ± S.E.M of six cultures from one of two experiments, both showing comparable results. *P < 0.05, treatment vs. control.

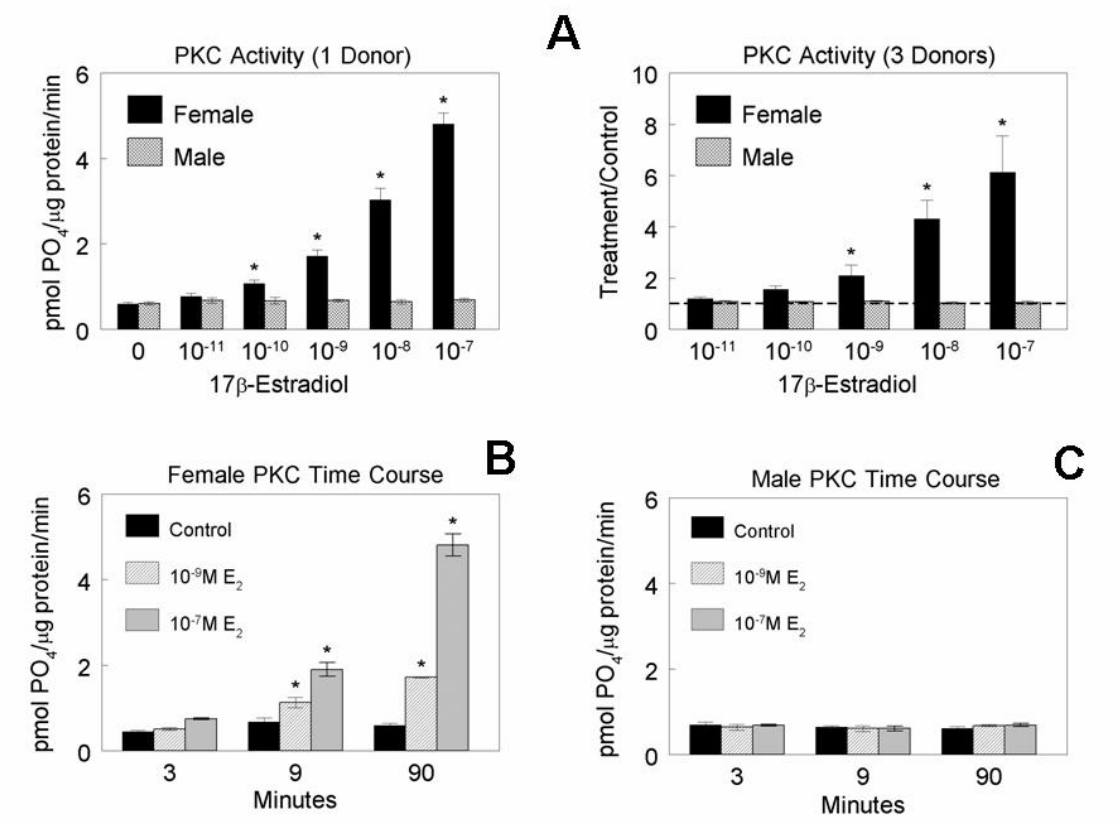

Figure 3.3: Effect of 17β-estradiol on protein kinase C specific activity

Second passage human articular chondrocytes (HACs) were cultured in monolayers and treated with 10^{-11} to 10^{-7} M 17β-estradiol (E_2) for 3, 9, 90, or 270 minutes. Cells were harvested and protein kinase C (PKC) specific activity was measured. **(A)** Female chondrocytes showed a significant response compared to control at 10^{-9} to 10^{-7} M E_2 while male cells did not show a response. **(B)** The effect of E_2 on PKC activity was time dependent for female chondrocytes with a significant response at 9 min, a maximal response at 90 min, and a return to baseline levels at 270 min. **(C)** Male chondrocytes did not show a response at any of the time points tested. Values are the mean ± S.E.M of six cultures from one of two experiments, both showing comparable results. *P < 0.05, treatment vs. control.

Response to 17β-Estradiol

HAC exhibited clear sexual dimorphism in their physiological response to E_2. Chondrocytes from all three female donors showed dose-dependent increases in [^{3}H]-thymidine incorporation, significant at 10^{-9} M E_2 (Figure 3.2A). DNA synthesis in male cells did not show any significant response to estrogen at the concentrations used. E_2 also regulated chondrocyte differentiation in a sex-specific manner. Cells from female donors showed dose-dependent increases in alkaline phosphatase activity, significant at 10^{-10} M (Figure 3.2B). Levels of alkaline phosphatase activity in male chondrocytes were unchanged by estrogen treatment. Similarly, E_2 treatment caused sex-specific and dose-dependent increases in [^{35}S]-sulfate incorporation (Figure 3.2C), which were found in chondrocytes from all three female donors at 10^{-10} M. E_2 did not affect this parameter in chondrocytes from male donors.

Both male and female chondrocytes expressed mRNA for ERα (Figure 3.1) and there were no apparent differences in mRNA levels due to donor sex. The presence of ERs in both sexes suggests the sex-specific response to E_2 acts through a different mechanism. PKC-dependent signaling is clearly involved. As noted previously for female RGPC cells [45] and human colon cancer cells [79], only female human articular chondrocytes showed a rapid dose-dependent increase in PKC activity in response to estrogen (Figure 3.3). The effect was significant at 9 minutes, reached a maximum at 90 minutes, and was found at concentrations as low as 10^{-10} M E_2 for individual patients and at 10^{-9} M E_2 when the results for all three patients were combined. In contrast, chondrocytes from male donors did not exhibit a significant response to E_2 at any of the

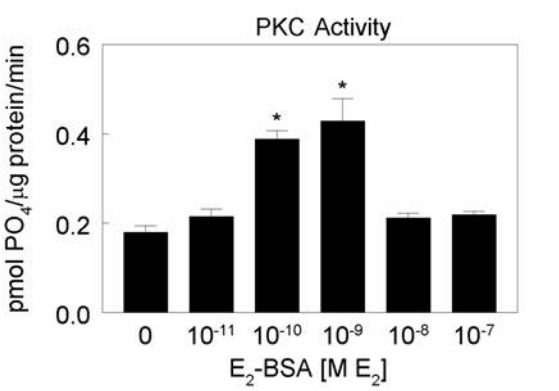

Figure 3.4: Isolation of the rapid membrane mediated response

Second passage human articular chondrocytes (HACs) were cultured in monolayers and treated with 10^{-11} to 10^{-7} M 17β-estradiol conjugated with bovine serum albumin (E_2-BSA) for 90 minutes. Cells were harvested and protein kinase C (PKC) specific activity was measured. Female chondrocytes showed a significant response compared to control at 10^{-10} to 10^{-9} M E_2. Values are the mean ± S.E.M of six cultures from one of two experiments, both showing comparable results. *P < 0.05, treatment vs. control.

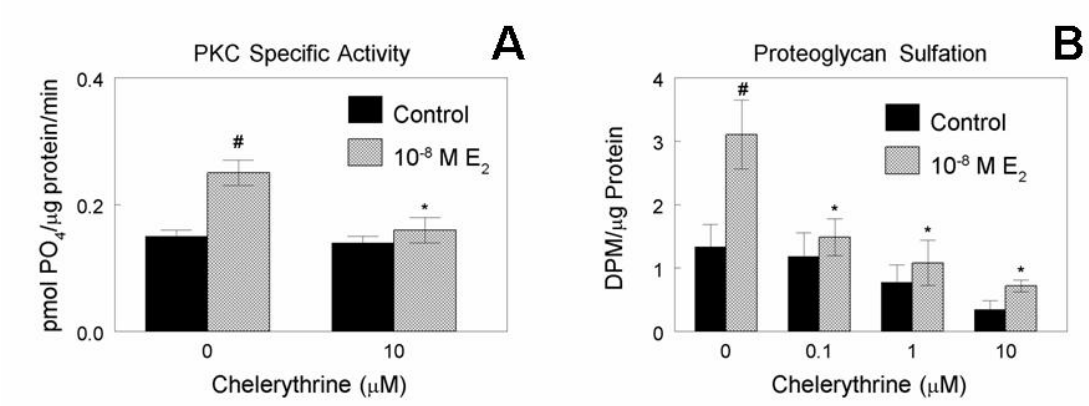

Figure 3.5: Effect of protein kinase C inhibition on 17β-estradiol stimulated matrix synthesis

Confluent second passage chondrocytes were treated for 24 h with control media or 10^{-8} M E_2 containing 0.1, 1, or 10 μM chelerythrine, a general PKC inhibitor. **(A)** Chelerythrine inhibited E_2 stimulation of PKC activity. **(B)** The increase in proteoglycan production associated with E_2 treatment was completely blocked by the addition of chelerythrine. Values are the mean ± S.E.M of six cultures from one of two experiments, both showing comparable results. #P < 0.05, treatment vs. control. *P < 0.05, inhibitor vs. treatment.

concentrations or time points tested. Female HACs also showed a significant increase in PKC activity when treated with10^{-10} M and 10^{-9} M E_2-BSA for 90 minutes (Figure 3.4). The large hydrophilic BSA molecules are incapable of passing through the plasma membrane, which indicates a rapid membrane-associated response

Effect of PKC Inhibition

Treatment of the cells with chelerythrine blocked the stimulatory effect of the hormone on PKC (Figure 3.5A) and proteoglycan synthesis (Figure 3.5B). The effects of chelerythrine were dose-dependent. At the lowest dose (0.1 μM), the inhibitor reduced [^{35}S]-sulfate incorporation in E_2 treated cultures to control levels, completely abrogating the effect of the hormone. Chelerythrine also appeared to decrease [^{35}S]-sulfate incorporation in untreated cultures but this effect was not significant.

DISCUSSION

It has been difficult to study the effects of hormones on articular chondrocytes *in vitro* because they undergo a process known as dedifferentiation when cultured on two-dimensional surfaces. The lack of a three-dimensional matrix causes the down-regulation of cartilage specific processes. Chondrocyte dedifferentiation was first described in embryonic chick chondrocytes as changes in collagen synthesis [50], and was later confirmed in rabbit and human articular chondrocytes [90]. Current biochemical analysis has shown that adult rabbit articular chondrocytes have complete loss of collagen type II mRNA expression and protein synthesis after two passages when seeded at low densities [62], defined as 10^4 cells/cm^2. Experiments on human fetal articular chondrocytes have also shown decreased collagen type II mRNA expression in primary cultures after 7-10 days

of low density culture [63]. Recently it was shown that dedifferentiation of HAC occurs rapidly within the first few passages following primary culture [51]. Our adult HAC model had undetectable levels of collagen type II mRNA after two passages, but continued to strongly express aggrecan, a chondrocyte-specific proteoglycan core protein**.** We were unable to verify that the original primary cells produced collagen type II because we used banked chondrocytes. In addition, the first passage cell stocks needed to be subpassaged at least once to obtain the number of cells needed for the experiments. This allowed the same six donors to be used for all the experiments, thereby decreasing genetic variability. The use of primary cells is preferred, but it is not practical in an adult human articular chondrocyte model.

It is possible that the sex-specific differences we see are due to the dedifferentiation effects, but it is unlikely. The dedifferentiation process does not appear to be sex-specific using the standard chondrocytic markers. However, if monolayer cell culture does indeed result in sex-specific changes in the biochemistry of cells then these results are even more relevant to the biological research community at large and should be further investigated.

Our results suggest that the sex-specific effects of E_2 on proteoglycan production are mediated by PKC. Inhibition of PKC with chelerythrine at concentrations as low as 0.1 μM completely blocked the stimulatory effects of the hormone. We previously examined the effect of E_2 on RGPC with and without chelerythrine and compared immunoprecipitation kinase assays using isoform specific antibodies [45]. Chelerythrine was shown to specifically inhibit PKCα, which was the isoform shown to be up-regulated by E_2 in RGPC cells. We also compared the effects of three PKC-specific inhibitors

(chelerythrine, staurosporine, and H7) on TGF-β1 stimulated PKC activity in the same rat growth plate model and found similar results with all three inhibitors [89]. Chelerythrine has also been used as a PKC-specific inhibitor in other musculoskeletal cell models [91-93]. However, chelerythrine has been shown to affect other signaling pathways in non-musculoskeletal cells [94, 95] and has variable effects on PKC in brain tissue [86, 96]. Recently, investigators have reported that they failed to observe PKC inhibition when using chelerythrine [94, 95], but the assays used in these studies were different from the ones reported here and the tissues involved were non-skeletal. While it is likely that E_2 exerts its effects via multiple pathways, the results presented here implicate PKC in the mechanism.

The fact that increased PKC activity occurs within minutes suggests that E_2 may activate a non-genomic signaling pathway through a membrane-associated receptor. This is further supported by the increase in PKC activity observed when E_2 was conjugated to BSA. Recent studies have identified both ERα and ERβ in the plasma membrane of estrogen-responsive cells [34, 97], as well as the presence of truncated forms of these receptors [98]. It is not yet known if one or more of these entities are responsible for PKC activation and translocation. It is possible that male chondrocytes do not express some component of this membrane receptor and therefore are not affected by E_2. It is also important to note that male chondrocytes are deficient in some part of the genomic estrogen signaling pathway since they did not show any response to E_2 after 24 hours of treatment even though they express ER. Not all responses to E_2 are sex-specific however. Both male and female osteoblasts respond to E_2 with increased src-dependent MAPK [99]. Also of note was a shift in the dose response curve of PKC activity in response to E_2-

BSA compared to E_2. This could have been the result of a higher relative concentration of E_2 at the plasma membrane due to BSA restricting diffusion into the cell.

In vivo, both male and female chondrocytes produce estrogen via aromatization of testosterone [100], but male cells also convert testosterone to 5-hydroxytestosterone (DHT) via 5-alpha reductase [101]. Some effects of testosterone are also sex-specific and are mediated by DHT [102]. It is unknown what additional effects estrogen metabolites may have on male cells.

Under normal physiological conditions, female cells would be exposed to higher levels of estrogen, both systemically as well as locally. Studies using RGPC cells as the model indicate that local levels of estrogen can be as high as 10^{-8} M [103], which is the concentration at with the membrane-associated PKC-dependent signaling is maximally stimulated. These observations support the hypothesis that the female response to estrogen involves membrane-associated signaling via PKC in addition to traditional nuclear receptor mediated mechanisms, as noted by others for female colon cancer cells [79] and female rat distal colon [80]. The present study is the first to show a clear sex-specific effect of the hormone in a normal human cell model.

Although there are many similarities between the response of RGPC and HAC to E_2, there are also differences. Most notably, E_2 inhibits DNA synthesis in RGPC [46], whereas it stimulates [^{3}H]-thymidine incorporation in human articular chondrocytes. In both instances the effects of the hormone are sex-specific. Our results indicate that there are fundamental differences between human male and female chondrocytes that modulate how their response to normal physiological regulators. This sexual dimorphism has important implications for applications that require functional adaptation of donor cells of

one sex in hosts of another sex. Certainly sex is a variable that must be considered in interpreting results describing cell behavior in culture and *in vivo*. The greater incidence in females of osteoarthritis and inflammatory diseases affecting cartilage [27-30] support the hypothesis that development of pathology may be due in part to intrinsic sex-specific differences in female and male chondrocytes.

CHAPTER 4

Osteoinductivity of Demineralized Bone Matrix in Immunocompromised Mice and Rats is Decreased by Ovariectomy and Restored by Estrogen Replacement

INTRODUCTION

The high prevalence of osteoporosis and osteoarthritis in post-menopausal women creates a demand for autograft in many orthopaedic procedures, including joint replacements, spinal fusions, and fracture repair, as well as for increasing bone mass for placement of dental implants. However, the osteopenia present in this patient population can make it difficult to obtain sufficient autologous bone graft to meet these clinical needs, resulting in the need for allografts and bone graft substitutes [104]. These synthetic materials provide osteoconductive surfaces, but they may not be sufficiently osteogenic in many applications. It is often desirable to use an osteogenic material like demineralized bone matrix (DBM) to boost the bone forming potential of many bone graft substitutes [105, 106].

DBM has been termed an osteoinductive material based on its ability to induce endochondral bone formation when implanted in mesenchymal tissues that would otherwise not form bone [107, 108]. Reddi and his colleagues have demonstrated that when rat DBM is implanted in subcutaneously in rats, a series of events is initiated that follows a well defined time course, beginning with chondrogenesis and resulting in the formation of one or more ossicles consisting of a lamellar bone cortex with trabeculae extending

into a marrow cavity [109]. The specific components responsible for DBM-induced bone formation are not yet fully defined, but there appears to be a correlation between osteoinductivity and bone morphogenetic protein content [110]. The response tends to be more robust when rodent DBM is used in the same species of rodent, but it is clear that the osteoinductive property of DBM is conserved across species, based on studies in which the DBM is tested as a xenograft [111-116].

Commercial preparations of human DBM are assayed for their ability to induce bone formation as part of the production process. Because these are human-derived materials, they are tested in immunocompromised mice and rats [117-121]. In this assay, DBM granules are placed intramuscularly and then implanted tissue is examined histologically for evidence of endochondral ossification. Depending on the relative activity of the DBM preparation, one or more ossicles will form in association with the implant. Using this assay, we and others have shown that human DBM is osteoinductive but the degree of osteoinductivity may vary considerably for a number of reasons including donor age, as well as DBM processing and sterilization [122-124].

Host physiology can also affect the osteoinduction response to DBM. A number of studies have shown that aging can negatively impact the ability of DBM to induce bone formation [125-129]. Others have shown that treatment with pulsed electromagnetic fields can increase the amount of new bone produced in response to DBM [130-132]. Thus, both intrinsic and extrinsic factors play a role in the overall outcome. However, little is known about how estrogen deficiency typical of menopause affects induced osteogenesis, or if estrogen replacement might modify the effects of estrogen loss.

Estrogen is one of the major regulating factors responsible for bone formation and maintenance, and the loss of this hormone after menopause often leads to bone loss in women [133, 134]. Estrogen may affect osteoinduction in multiple ways. The hormone has direct effects on chondrocytes in the endochondral pathway [46, 47, 49], as well as on osteoblasts [135, 136]. Estrogen may also affect remodeling and ultimately resorption of the induced ossicles. It increases production of transforming growth factor beta-1 (TGF-β1) by T-cells [137], and reduces production of tumor necrosis factor alpha (TNF-α) [138]. This results in a decrease in osteoclast activity [139]. In the absence of estrogen, TNF-α is increased and bone resorption is stimulated [140, 141].

These observations suggest that human DBM-induced bone formation will be decreased in the absence of endogenous estrogen and that this reduction can be ameliorated by estrogen replacement. To test this hypothesis, we took advantage of the muscle pouch implantation assays typically performed using athymic mice or rats. In general, male animals have been used for osteoinductivity assays for reasons of cost and convenience. It is not known if immunocompromised female animals will respond to DBM as has been shown using male animals. In addition, although both mice and rats are used for qualitative scoring of osteoinductivity [119, 142-144], no studies have directly investigated whether both animal species respond to commercially available preparations of human DBM in a comparable manner using quantitative assessments of the same DBM samples.

The response of athymic mice and rats to ovariectomy adds a further level of complexity to the *in vivo* assay outcomes. Ovariectomy does not affect bone formation or increase bone turnover in athymic mice because these animals lack T-cells [145].

Athymic rats also have reduced levels of T-cells, but some T-cells persist [146]. This may be the reason why athymic rats, unlike athymic mice, exhibit ovariectomy-induced bone loss [147]. The initial event in DBM-induced bone formation at muscle sites is a transient inflammatory response that includes monocytes and macrophages [148], but it is not known what role these cells play in the osteoinduction process. The differences in T-cell populations in these two animal species suggests that the amount of bone formation may vary between the two animal species even in sham operated controls, and further differences will result after ovariectomy and estrogen replacement.

The overall goal of this study was to determine whether estrogen status affects the osteoinductivity of human DBM. The experiments were designed to test the hypothesis that estrogen loss due to ovariectomy results in reduced new bone formation and this can be restored by estrogen therapy. Because human DBM is a xenograft, it was necessary to test this hypothesis in an immunocompromised animal model but it was not known whether the response of athymic female mice to human DBM would differ from the response of athymic female rats. Accordingly, we examined human DBM osteoinductivity in both species.

MATERIALS AND METHODS

Selection of Host Animals

Twenty-four inbred albino female Nu/Nu mice (athymic mice) (Harlan, Indianapolis, IN) and twenty-four inbred albino female Nu/Nu rats (athymic rats) (Taconic, Germantown, NY) were used in this study. Athymic animals were chosen to minimize any immune response to the xenografts, as required by the Institutional Animal

Care and Use Committee (IACUC) at the Georgia Institute of Technology. Moreover, athymic animals are typically used by industry to assay osteoinduction ability of commercial preparations of human DBM for this reason. The athymic mice used were purchased at 5-6 weeks and acclimatized for three weeks prior to surgery. The mice underwent the surgical procedures when skeletally mature at 8 to 9 weeks of age. The athymic rats were purchased at 11 weeks of age and acclimatized for one week prior to surgery. At 12 weeks of age, when skeletally mature, the rats underwent the surgical procedures. These ages were selected based on information supplied by Harlan and Taconic.

Preparation of DBM Implants

Human DBM particles, prepared for human clinical use and ranging in size from 200-500 μm, were obtained as a generous gift from LifeNet, Inc. (Virginia Beach, VA). Previously, we used the athymic mouse muscle implantation assay to assess the bone induction ability of 27 batches of DBM from LifeNet [143], and from this assortment we selected a batch with high osteoinduction activity for the present study. The DBM particles were measured on weighing paper (10 mg for mice and 15 mg for rats) and transferred using a metal spatula to #5 gelatin capsules in order to facilitate their implantation. The difference in implant size was not based on animal weight but was done to reflect the use of larger DBM implants in rats compared to mice noted in the literature [119, 142, 144]. Because the gelatin capsules were not pre-sterilized and the weighing and packing of DBM was not performed under clean room conditions, all loaded capsules were sterilized by UV light overnight. We have repeatedly tested control

batches of the LifeNet DBM using this method of sterilization and it has been shown to not diminish the osteoinductive properties of DBM [119, 143].

Ovariectomy and Implant Procedures

All surgical procedures on an animal were performed at the same session under isoflurane inhalation anesthesia. Mice and rats were randomly assigned to one of three surgical groups: sham-operated controls (SHAM); ovariectomized (OVX); and ovariectomized plus 17β-estradiol (E_2) supplementation (OVX+E_2). All animals received DBM implants bilaterally in the gastrocnemius muscle of the hind limb as described below. This protocol was approved by the Institutional Animal Care and Use Committee at the Georgia Institute of Technology.

A dorsal approach was used to remove the ovaries as previously described [149]. For the implantation of DBM, small skin incisions were made over the calf region of each hind limb following disinfection, and a pouch was prepared in the muscle by blunt dissection [119]. One gelatin capsule was inserted into each pouch and the incision closed by clips.

In those animals receiving estrogen replacement, a slow release device (Innovative Research of America, Sarasota, FL) was implanted subcutaneously in the nuchal region of the back using the same incision used for the ovariectomy. A narrow path was made by blunt dissection of the subcutaneous tissue from the initial incision to the area of implantation. The slow release device was then inserted into the nuchal subcutaneous pocket uses forceps. The skin over the wound was then closed with clips, taking care not to pinch the implant. Each mouse was implanted with a 60 day release pellet containing 10 μg E_2 (0.17 μg/day), and each rat received a 60 day release pellet

containing 120 μg E_2 (2.0 μg/day). The dosage was based on the minimum dosage necessary to restore uterine weight to ovariectomized athymic mice [150], and then scaled up for the rats as a function of animal weight.

Pair Feeding of Animals

Rats and mice that have been ovariectomized tend to have increased appetites and gain weight. In order to eliminate weight gain as a confounding variable [151, 152], the animals in this study were pair fed. The consumption of food by the ovariectomized animals was metered by the intake of the sham-operated controls. The success of the pair feeding regimen was verified by weighing the animals at the time of surgery and then weekly thereafter.

Effectiveness of the Ovariectomy and Estrogen Replacement Regime

To verify the success of ovariectomy, estrogen levels were measured from blood samples collected at the time of euthanasia. At the ends of the two study periods (35 and 56 days), the animals were euthanized by thoracotomy under isoflurane anesthesia. This method of euthanasia facilitated the drawing of blood directly from the heart cavity sufficient for estrogen analysis. Estrogen levels in the blood samples were determined using an ultra-sensitive estradiol radioimmunoassay (RIA) kit (Diagnostic Systems Laboratories, Webster, TX). In addition, the uteri were removed by sharp dissection and weighed.

Histological Evaluation

Following euthanasia at 35 or 56 days, the whole of the calf region was excised to ensure complete recovery of the implant site and then fixed in 10% neutral buffered formalin. Histological processing was done at North American Science Associates

(NAMSA), Inc. (Northwood, OH). After decalcification in 5% formic acid, tissues were embedded in paraffin, sectioned and stained with hematoxylin and eosin. Three consecutive cross-sectional cuts (3-4 μm each) were made at three different levels of the limb (9 total sections per leg) to ensure visualization of the implant site.

One section from each implant was used for all analyses. To determine which section to use, all nine sections from each block were evaluated for the presence or absence of DBM particles, new bone and new cartilage, as described previously [119]. Briefly, the methods used were as follows. To ensure that any ossicles were due to DBM-induced bone formation and not because of osteoconduction due to approximation of DBM particles to host bone, the tibia and fibula were used as landmarks and only those sections in which ossicle formation was clearly not associated with either bone were considered for further analysis. From this subset, one section from each implant was chosen based on the amount of new bone and/or cartilage. Because the selected section was the one with the greatest amount of new bone and/or cartilage, the results were biased positively.

A qualitative score was used to indicate whether bone or cartilage induction had occurred and to provide an assessment of the number of ossicles that had formed. Each section was evaluated by two independent examiners and any differences between the examiners were resolved by a third examiner. Third party arbitration was required for 5 sections of the 864 sections examined, indicating a high intra-observer correlation. The qualitative scoring system for bone was based on the following parameters. When DBM was present but with no cartilage or bone induction, the value "1" was given. When an ossicle was observed, the score of "2" was given, and when 2 or more ossicles were

present, the value was "3". In sections with very osteoinductive implants, where 70% or more of the slide at 10X magnification was covered with one or more ossicles, a value of "4" was ascribed. Thus a section with a single large ossicle covering 70% or more of the field at a magnification of 10X would receive a score of 4, rather than a score of 2. While this is not a common finding, we have recorded a score of 4 for implants containing BMP-2 [153, 154].

There are no "ossicle equivalents" for cartilage, so the qualitative score for cartilage was determined by the number of cartilage sites in the selected section. When DBM was observed but no cartilage was present, a score of "1" was given. One cartilage site was scored "2", and two or more sites received a score of "3". In a section where 70% or more of the slide at 10X magnification was covered with cartilage, a value of "4" was assigned.

Quantitative measurements were made to provide an assessment of the amount of new bone and/or cartilage. Histomorphometric analyses were performed on the same histologic sections using a computerized analysis system (Image-Pro Plus, Media Cybernetics, Silver Springs, MD). Areas of the sections to be measured were captured at the appropriate magnification by a video camera. Calibration was performed according to the instructions accompanying the software. The following were measured using a stylus to outline each feature: ossicle area composed of the marrow space and surrounding cortex (DBM and new bone), marrow area, new bone area (distinct from DBM and limb bones), cartilage area, and the total area of residual DBM particles.

Statistical Analysis

The results of the qualitative and morphometric analyses were calculated as the means ± SEM for each variable. The values for all groups represented findings from 4 animals, each having two implants, providing a sample size of 8. Previous studies have shown the validity of treating each implant as a unit rather than each animal as a unit (2 sites/animal) [143]. Statistically significant differences between groups of the same species were determined by two-way ANOVA and the use of Bonferroni's modification of Student's t-test. For both statistical tests, P values ≤ 0.05 were considered significant. Power calculations showed that the power varied between 0.54 and 0.89, depending on the parameter being measured. A quantitative statistical comparison of interspecies results was not performed due to differences in the two animal species.

RESULTS

Evaluation of Pair Feeding, Ovariectomy and Estrogen Replacement

No animals were excluded from the study on clinical grounds after the study began. All animals healed normally following the surgical procedures and there was no evidence of infection.

OVX and OVX+E_2 mice grew at the same rate as the SHAM mice, demonstrating the pair-feeding regimen was successful (Figure 4.1A). However, the OVX mice did have a statistically significant decrease in weight at 1 week that was not seen in the SHAM or OVX+E_2. OVX rats grew at a slightly greater rate than SHAM rats; however, the increase was only statistically significant at 6 weeks (Figure 4.1B). The growth of OVX+E_2 rats was significantly inhibited from 3 to 6 weeks post-surgery, but eventually recovered at 7 weeks to that of the SHAM controls.

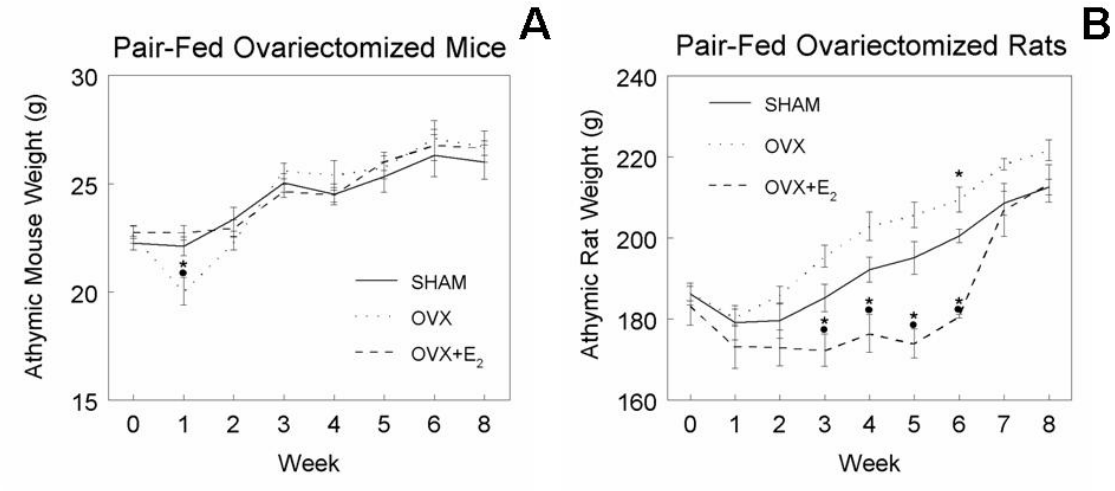

Figure 4.1: Analysis of pair feeding regimen

The success of the pair feeding regimen was verified by weighing the animals at the time of surgery and then weekly thereafter. The consumption of food by the ovariectomized (OVX and OVX+E_2) animals was metered by the intake of the sham-operated (SHAM) animals. **(A)** Mice; **(B)** Rats. Values are means ± SEM for N = 8 mice per group through 5 weeks (35 days) and N = 4 mice for weeks 6 to 8 (56 days total). *P < 0.05, SHAM vs. treatment. ●P< 0.05, OVX vs. OVX+E_2.

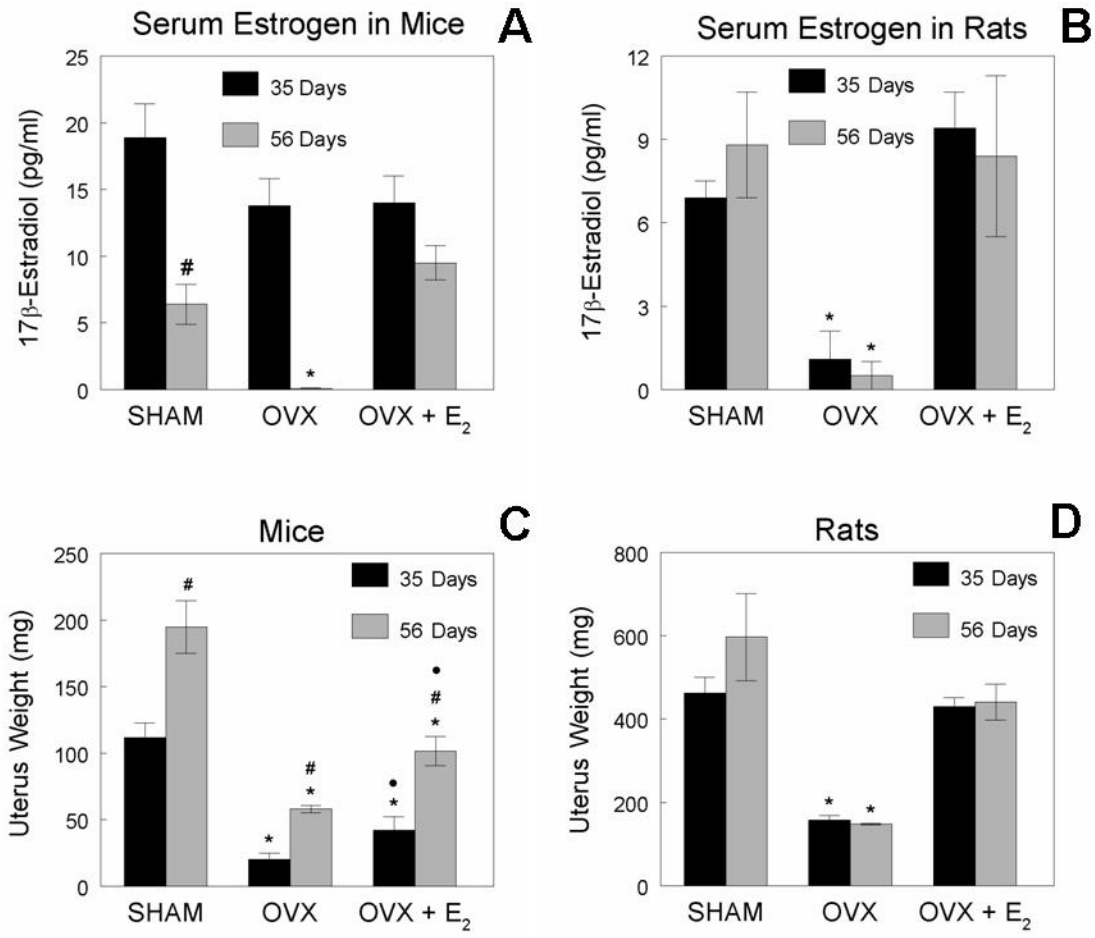

Figure 4.2: Analysis of ovariectomy effectiveness

The effectiveness of bilateral ovariectomy (OVX) on athymic mice and rats was determined by blood serum estrogen levels and uterine weight at 35 days and 56 days post surgery. Sham-operated animals (SHAM) and ovariectomized animals with 17β-estradiol supplementation (OVX+E_2) were used as controls. Blood serum estrogen levels were determined using a radioimmunoassay kit. **(A)** Athymic mice in the SHAM and OVX groups showed lower estrogen levels at 56 days than 35 days. OVX resulted in a decrease in serum estrogen at 56 days but not 35 days. **(B)** Athymic rats did not show a difference in estrogen levels over time and the OVX groups demonstrated a significant decrease in estrogen levels at both time points. **(C)** Athymic mice showed a significant increase in uterus weight from 35 days to 56 days in all experimental groups. OVX caused a decrease in weight that was partially restored with estrogen. **(D)** Uterus weight in the athymic rat was stable over time. OVX resulted in a significant decrease that was restored with estrogen. Values are the mean ± S.E.M of four animals. *$P < 0.05$, SHAM vs. treatment. #$P < 0.05$, 35 days vs. 56 days. ●$P < 0.05$, OVX vs. OVX+E_2.

OVX mice had reduced levels of serum estrogen at 35 days in comparison to control animals, but this was not statistically significant and no effect of estrogen replacement was evident (Figure 4.2A). At 56 days, no systemic estrogen could be detected in the OVX mice and estrogen treatment restored the hormone to levels measured in the sham-operated mice. In addition, systemic estrogen levels decreased with time in the mice. Ovariectomy of athymic rats reduced serum estrogen levels by more than 80% within the first 35 days (Figure 4.2B). Estrogen replacement restored levels of the hormone to those seen in the sham-operated animals.

Uterine weight doubled between 35 and 56 days in all mouse treatment groups (Figure 4.2C). Uterine weight in the ovariectomized animals was 75% less than in the sham operated controls and this difference was maintained over time. Estrogen treatment increased uterine weight by 100% in comparison to the OVX mice that did not receive the hormone, but the weight of the uterus was not equivalent to that of sham-operated mice, even at 56 days. Unlike the mice, there was no age-related change in uterine weight in the rats (Figure 4.2D). Uterine weight in the ovariectomized rats was more than 50% lower than in sham-operated rats, and treatment with estrogen restored uterine weight to that seen in the sham-operated controls. The changes in uterine weight correlated with changes in systemic estrogen.

Histological Evaluation of Osteoinduction

All implant sites exhibited DBM at the time of harvest. Histological evaluation of the DBM-implanted tissues demonstrated differences in the response between the two animal species (Figure 4.3). The athymic mouse exhibited the typical structure of large

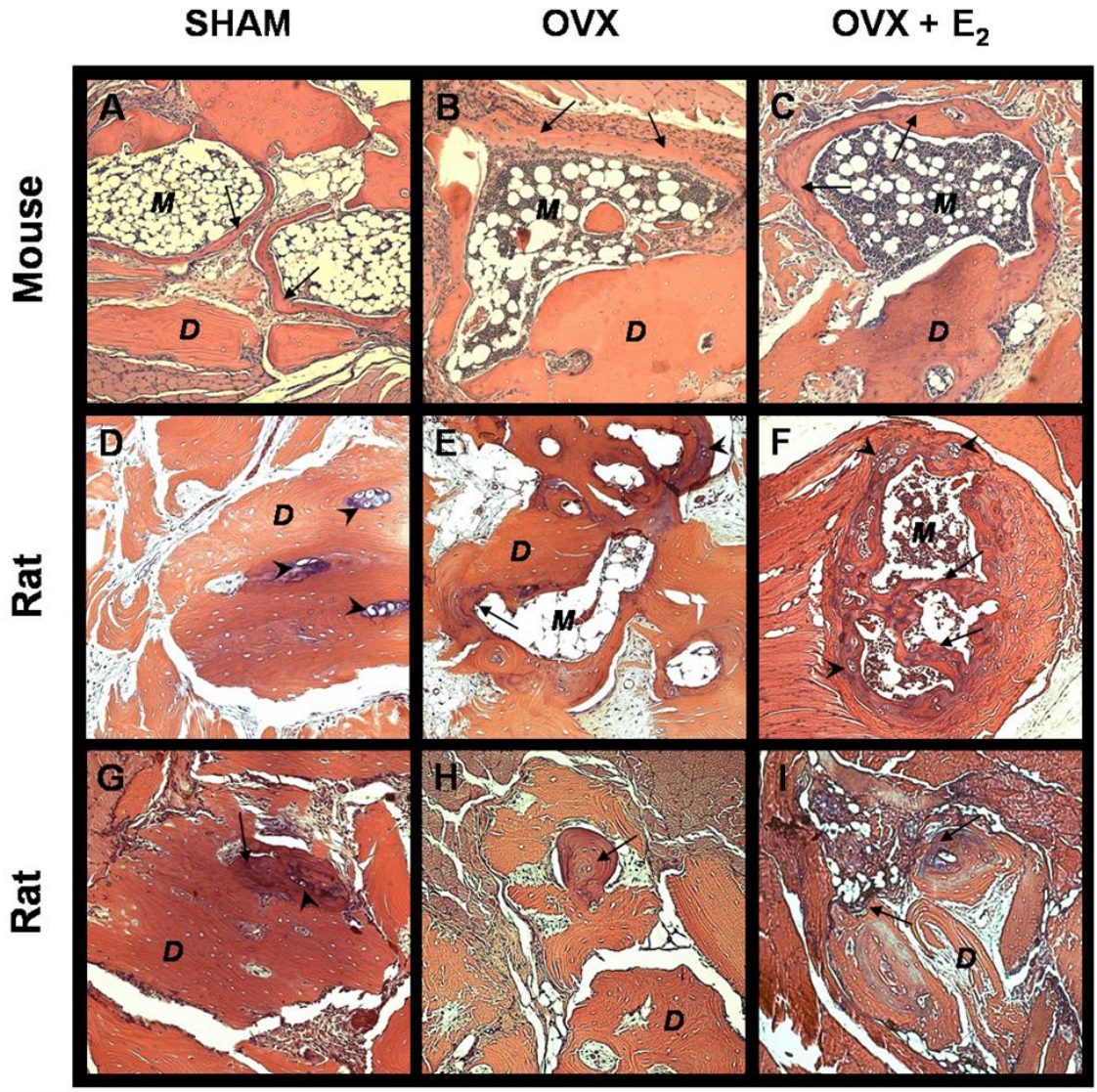

Figure 4.3: Histological evaluation of DBM induced endochondral ossification

The effects of estrogen on the osteoinductive properties of human demineralized bone matrix (DBM) at 35 days and 56 days were determined using a rodent muscle implant model. Athymic mice and rats were ovariectomized (OVX) and DBM was implanted in the hind gastrocnemius muscle. Sham-operated animals (SHAM) and ovariectomized animals with 17β-estradiol supplementation (OVX+E_2) were used as controls. The hind limbs were dissected, decalcified, sectioned and stained with hematoxylin and eosin. Images shown are from samples harvested at 56 days. **(A)** Athymic mice showed large ossicles composed of a marrow cavity (*M*) surrounded by DBM particles (*D*) and new bone (*arrow*). **(B, C)** Estrogen levels did not affect the general appearance of the ossicles in athymic mice. Osteoinduction in athymic rats was more variable than the mice. **(D)** Cartilage (*arrowhead*) formation could be seen within the DBM without the formation of ossicles. **(G, H)** Large nodules of new bone attached to DBM were also noted. **(E, F, I)** When ossicles did form they were usually smaller in size compared to the mice and were surrounded by a mixture of cartilage and new bone.

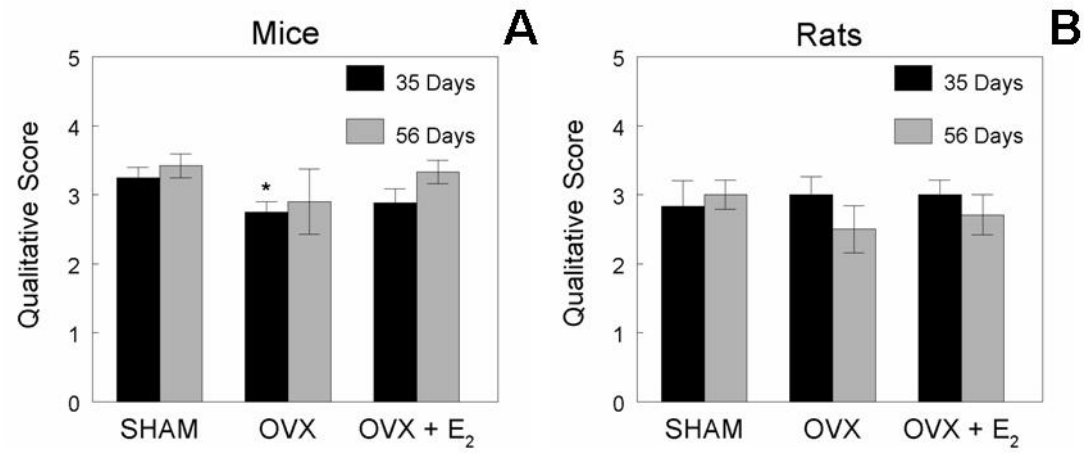

Figure 4.4: Assessment of osteoinduction using a qualitative scoring system

Osteoinduction in ovariectomized (OVX) athymic mice and rats at 35 days and 56 days was measured using the following qualitative scoring system. DBM without bone or cartilage was given a value of "1". When an ossicle was observed, the score of "2" was given, and when 2 or more ossicles were present, the value was "3". Implants where 70% or more of the slide at 10X magnification was covered with ossicles were given a value of "4". Sham-operated animals (SHAM) and ovariectomized animals with 17β-estradiol supplementation (OVX+E_2) were used as controls. **(A, B)** All experimental groups for both animal species showed significant osteoinduction. There was a small decrease detected in athymic mice compared to controls in the OVX group at 35 days. Values are the mean ± S.E.M of eight implants. *$P < 0.05$, SHAM vs. treatment.

ossicles filled with bone marrow surrounded by a combination of implanted DBM and new bone (Figure 4.3A). This general appearance was independent of the estrogen status of the mouse (Figure 4.3B and 4.3C). The athymic rat produced much more variable results. In some cases small amounts of new cartilage formed within the DBM particle mass without the presence of new bone or a marrow cavity (Figure 4.3D). In other cases large nodules of new bone could be found connected to the DBM particles without the formation of an ossicle (Figure 4.3G and 4.3H). When ossicles did form they were smaller compared to the athymic mouse and were usually surrounded by a mixture of new bone and cartilage (Figure 4.3E, 4.3F, and 4.3I). The presence of cartilage or the formation of ossicles in the athymic rat did not appear to be correlated with the estrogen status of the animal.

Qualitative assessment of osteoinductivity was similar regarding the two different species (Figure 4.4). The osteoinductivity index was higher in the sham-operated mice than in the rats, but in both cases the score was not statistically different from 3. Ovariectomy resulted in a small but significant decrease in osteoinductivity at 35 days in the mice, but this decrease was no longer evident at 56 days, and estrogen replacement prevented the decrease at the early time point (Figure 4.4A). The qualitative assessment of osteoinductivity in the rat indicated that neither ovariectomy nor estrogen treatment altered the number of sites of bone formation (Figure 4.4B).

While the number of bone formation sites was relatively unaffected by ovariectomy, ovariectomy did alter the kinetics of bone formation and this was species specific (Figure 4.5). New bone area was significantly lower in OVX mice at both 35

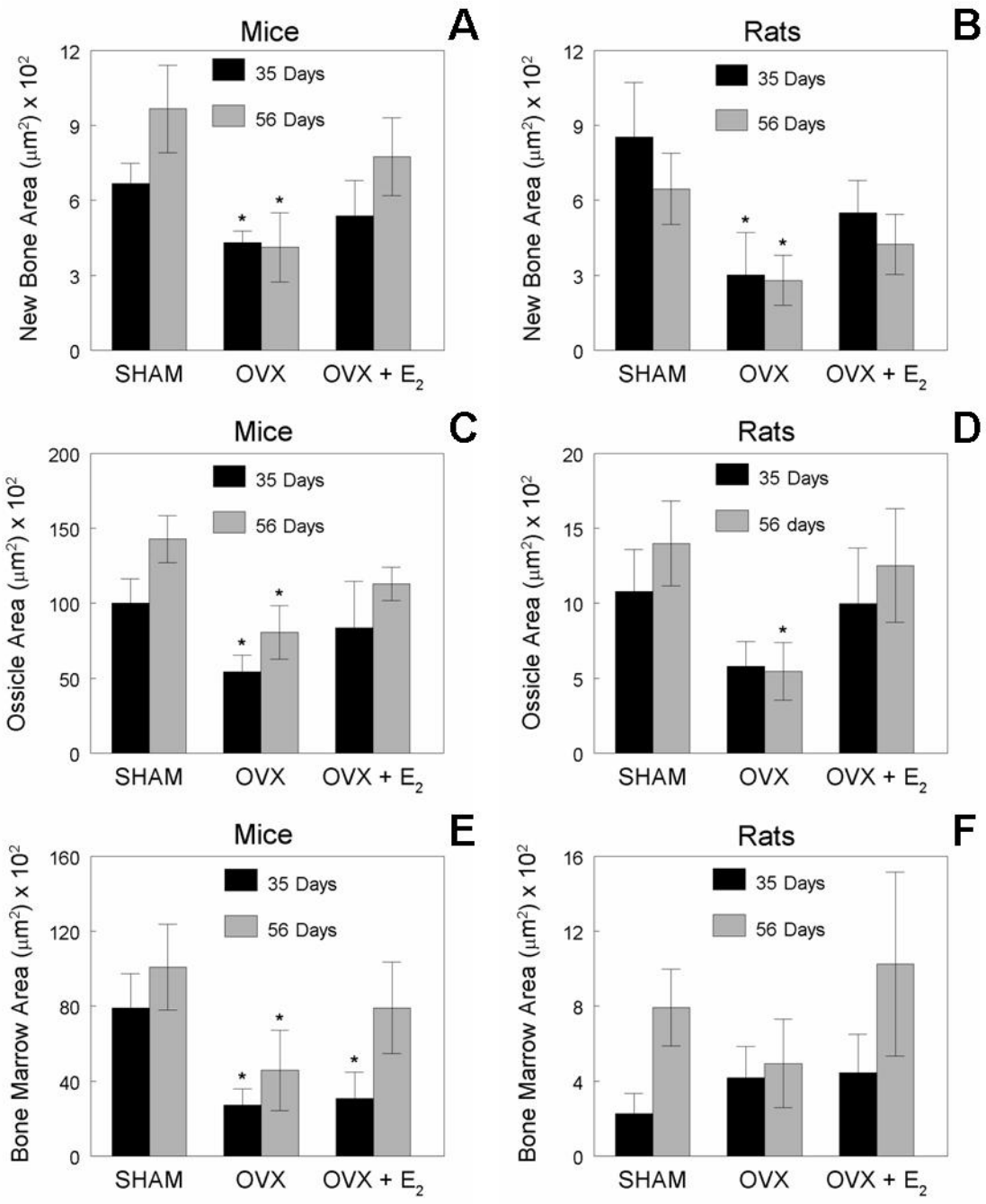

Figure 4.5: Quantitative assessment of osteoinduction using histomorphometry

Osteoinduction in ovariectomized (OVX) athymic mice and rats at 35 days and 56 days was measured quantitatively by morphometric analysis of new bone area, ossicle area, and bone marrow area. Sham-operated animals (SHAM) and ovariectomized animals with 17β-estradiol supplementation (OVX+E_2) were used as controls. **(A)** OVX resulted in a decrease in new bone formation in athymic mice and was restored by estrogen treatment. **(B)** A similar response was seen in the OVX athymic rats. **(C, D)** Ossicle area also decreased with OVX in both species, although this was not significant at 35 days for the rats. **(E)** Bone marrow area was significantly decreased in the athymic

(Figure 4.5 continued) mouse after OVX and was only restored after 56 days of estrogen replacement. **(F)** The rats did not show any change in bone marrow area with estrogen status. Values are the mean ± S.E.M of eight implants. *P < 0.05, SHAM vs. treatment.

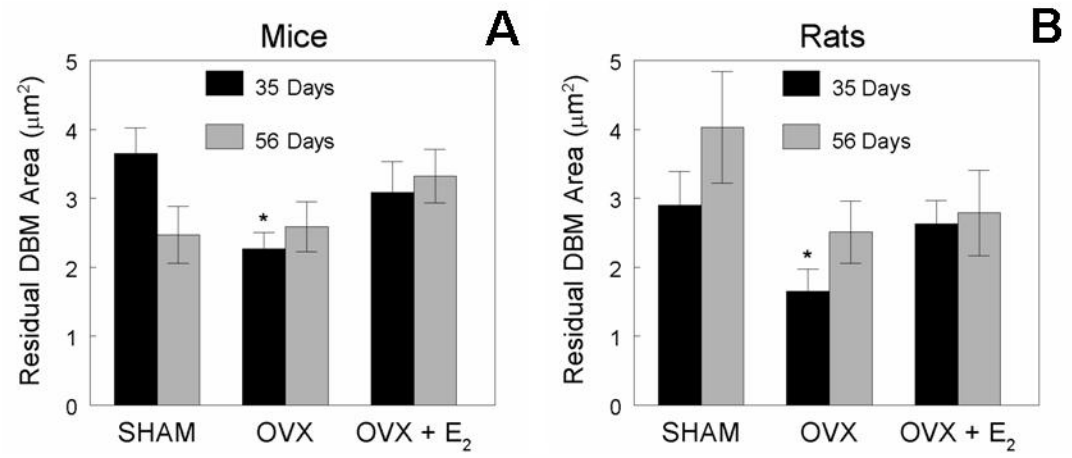

Figure 4.6: Analysis of DBM resorption

Residual DBM area was measured in ovariectomized (OVX) athymic mice and rats with muscle implants. Sham-operated animals (SHAM) and ovariectomized animals with 17β-estradiol supplementation (OVX+E_2) were used as controls. **(A, B)** Residual DBM particles were seen in all implants at both time points. OVX caused a small resorption of DBM in both species. Values are the mean ± S.E.M of eight implants. *P < 0.05, SHAM vs. treatment.

and 56 days (Figure 4.5A). The ossicle size was approximately 50% lower in OVX mice at 35 days and this persisted in the OVX animals even though there was a further increase in ossicle size in the sham-operated animals (Figure 4.5C). Estrogen replacement resulted in greater ossicle area but there was considerable variability among the mice that precluded demonstration of statistical significance. The marrow space was also less in the OVX mice compared to sham-operated animals (Figure 4.5E). Estrogen did not alter this at 35 days, but at 56 days, the size of the marrow cavity within the ossicle was comparable to that of sham-operated controls.

New bone area in the ovariectomized rats was less than 50% of the new bone area in sham-operated animals. Estrogen replacement increased new bone formation but the levels achieved were not as great as in the sham-operated rats (Figure 4.5B). OVX rats also had 50% less ossicle area at 35 days, and this effect was maintained at 56 days (Figure 4.5D). Estrogen treatment restored ossicle area to that of sham-operated control rats. Unlike the OVX mice, there was no time-dependent change in the size of the marrow cavity in OVX rats (Figure 4.5F). In addition, ovariectomy and estrogen did not significantly affect the marrow area in the athymic rat.

The amount of residual DBM was similar in both animal species. Ovariectomized mice had a small but statistically significant reduction in the amount of residual DBM (Figure 4.6A), as did ovariectomized rats (Figure 4.6B). Estrogen replacement prevented this loss in both species.

Although DBM acts via endochondral ossification, evidence of cartilage was found only in the rat implants. Ovariectomy had no effect on the number of cartilage sites at either time point, whether the animals were treated with estrogen or not (Figure

4.7A). In addition, it was not possible to demonstrate statistically significant differences in new cartilage area due the high variability of the sample population, although the trend would suggest ovariectomy in rats may result in increased cartilage formation in response to DBM (Figure 4.7B). Because delayed cartilage formation or chondroclasis had not been anticipated, the study was not designed with sufficient power to assess statistically significant differences in these parameters.

DISCUSSION

It is known that estrogen regulates normal bone growth and development; this study demonstrated for rats and mice that it also regulates endochondral bone formation stimulated by an osteoinductive agent, human DBM. As noted previously for rat DBM implanted in ovariectomized rats [155], the number of sites of human DBM-induced new bone formation was not significantly affected by estrogen loss. However, measurement of ossicle area showed that the ossicles in estrogen deficient animals were smaller than in sham-operated control animals. Moreover, the present study demonstrated that this reduction in size could be prevented in part by estrogen replacement. These observations indicate that estrogen regulated bone growth and not the initial osteoinduction event per se.

This study is the first to examine the response of athymic mice and rats to the same commercial preparation of human DBM. Athymic mice and rats are frequently used to test xenogeneic materials because of their compromised immune systems, but they are very different with respect to the nature of their T-cell impairment. Although the

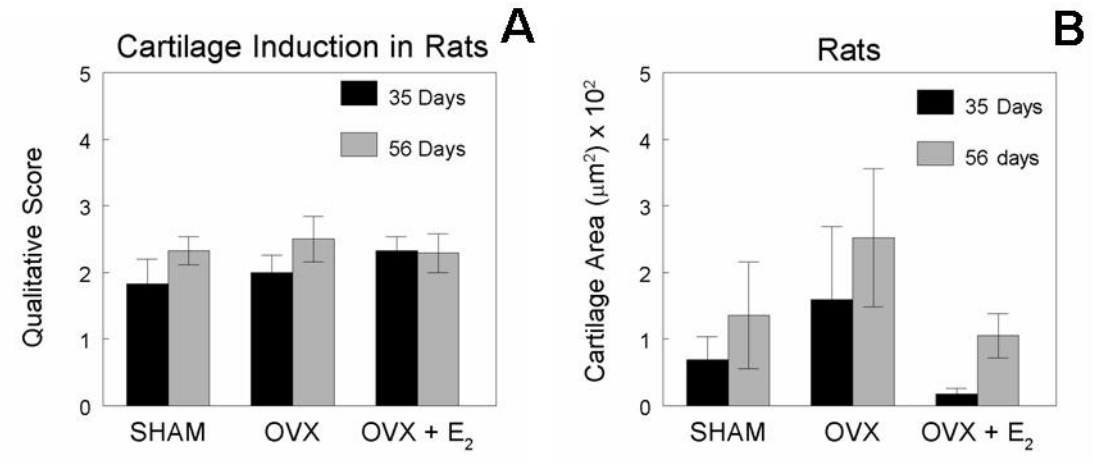

Figure 4.7: Assessment of DBM induced chondrogenesis

Cartilage induction in ovariectomized (OVX) athymic rats at 35 days and 56 days was measured using the following qualitative scoring system. When DBM was observed but no cartilage was present, a score of "1" was given. One cartilage site was scored "2", and two or more sites received a score of "3". In a section where 70% or more of the slide at 10X magnification was covered with cartilage, a value of "4" was assigned. Sham-operated rats (SHAM) and ovariectomized rats with 17β-estradiol supplementation (OVX+E_2) were used as controls. **(A)** All experimental groups for both animal species showed significant cartilage formation but there was no difference detected due to OVX. **(B)** Quantitative morphometric analysis of the cartilage area also did not show any significant differences between the experimental groups. Values are the mean ± S.E.M of eight implants.

difference in DBM dose and body size precludes a direct comparison between these two inbred animal species, the results show that human DBM is capable of initiating new bone formation in ectopic muscles sites of both species, but the nature of the response appears to be species dependent. We observed classic ossicles in the mouse, characterized by a well defined marrow space surrounded by cortical bone. In contrast, bone induction in the rat was characterized by new bone linking adjacent DBM particles, and only infrequently were well defined ossicles present.

Differences were also noted with respect to the rate of osteoinduction. Ossicle size increased in the mouse with time in all treatment groups, suggesting the possibility that osteoinduction may have been influenced by factors associated with normal animal growth, even after skeletal maturity. Given that no cartilage was evident in the mouse ossicles, we have concluded that the increase was due to direct apposition of bone. In contrast, rat ossicle size did not change with time, although the rats increased in weight. Moreover, even at 56 days post-implantation, DBM-induced cartilage persisted in the OVX rats, suggesting that endochondral ossification was at a slower rate. Estrogen stimulates the differentiation of growth plate chondrocytes *in vitro* and *in vivo* [44, 156-158], supporting the hypothesis that the presence of cartilage at 56 days in the OVX rats was a consequence of delayed endochondral maturation.

We attempted to control for differences in age of the animals by using mice and rats at the time they become skeletally mature, based on information supplied by Harlan and Taconic. It is possible that the differences we observed reflected differences in sexual and skeletal maturity, but it is also likely that species differences played a role.

We suggest that results from an assay in one animal species can be compared to another only with caution.

Reduction in uterine weight and serum estrogen levels in the OVX animals indicated that the surgical procedure was successful. Similarly, restoration of uterine weight and serum estrogen in the animals implanted with slow release estrogen capsules show that estrogen replacement therapy was effective. There were some differences in the two species, however, that may have impacted the results. In the mice, serum estrogen was not reduced at 35 days, suggesting that although the ovaries were excised, other sources of estrogen were available. This may also explain the increase in ossicle area and marrow space observed in the mice. By 56 days, serum estrogen was depleted in the OVX mice and this corresponded with a decrease in uterine weight.

Growth of the OVX+E_2 rats was delayed despite the pair feeding regimen. Because the OVX rats grew at the same rate as the SHAM controls, the growth suppression in the OVX+E_2 rats must have been related to the E_2-supplementation. The fact that serum E_2 at harvest was restored to normal levels in these animals suggests that the time release implants were functional. However, E_2 levels were not measured at times prior to harvest, so we were not able to determine if E_2 release was linear or if serum E_2 was comparable to SHAM control levels at earlier time points. Another possibility is trauma due to the additional surgical procedures. How or if this reduced growth impacted the osteoinduction response of to DBM is not known. The OVX mice had a small decrease in weight at 1 week. The reduced hormone levels may have resulted in a greater difficulty in recovering from the surgical-induced stress.

Our observations implicate differences in the T-cell defect that is expressed by the athymic mice and rats used in this study. The complex biological relationship between estrogen, the immune system, and bone has been well studied in rodent models. Estrogen has been shown to decrease osteoclast formation [140, 141] and increase osteoclast apoptosis [139]. It is believed that estrogen regulates osteoclast function via T-cells. Estrogen deficiency induces bone loss by enhancing T-cell production of TNF-α [138] and estrogen prevents bone loss through TGF-β signaling in T-cells [137]. Athymic mice, which lack functional T-cells, do not exhibit ovariectomy-induced bone loss. However, differences in the skeletal physiology of euthymic and athymic mice have been demonstrated [124], suggesting that bone formation is also regulated via T-cell dependent mechanisms. For instance, athymic mice have lower serum calcium and alkaline phosphatase, greater femur density, and a lower percent ash weight of dry bone compared to euthymic mice. This modified skeletal physiology characterized by a lack of T-cells could, therefore, influence bone formation as a result of induction by DBM. The importance of the immune system in bone homeostasis has also been shown in rats. The administration of an immunosuppressant, cyclosporine A, induced rapid bone loss [159]. Moreover, ovariectomy of athymic rats has been shown to result in loss of trabecular bone volume and trabecular area after 2 weeks [147] due in part to the fact that functional T-cells are still present, although reduced in number [146].

These observations indicate that there are important differences between the two animal species that could impact osteogenesis induced by DBM. We were not able to compare the response of athymic animals with that of euthymic animals because human DBM was considered to be a xenograft, and for this reason we could not directly address

the role of T-cells in the osteoinduction process. However, the present study confirms that there are differences in how the two animal species respond to an osteoinductive stimulus, suggesting that T-cells play a role. The fact that human DBM-induced osteogenesis in male athymic mice produces results comparable to those seen in SHAM female mice for both qualitative and quantitative measurements [119], further supports the interpretation that the difference in the two species is T-cell related, and not due to a sex-specific characteristic unique to females.

In summary, this study clearly demonstrates that estrogen is important for induced osteogenesis. Ovariectomy reduced, but did not completely block, osteoinduction by human DBM in both animal species, and estrogen replacement was able to restore the osteoinductive properties of human DBM. It is important to emphasize that the effects of ovariectomy and estrogen on ectopic endochondral bone formation were not evident when using a qualitative scoring system, either in the present study using human DBM or in previous reports using rat DBM in ovariectomized rats [155]. Quantitative measurements were needed to show the decreased osteogenesis present in the ovariectomized animals. The qualitative score provides information on the number of sites of new bone formation, and if any sites are particularly large, whereas histomorphometric measurements of the tissues indicates whether differences in ossicle size are due to differences in the marrow cavity or amount of new bone. Thus, both parameters are valuable tools for assessing osteoinductivity and qualitative methods alone may be inadequate as a method for discriminating between the relative effectiveness of materials like human DBM.

This study also shows that there are species differences that can impact the results obtained when testing the osteoinduction ability of human DBM preparations, indicating

the need to independently validate each animal species. Regardless of animal species, however, our results demonstrate that estrogen sufficiency is an important variable for the success use of human DBM as an osteoinductive agent in musculoskeletal therapies. The present study did not address the use of human DBM in orthotopic sites, or if estrogen replacement can improve clinical outcomes [160-162], although the results suggest that this may be the case. Further research is required to determine the role of estrogen in human DBM-induced osteogenesis and to develop optimal therapies for musculoskeletal pathologies in patients with altered hormone levels like post-menopausal women.

CHAPTER 5

Rat Growth Plate Chondrocytes Maintain their Phenotype when Microencapsulated in Alginate using High Electrostatic Potential

INTRODUCTION

It is estimated that 37% of children will sustain a fracture during their childhood [163] with 15-30% of those injuries involving the growth plate [164]. Of these injuries, over 1% are severe enough to completely arrest limb growth and can lead to significant disability for the lifetime of the child [165]. A tissue engineered product could be beneficial for these patients as well as others affected by various osteochondrodysplasias.

Cartilage tissue engineering has been difficult due to the propensity of chondrocytes to undergo a process referred to as "dedifferentiation" when expanded in monolayer cultures. The lack of a three-dimensional matrix results in the chondrocytes expressing a fibroblastic phenotype and the down-regulation of cartilage specific processes [50, 90, 166]. It is believed the dedifferentiation process is a result of actin stress fibers that form during attachment and spreading of the cells to a two dimensional surface [52-55]. Although cells in the resting zone of the rat growth plate are surrounded with an extracellular matrix similar to articular cartilage, less is known about the dedifferentiation process in these cells. This is particularly true for costochondral chondrocytes, which have been shown to retain many of their *in vivo* properties through several passages in monolayer culture [167].

It has been well established that three dimensional encapsulation of chondrocytes in hydrogels can reverse the dedifferentiation process by maintaining the rounded morphology of the cell [56, 57]. It is theorized that encapsulation of chondrocytes changes the mechanical stresses on the cell to those seen *in vivo* and promotes the expression of cartilage specific matrix molecules. Alginate has been one of the more commonly used hydrogels for encapsulation due to its inherent physical and chemical properties. The linear polysaccharide chains of mannuronate and guluronate rapidly cross link in the presence of divalent cations such as Ca^{2+} to form a solid gel and entrap the chondrocytes. A chelating agent can then be added to break down the alginate matrix and release the cells and extracellular components. Alginate encapsulation has been shown by several research groups to effectively reestablish a chondrocytic phenotype in a variety of dedifferentiated *in vitro* chondrocyte cultures including bovine [60, 168], rabbit [62], and human [59, 63, 64] articular chondrocytes. However, there has been limited research on the encapsulation of growth plate chondrocytes.

It has been shown that growth plate chondrocytes can be cultured in alginate beads for up to one year [169]. During this time the cells produce cartilage specific matrix and undergo apoptosis, which is part of the normal behavior for growth plate chondrocytes and necessary for endochondral bone formation. Alginate encapsulated growth plate chondrocytes have also been shown to proliferate in response to growth factor supplementation [170] and this growth can be directed by creating microchannels within the alginate to mimic *in situ* organization of the tissue [171].

The growth plate provides a challenging engineering problem due to the variable and complex anatomical geometry of the tissue. High electrostatic potentials can be used

to reduce alginate bead size by disrupting the surface tension of the alginate droplets [70, 75]. The beads produced are up to one hundred times smaller in volume than those produced using other disruption methods. Beads of this size may allow minimally invasive injectable cell therapies that are capable of filling a range of both growth plate and articular defects. The smaller bead size could reduce mass transfer limitations [172], a common problem among larger tissue engineered constructs that can lead to necrotic cores. Moreover, the biocompatibility of alginate implants has been shown to be improved by decreasing bead size [74, 173].

It is not known, however, what consequences the exposure to high electrostatic potential may have on chondrocyte viability and phenotypic expression. Electrostatic alginate encapsulation of cells has been limited mostly to hybridomas [174] or pancreatic islets [175-177]. Some recent work has been done with mesenchymal stem cells [178], but this study did not characterize how the high electrostatic encapsulation process impacted the phenotype of the cells; instead it focused on the effects of cell density and alginate concentration on bead morphometry. Therefore, the goal of this study was to develop a method for microencapsulating growth plate chondrocytes in alginate using high electrostatic potentials and characterize the effects of the encapsulation process on the phenotype of the cells.

MATERIALS AND METHODS

Rat Resting Zone Growth Plate Chondrocyte Harvest and Culture

Costochondral resting zone growth plate chondrocytes (RC) were isolated from the ribs of 125g male Sprague-Dawley rats (Harlan, Indianapolis, IN). The resting zone

cartilage of the rib growth plates was cut into small pieces, washed, and then digested with collagenase. The digested suspension was passed though a 40μm mesh sieve and centrifuged at 2000 rpm for 10 minutes. The supernatant was removed and the chondrocytes resuspended in full media containing Dulbecco's Modified Eagle's Medium (DMEM), 10% fetal bovine serum (FBS), 1% penicillin/streptomycin, and 50 μg/ml L-ascorbic acid. Isolated primary chondrocytes were plated on T75 flasks, grown to confluence, and passaged using 0.25% trypsin-1mM ethylenediamine tetraacetic acid (EDTA). Fourth passage RC cells were used for all experiments.

Alginate Encapsulation and Optimization

Ultrapure alginates (NovaMatrix, Drammen, Norway) were used to microencapsulate RC cells using a Nisco Encapsulator VAR V1 LIN-0043 (Nisco Engineering AG, Zurich, Switzerland). Four different alginate compositions (Table 5.1) were used to investigate the role of molecular weight and monomer content on the encapsulation process and cellular phenotype. Each alginate powder was sterilized using UV light and dissolved in 0.9% phosphate buffered saline (PBS) to produce a 2% (w/v) alginate solution. RC cells were suspended in a minimum volume of PBS and added to the alginate solution resulting in $6x10^6$ cells/ml (low density) or $50x10^6$ cells/ml (high density). The solution was then extruded through a 0.18mm (inner diameter) needle at 10 ml/hr into a gelation solution consisting of 50 mM $CaCl_2$ plus 150 mM glucose. A 6 kV electrostatic potential between the gelation solution and needle was used to overcome the surface tension.

Morphometric and viability analyses were performed on microbeads of all four alginate compositions (LVM, LVG, MVM, and MVG). LVM alginate has faster

degradation kinetics as a result of lower molecular weight and decreased cross-linking due to low guluronate content. Tissue formation has been shown to be enhanced by more rapid degradation of the alginate [179, 180]. For these reasons, LVM alginate was selected for additional experiments including mRNA measurement, light and electron microscopy, and *in vivo* implantation.

Microbead Morphometrics

Morphometric analysis of low density ($6x10^6$ cells/ml) microbeads of all four alginate compositions (LVM, LVG, MVM, and MVG) was performed using a computerized analysis system (Image-Pro Plus, Media Cybernetics, Silver Springs, MD). Areas of the sections to be measured were captured at the 10x magnification by a video camera. Calibration was performed according to the instructions accompanying the software. The cross sectional area and cell number were measured. The average bead diameter was then calculated from the cross sectional area.

Viability

Viability of RC cells seeded at low density ($6x10^6$ cells/ml) in all four alginate compositions was measured using fluorescent confocal microscopy and a calcein/ethidium homodimer-1 stain (Molecular Probes, Eugene, OR). Alginate encapsulated chondrocytes were cultured for 0, 1, or 2 weeks. Culture medium was removed and the beads washed with PBS containing 1mM $CaCl_2$ to maintain bead integrity. The samples were then incubated for 30 minutes in a PBS solution containing 1 mM $CaCl_2$, 4 μM ethidium homodimer-1, and 2 μM calcein. Images were obtained using a LSM 510 confocal microscope (Carl Zeiss MicroImaging Inc., Thornwood, NY). Viability was also measured for high density ($50x10^6$ cells/ml) LVM microbeads

Table 5.1: Alginate Compositions

	Guluronate Content (%)	Molecular Weight (g/mole)
LVG	66	170,000
LVM	44	130,000
MVG	69	240,000
MVM	43	220,000

Table 5.2: RT-PCR Primers for Fourth Passage Rat Growth Plate Chondrocytes

	Sense Primer	Anti-Sense Primer	Anneal Temp.	Product
Aggrecan	5'-CTC TGG CGA CCT TGA CTC-3'	5'-TGA CAT CCT CTA CAC CTG AAG-3'	58 °C	538 bp
Collagen 1	5'-GTC AGG CTG GTG TGA TGG GA-3'	5'-AAC CTC TCT CGC CTC TTG CT-3'	60 °C	318 bp
Collagen 2	5'-GCG GAG ACT ACT GGA TTG-3'	5'-AGT GGT AGG TGA TGT TCT G-3'	55 °C	293 bp
SOX-9	5'-TGT GAA CTG GTA GAT CTG GT-3'	5'-AAG AAG TGG AAT AAG TGG GCT-3'	60 °C	292 bp

PCR Analysis

After 0, 1, 3, 5, 7, or 14 days in culture, low density LVM microbeads were washed with saline and the alginate dissolved using 75 mM sodium citrate. The samples were centrifuged to pellet the cells and the alginate removed. RNA was extracted using the Qiagen miniprep kit (Qiagen, Valencia, CA) and quantified by UV spectroscopy. Reverse transcription PCR (RT-PCR) was used to assess expression of collagen type I, collagen type II, aggrecan, and the chondrocyte transcription factor, SRY-box containing gene (SOX-9). RT-PCR was performed on confluent monolayer cultures as a control, and RNA extracted from rat native growth plate cartilage tissue or human lymphocytes were used as positive or negative controls, respectively, to verify the specificity of the primers. RT-PCR primer information is summarized in Table 5.2.

The total RNA sample from each sample was reverse transcribed using the First-strand cDNA Synthesis Kit (Amersham-Biosciences, Piscataway, NJ) and the specific anti-sense primer for each mRNA of interest. The cDNA was amplified using the Fisher PCR kit (Fisher Scientific International, Hampton, NH) and the specific sense and anti-sense primers. PCR conditions for each cycle included a 30 second denaturation at 94 ^{o}C, a 60 second annealing at 50-65 ^{o}C depending on the primer used, and a 30 second extension at 72 ^{o}C. The PCR-amplified products were run on 5% polyacrylamide gels using a buffer consisting of 0.9 M Trizma® base (tris[hydroxymethyl]aminomethane), 0.9 M boric acid, and 20 mM EDTA.

In vitro Histology and Transmission Electron Microscopy

High density ($50x10^6$ cells/ml) LVM alginate microbeads were used for microscopy analysis to maximize the number of cells visible per section. The microbeads

were cultured for 2 weeks, fixed with 2.5% gluteraldehyde in 0.1 M cacodylate buffer, embedded in polyacrylate resin, and sectioned. General cell appearance and matrix deposition were assessed using toluidine blue and safranin-O stained sections (Winship Cancer Institute Pathology Core Lab, Atlanta, GA). Ultrathin sections were examined by TEM to evaluate the subcellular structure of microencapsulated cells (Emory School of Medicine Microscopy Core, Atlanta, GA).

Glycosaminoglycan Quantification

The production of proteoglycans was measured in monolayer and alginate microbead cultures. RC cells were either cultured as monolayers in 6-well plates or in low cell density LVM microbeads. Both monolayer and microbead samples contained approximately 500,000 cells. At 3, 5, 7, 10, 12, and 14 days post-confluence or post-encapsulation, the culture media was exchanged and the amount of free glycosaminoglcyans (GAGs) quantified using 1,9-dimethylene blue (DMMB) dye. Monolayer and microbead samples were also harvested at 1 and 2 weeks and the total accumulated GAGs quantified. Monolayer samples were harvested using trypsin and microbead samples were harvested by dissolution in 75 mM NaCitrate.

The DMMB dye solution was prepared by mixing 16 mg of DMMB with 5 ml of 100% ethanol. The dissolved DMMB was then added to a 950 ml solution containing 40.5 mM glycine and 40.5 mM NaCl. The pH was adjusted to 1.5 using 1 M HCl to reduce interference by the alginate [181], and the solution brought up to 1 liter volume using dilute HCl. The final absorbance of the solution was between 0.30 and 0.34 at 525 nm, and between 1.25 and 1.33 at 592 nm. Chondroitin sulfate diluted in the appropriate solution was used a the standard: full culture media for free GAG samples, 50%

trypsin:50% full media for monolayer samples, and 75mM NaCitrate with 0.05% LVM alginate for micobead samples. Eight microliters of sample were aliquoted into 96-well plates and 200 μl of DMMB dye were added. The samples were incubated at room temperature for 5 minutes and the absorbance measured at 592 nm using a microplate reader.

Athymic Mouse Intramuscular Implant Model

An athymic mouse intramuscular implant model was used to assess the *in vivo* response of the LVM alginate microbeads. Six week old athymic nude (Nu/Nu) mice (Taconic, Germantown, NY) were anesthetized using isoflurane gas. A small skin incision was made over the calf region of the hind limb following disinfection, and a pouch was prepared in the muscle by blunt dissection [119]. One gelatin capsule filled with 50 μl alginate microbeads containing approximately $3x10^5$ (low density) RC cells was inserted into the gastrocnemius muscle. The same number of unencapsulated RC cells or an equal volume of blank beads with no cells were implanted as controls. Implants were placed bilaterally such that each animal had two implants of the same type (N = 8 implants; N = 4 mice/formulation). The animals were euthanized by CO_2 inhalation at 4, 8, or 12 weeks and the legs harvested and processed for histological analysis. An additional experiment using $2.5x10^6$ (high density) RC cells was performed for 12 weeks using the same procedure described above. The protocol was approved by the Institutional Animal Care and Use Committee at the Georgia Institute of Technology.

In vivo Histology

Following euthanasia at 4, 8, or 12 weeks, the whole of the calf region was excised to ensure complete recovery of the implant site and then fixed in 10% neutral

buffered formalin. Histological processing was performed by AppTec (St. Paul, MN). After decalcification in 5% formic acid, tissues were embedded in paraffin, sectioned and stained with hematoxylin and eosin. Cross-sectional cuts (3-4 μm each) were made at three different levels of the limb (3 total sections per leg) to ensure visualization of the implant site.

Statistical Analysis

The results of the morphometry, viability and GAG quantification were calculated as the means ± SEM for each variable. The values for morphometry and viability represented measurements from ten micrographs at 10x magnification. The GAG quantification values represent six individual cultures. The amount of total free GAG released over time was calculated by summing the values of the current and preceding time points, and the variability calculated using propagation of error. Statistical significance of morphometry and viability samples was determined by one or two-way ANOVA followed by use of Bonferroni's modification of Student's t-test. Statistical significance of GAG quantification samples was determined by use of the Mann-Whitney rank sum test. P values ≤ 0.05 were considered significant.

RESULTS

Characterization of Encapsulation Method

The average bead diameter varied from 176±2 μm to 194±7 μm depending on the alginate composition used (Figure 5.1A), but there were no statistically significant differences among the formulations. In addition, no significant change in bead diameter

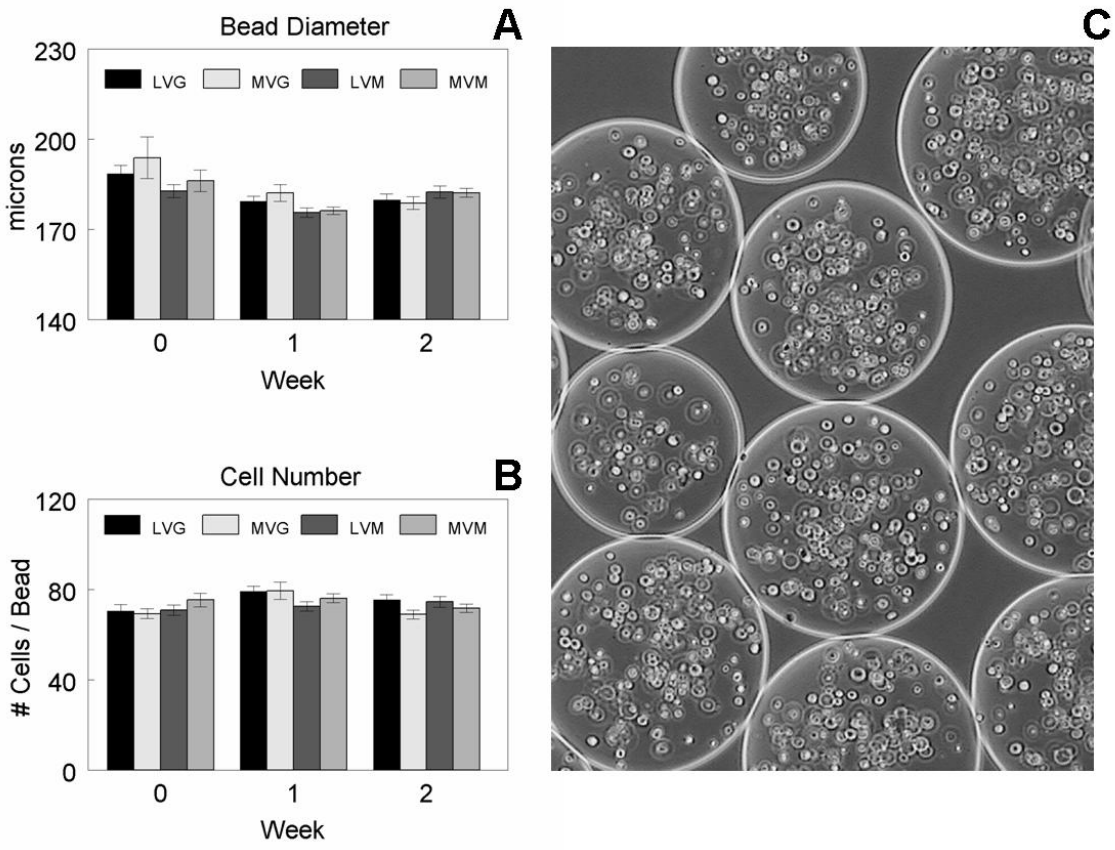

Figure 5.1: Quantitative morphometric analysis of alginate microbeads

Fourth passage rat costochondral resting zone growth plate chondrocytes (RC) were suspended in several formulations of ultrapure alginate with variable molecular weights and compositions (LVG, MVG, LVM, MVM). Microbeads were formed by extruding the suspension through a needle into an isotonic gelation bath containing calcium chloride and glucose. A 6 kV electrostatic potential between the needle and bath was used to disrupt the surface tension and reduce bead size. Morphometrics were performed using ten micrographs at 10x magnification. **(A)** The average bead diameter directly after encapsulation was 176±2 to 194±7 μm. There was no statistical difference based on alginate formulation and the bead size remained constant during the 2 week culture period. **(B)** The average cell number per bead following encapsulation was 69±2 to 80±4, which corresponded to the initial seeding density of $6x10^6$ cells/ml. There was no statistical difference based on alginate formulation or culture time, indicating minimal proliferation of the cells. **(C)** The beads and cells were easily viewed by light microscopy and remained intact and uniform after 2 weeks. The micrograph illustrates RC cells microencapsulated in LVG alginate after 2 weeks of *in vitro* culture.

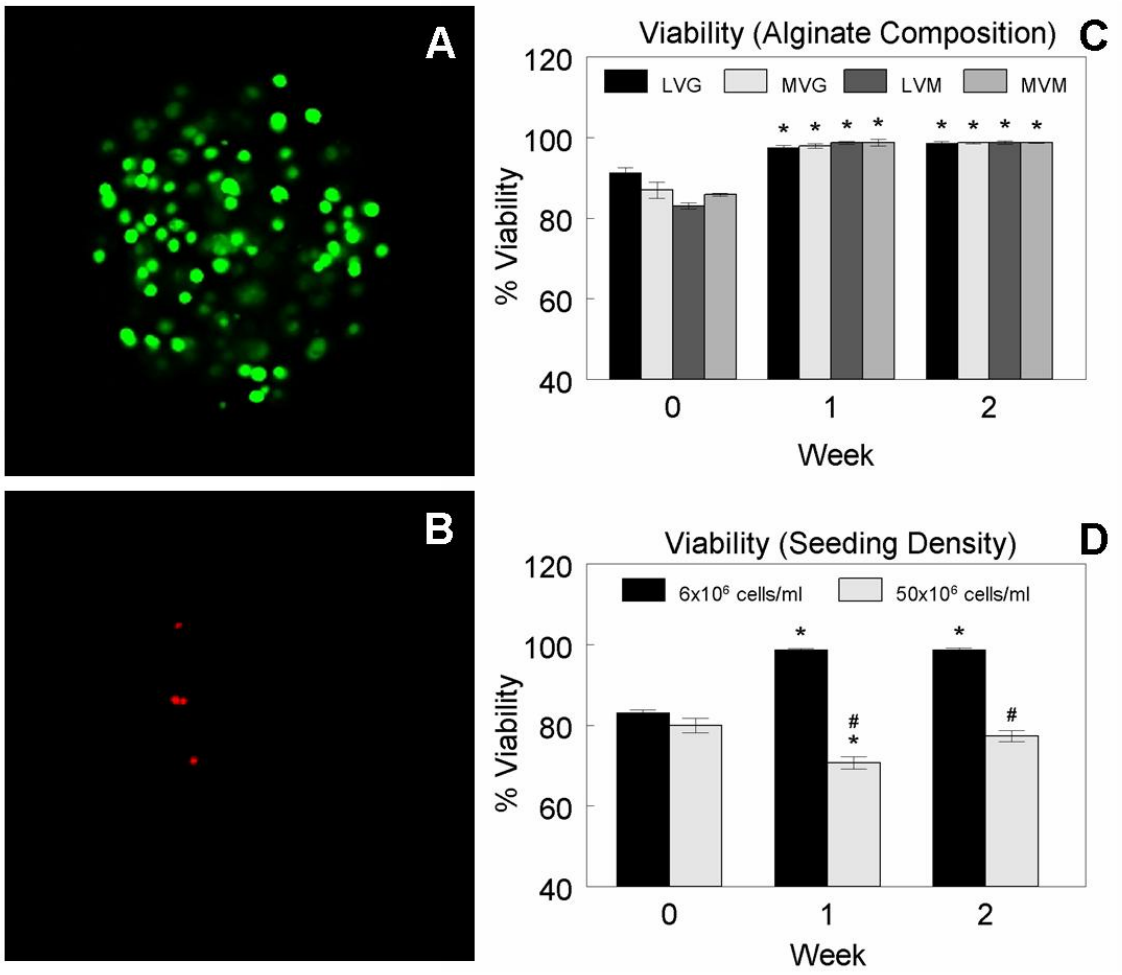

Figure 5.2: Viability of rat growth plate chondrocytes in alginate microbeads
Fourth passage rat costochondral resting zone growth plate chondrocytes (RC) were microencapsulated in various alginate formulations (LVG, MVG, LVM, MVM) and the viability measured using fluorescent confocal microscopy and a calcein/ethidium homodimer-1 stain. **(A)** The micrograph shows calcein stained RC cells microencapsulated for 2 weeks at low cell density ($6x10^6$ cells/ml) in MVM alginate. Viable cells were evenly distributed throughout the microbead indicating sufficient mass transfer to the center of the construct. **(B)** The same construct stained with ethidium homodimer-1 shows minimal cell death after 2 weeks of culture. **(C)** Viability was quantified using ten micrographs at 10x magnification. The initial viability was 83% to 91% and increased significantly after 1 week to >98% for all alginate compositions. **(D)** The effect of seeding density was determined by microencapsulating RC cells in LVM alginate at low ($6x10^6$ cells/ml) and high ($50x10^6$ cells/ml) density. The initial viability after encapsulation was not significantly different, but after 1 week of *in vitro* culture there was more cell death observed in the high density constructs. *$P < 0.05$, Initial vs. End Time Point. #$P < 0.05$, Low vs. High Cell Density.

was measured during the two weeks of *in vitro* culture. In the low cell density microbeads, the initial cell number per bead was 69±2 to 75±3 (Figure 5.1B), which corresponded to the loading density of 6 x10^6 cells/ml. No significant change in cell number per bead was observed over two weeks in any of the alginate compositions. The beads and encapsulated cells were easily viewed by light microscopy and remained intact and uniform during the two weeks of culture (Figure 5.1C).

The viability of low cell density microbeads was measured in all four alginate compositions using calcein (Figure 5.2A) to stain the cytoplasm of live cells and ethidium homodimer-1 (Figure 5.2B) to stain of the nuclei of dead cells. The live cells were evenly distributed throughout the beads with an initial viability of 83% to 91% (Figure 5.2C). Viability increased after one week in culture to greater than 98% for all alginate compositions and remained constant up to two weeks. No statistically significant differences in viability were observed between the different alginate compositions on cell viability during the *in vitro* culture of low cell density microbeads. High cell density LVM microbeads were also cultured *in vitro* for 2 weeks (Figure 5.2D). The initial viability of 80% was not statistically different compared to low cell density LVM microbeads, but after one week in culture the viability significantly decreased to 70%. The viability recovered during the second week of culture to 77%; however, this was still significantly less than the 98%+ viability seen in low cell density LVM microbeads.

Phenotype Analysis

Monolayer cultured RC cells expressed mRNAs for aggrecan, collagen type I and collagen type II (Figure 5.3A). Alginate microencapsulated RC cells continued to

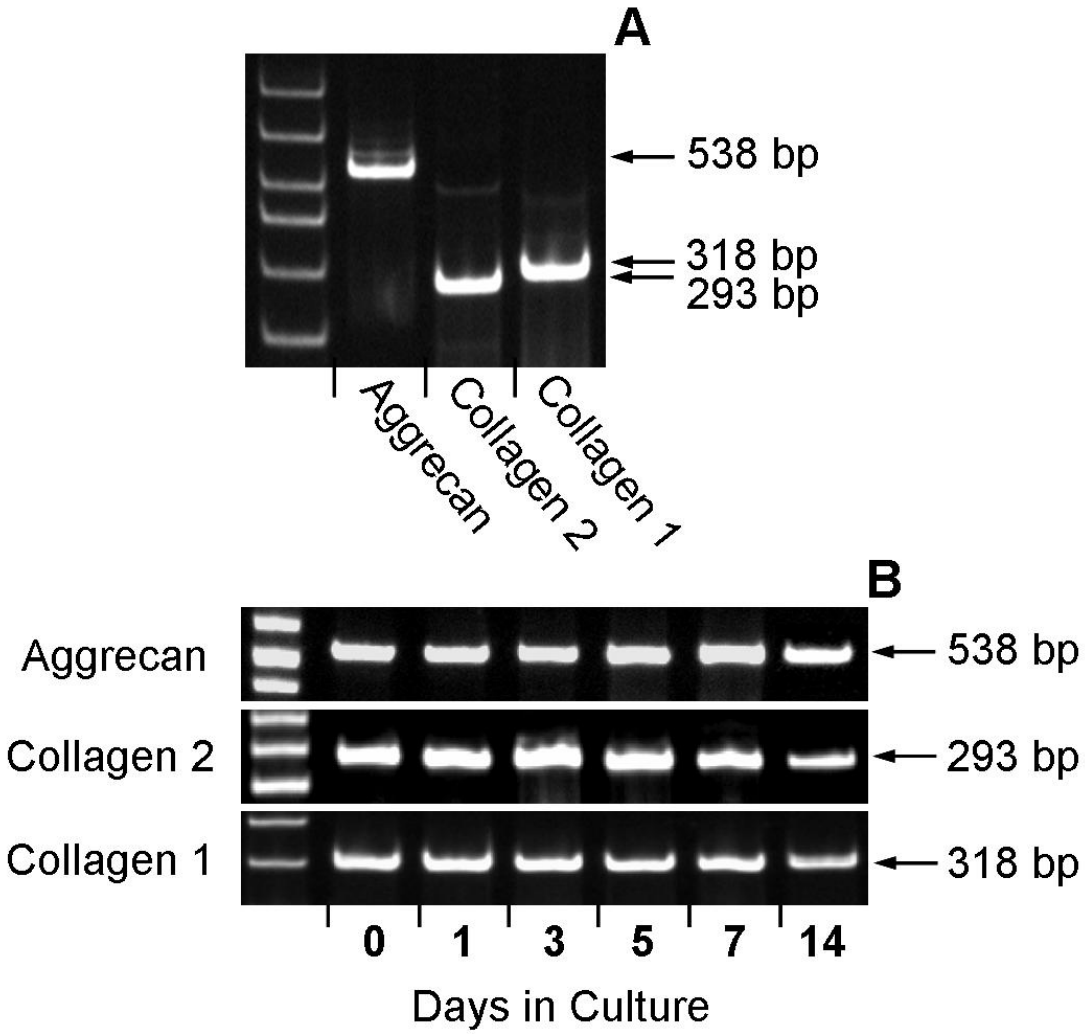

Figure 5.3: Analysis of mRNA expression of microencapsulated rat growth plate chondrocytes

Reverse transcription polymerase chain reaction (RT-PCR) was used to measure mRNA expression of cartilage specific genes in fourth passage rat costochondral resting zone growth plate chondrocytes (RC). **(A)** Monolayer RC cultures showed expression of the cartilage specific proteoglycan aggrecan, as well collagens type I and type II. **(B)** RC cells microencapsulated at low density ($6x10^6$ cells/ml) in LVM alginate maintained a constant level of aggrecan, collagen type I and collagen type II expression during the 2 week *in vitro* culture.

express constant levels of aggrecan, collagen type I, and collagen type II during the 14 day culture period (Figure 5.3B). SOX-9 expression was not detected in monolayer RC cell cultures or in alginate encapsulated cells at any of the time points during the two weeks of culture, but was detected in the positive controls of native rat growth plate cartilage.

Morphological Analysis

Toluidine blue staining of high density ($50x10^6$ cells/ml) microbeads after two weeks showed two distinct cell populations (Figure 5.4A). One population appeared to be viable cells with active formation of dark staining granules, while the other population looked inactive. This variation of staining could be a function of where the cells where sectioned or could possibly indicate cell death. Minimal extracellular matrix deposition was observed in either population. Further staining with safranin-O confirmed the lack of matrix deposition by the RC cells (Figure 5.4B).

TEM analysis did not demonstrate the presence of two distinct cell populations indicating the pale staining seen in the histology was possibly an artifact of the histology. RC cells showed highly active vesicle production (Figure 5.5A) containing dense coiled fibers (Figure 5.5B). In addition, the alginate matrix in contact with the RC cells appeared denser, indicating possible matrix deposition that was undetected with light microscopy (Figure 5.5C). The cells, however, did not appear to degrade the alginate and exhibited minimal mitosis due to the restriction of the alginate matrix. Moreover, they appeared to retract from the alginate to form a gap, potentially in the attempt to deposit extracellular matrix (Figure 5.5D).

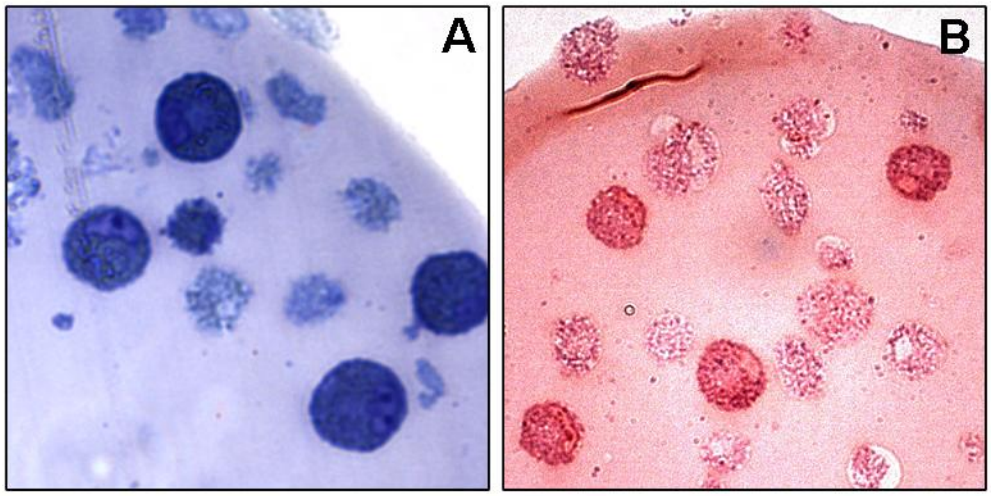

Figure 5.4: Light microscopy of microencapsulated rat growth plate chondrocytes

Histological analysis was performed on fourth passage rat costochondral resting zone growth plate chondrocytes (RC) encapsulated at high density ($50x10^6$ cells/ml) in LVM alginate microbeads after 2 weeks of *in vitro* culture. **(A)** Toluidine blue staining demonstrated active living cells with dark staining granules, but also a population of pale staining cells. The variation of cellular staining could be the result of where the cells were sectioned or could indicate less active or dead cells. There did not appear to be significant extracellular matrix deposition. **(B)** Safranin-O staining further confirmed the minimal deposition of matrix.

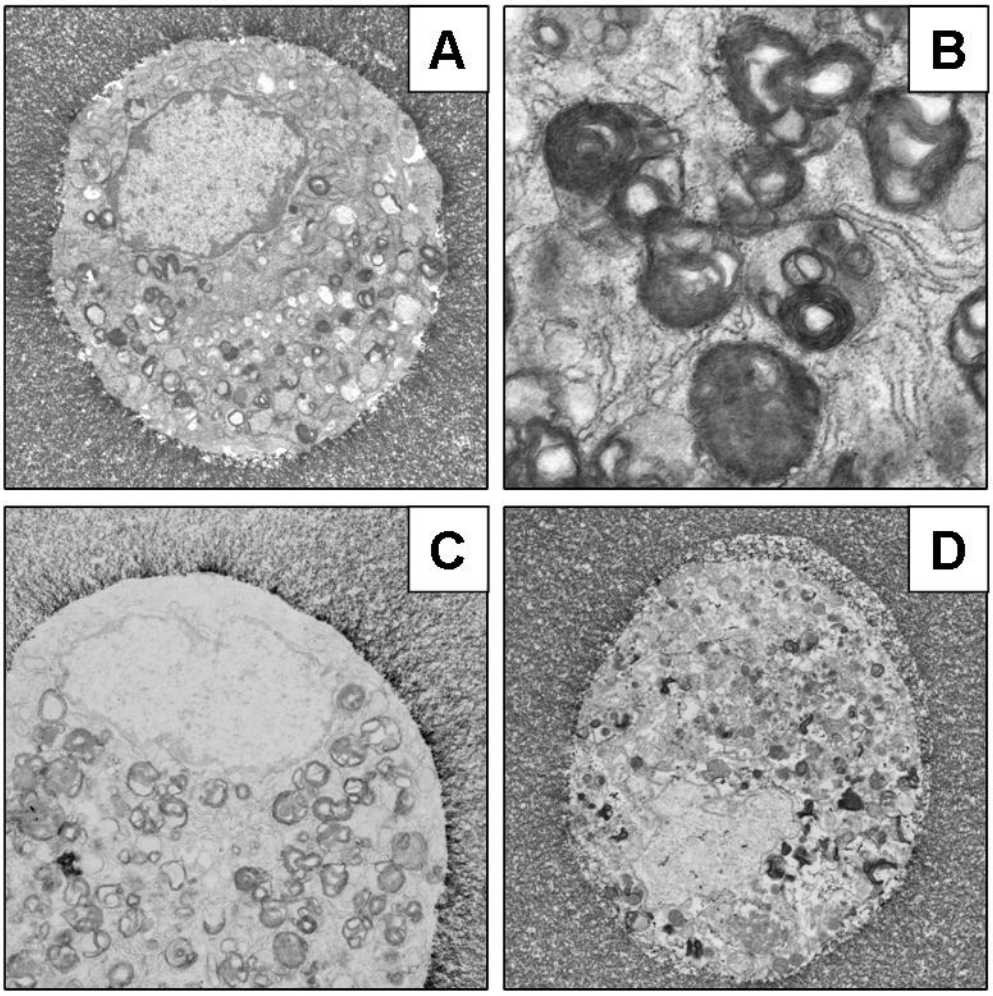

Figure 5.5: Transmission electron microscopy of microencapsulated rat growth plate chondrocytes

TEM was performed on fourth passage rat costochondral resting zone growth plate chondrocytes (RC) microencapsulated at high density in LVM alginate following 2 weeks of *in vitro* culture. Unlike light microscopy, TEM showed only one homogenous cell population. **(A)** RC cells appeared intact with a distinct nucleus and highly active vesicle production in the cytoplasm. **(B)** The vesicles contained dense coiled fibers most likely composed of extracellular matrix components. **(C)** The cell-alginate interface appeared denser signifying possible matrix deposition. **(D)** The presence of gaps between the cells and alginate could also indicate an attempt by the RC cells to release their matrix filled vesicles by retracting from the supporting matrix.

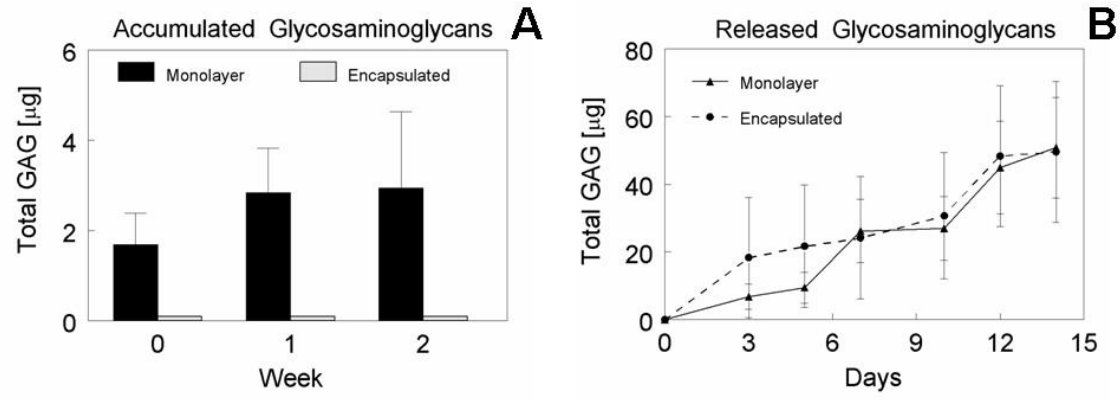

Figure 5.6: Analysis of matrix synthesis and secretion by rat growth plate chondrocytes

Fourth passage rat costochondral resting zone growth plate chondrocytes (RC) were cultured in monolayers or low density ($6x10^6$ cells/ml) LVM microbeads, and total glycosaminoglycan (GAG) production quantified by 1,9-dimethylene blue (DMMB) dye. **(A)** Monolayer and microbead samples were harvested at 1 and 2 weeks post-confluence or post-encapsulation and the total accumulated GAGs quantified. Less than four micrograms of GAGs accumulated in monolayer RC cultures over the two week culture period, and there were no detectable GAG levels in microbead cultures. **(B)** At 3, 5, 7, 10, 12, and 14 days post-confluence or post-encapsulation, the culture media was exchanged and the amount of free GAGs quantified. Over 40 micrograms of total GAGs were released into the culture media by both monolayer and microbead samples, indicating over ten times more GAG was released as free GAG than was sequestered as extracellular matrix. There was no significant difference between the total GAGs released by monolayer and microbead cultures.

In vitro Matrix Production

Most of the GAG synthesized by monolayer and alginate encapsulated RC cells was not sequestered as extracellular matrix but was instead released as free GAG into the culture media (Figure 5.6). Less than four micrograms of GAGs accumulated in post-confluent RC monolayer cultures over the two week culture period, and there were no detectable GAG levels in microbead cultures (Figure 5.6A). Over 40 micrograms of total GAGs were released into the culture media by both monolayer and microbead samples during the same two week incubation time (Figure 5.6B). There was no significant difference between the total GAGs released by monolayer or microbead cultures.

In vivo Implantation

Unencapsulated RC cell only controls formed cartilage nodules in muscle at 4, 8 (Figure 5.7A), and 12 weeks. Blank LVM microbeads without cells showed minimal degradation with highly cellular connective tissue surrounding the implants at four weeks. Significant degradation debris could be seen within the surrounding fibrosis at eight weeks (Figure 5.7B) and 12 weeks (Figure 5.7C), but most of the microbeads remained intact. Low cell density LVM beads at 4 (Figure 5.7D), 8 (Figure 5.7E), and 12 (Figure 5.7F) weeks showed viable RC cells but no obvious chondrogenesis. The host response appeared similar to blank microbead controls with significant surrounding fibrosis with the formation of granulation tissue at later time points. High cell density LVM microbeads implanted for 12 weeks showed large lacunae signifying RC cell hypertrophy and differentiation (Figure 5.7G). A large portion of the lacunae appeared empty suggesting apoptosis (Figure 5.7H). Moreover, some RC cells were surrounded by a positively charged matrix indicating pericellular protein deposition (Figure 5.7I).

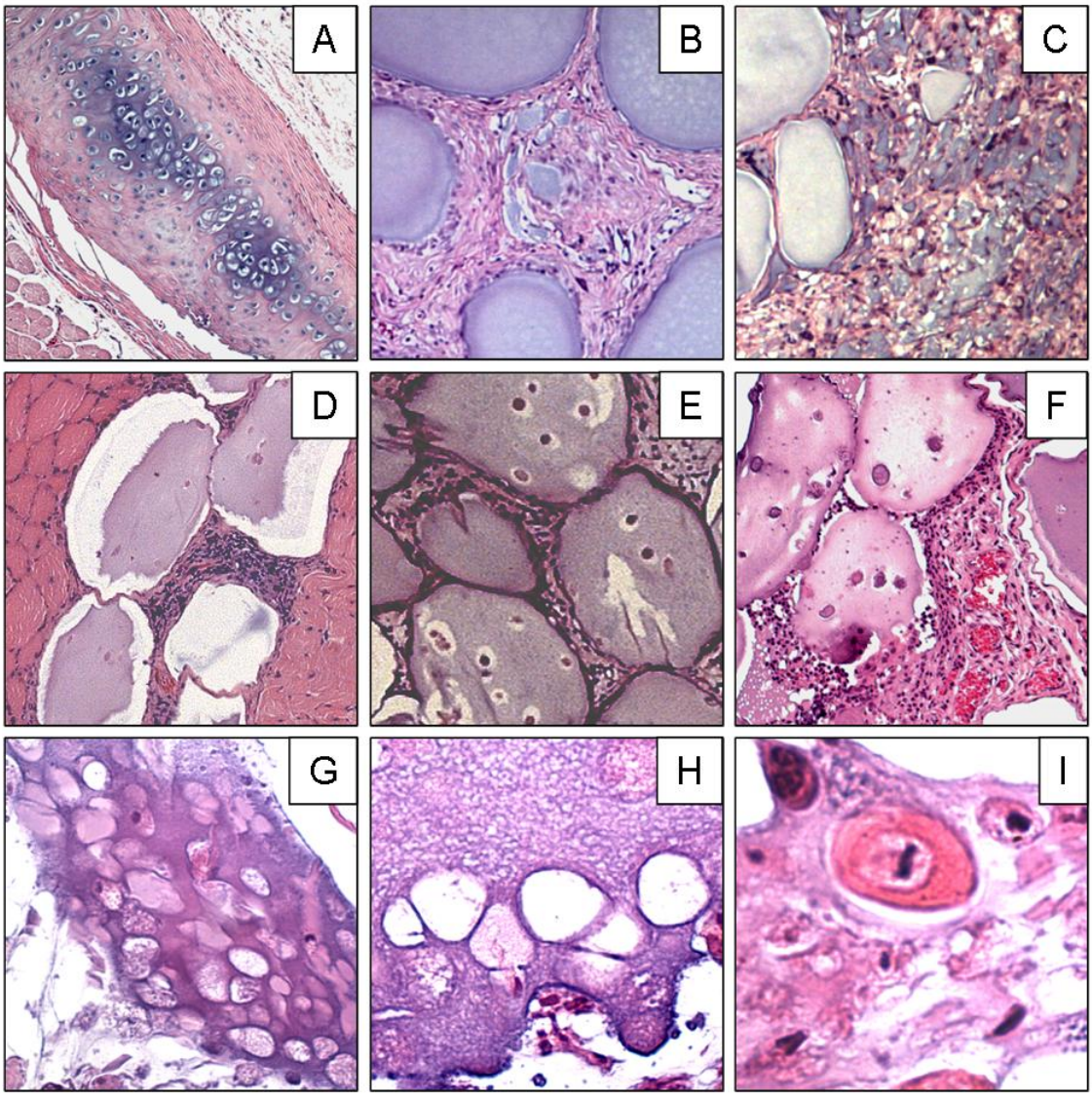

Figure 5.7: Histological analysis of *in vivo* implanted alginate microbeads

Fourth passage rat costochondral resting zone growth plate chondrocytes (RC) were microencapsulated at low ($6x10^6$ cells/ml) or high ($50x10^6$ cells/ml) density in LVM alginate. The microbeads were implanted intramuscularly into athymic mice for 4, 8, or 12 weeks. Unencapsulated RC cells and blank microbeads were also implanted as controls. **(A)** Unencapsulated cell only controls were capable of forming cartilage nodules in muscle at 4, 8, and 12 weeks. The micrograph depicts one such nodule at 8 weeks. **(B)** The host response to blank microbeads resulted in significant surrounding fibrosis at 4 weeks with evidence of degradation debris by 8 weeks. **(C)** The microbeads showed continued degradation at 12 weeks with remodeling of the fibrosis into vascularized granulation tissue. **(D)** Low cell density microbeads at 4 weeks showed a similar host response compared to blank controls but no chondrogenesis was apparent. **(E)** At 8 weeks the encapsulated RC cells still appeared viable but there was no evidence of chondrogenesis within or around the beads. **(F)** By 12 weeks there remained no obvious chondrogenesis, but some of the RC cells appeared to be hypertrophied. **(G)** RC

(Figure 5.7 continued) cells encapsulated at high cell density showed significant hypertrophy and the formation of lacunae at 12 weeks. **(H)** The appearance of empty lacunae indicated possible apoptosis and therefore terminal differentiation of the RC cells. **(I)** There was also evidence of positively charged matrix surrounding the cells within the lacunae, suggesting pericellular protein deposition.

DISCUSSION

The physical and biological properties of alginate can vary widely depending on the ratio of saccharide residues and the molecular weight of the polymers. Alginate composition did not appear to be an important factor in the fabrication of microbeads using electrostatic potential. All four alginate compositions produced spherical microbeads with similar size distributions. The morphology of the beads remained constant for up to two weeks in culture regardless of the alginate composition. Cell viability also did not vary by composition as previously reported in chondrocytes [182], indicating that mass transfer was not composition dependent. However, one study on mouse insulinoma cells has shown an increase in metabolic rate when encapsulated in alginates with lower guluronate content [183], thereby suggesting composition could be an important factor.

The alginate encapsulated RC cells showed minimal proliferation during the two week *in vitro* culture. Previous research has revealed that alginate encapsulation can inhibit the ability of the cells to grow and divide under static culture [184]. Moreover, the alginate composition and degradation rate can affect proliferation as well [185]. Our results, however, did not exhibit any difference between the four compositions tested, which is consistent with other published results [182]. Prior research suggests that both fast and slow degradation kinetics can be beneficial for *in vivo* tissue formation [186, 187]. It is currently unclear how the composition of alginate hydrogels should be modified to optimize chondrogenesis.

The degradation rate of the alginate matrix can also influence the differentiation pathway of the encapsulated cells [188]. The lack of proliferation could be a result of the

three dimensional alginate matrix stimulating normal homeostatic behavior. Resting zone chondrocytes do not normally proliferate until they prepare to differentiate into growth zone chondrocytes. Therefore, the static cell number could be considered phenotypically normal behavior for RC cells. Another option is the three dimensional hydrogel matrix could be ensuing further differentiation of the cells into a hypertrophic phenotype. The *in vivo* results we observed support this hypothesis.

Encapsulated RC cells expressed mRNA for the relevant matrix proteins but did not demonstrate noteworthy matrix deposition by histology or by DMMB quantification of GAG production. Monolayer cultures of RC cells were also unable to sequester GAGs into their extracellular matrix, indicating the ability to synthesize and secrete matrix but not assemble it correctly. The plastic monolayer surface or restrictive properties of the alginate could have prevented secretion and accumulation of large hyaluronan molecules that are necessary for the anchoring of proteoglycans to the collagen fiber network. Previous studies have also reported this lack of GAG accumulation in alginate suspended chondrocyte cultures [189, 190]. The composition of the surrounding extracellular matrix is critical for chondrogenesis [191], and the addition of extracellular matrix molecules like fibronectin or collagen to the alginate gel can significantly alter the phenotype of chondrocytes [192]. Supplementation of the alginate matrix with additional proteins or proteoglycans may aid the encapsulated chondrocytes in depositing their own stable matrix.

Modification of the culture conditions can enhance matrix deposition of alginate encapsulated chondrocytes. Possible future studies could involve supplementation of the growth media with chondrogenic factors like TGF-β2, IGF-1, FGF-2 [193] or BMP-2 [194],

which have been shown to increase matrix production. Moreover, the use of decreased oxygen tension can also be used to enhance chondrogenesis [168]. Xenogeneic serum has been shown to be less optimal than using allogeneic or autogenic serum for promoting chondrogenesis [195, 196]. However, the use of rat serum is not currently feasible, as fetal rats have a blood volume too small to effectively harvest substantial quantities for cell culture.

The electrostatic potential could have had additional unknown effects on both the alginate and the cells. For example, the degradation characteristics of the alginate could have been altered by the electrical charge. In addition, the production of heat due to resistance could damage or modify certain essential cell activities. Such studies with appropriate controls have not been done to date. Our results, however, suggest the electrostatic potential may have minimal effect given the fact the RC cells retained a chondrocytic phenotype and high viability.

The goal of producing microbeads was to enable minimally invasive injectable cell delivery. We chose to implant the constructs surgically to remove the additional variable of mechanical loading on the cells via the injection procedure. A significant host response to the implanted beads was observed despite prior literature suggesting otherwise [74]. It is possible the previous results were not due to size of bead, but rather a function of using two different methods of encapsulation.

Implanted unencapsulated RC cells were capable of forming phenotypical appearing cartilage nodules in the intramuscular implant. Implanted RC cells did not, however, form cartilaginous tissue in either low density or high density microbeads. The RC cells at low density could have been phenotypically chondrocytes, but the lack of

proliferation and minimal matrix production due to restriction by the alginate resulted in negligible cartilage tissue formation. High density microbeads on the other hand appeared phenotypically like hypertrophic growth plate chondrocytes. It is known that culture of chondrocytes in high density pellets promotes chondrogenesis [197]. The increased cell density could result in more interaction between cells and a higher local concentration of autocrine and paracrine signaling, thus promoting differentiation as seen in our high density cultures.

Alginate microbeads have many potential applications for tissue engineering and biotechnology. The small size allows for minimally invasive injectable cell therapies where the cells are protected by the hydrogel matrix, while being large enough to manipulate thereby permitting precise control over the number, type, and distribution of the cells implanted. Moreover, the decrease in volume reduces the mass transfer limitations associated with many constructs thus allowing for improved viability [198].

In summary, our research shows that rat growth plate chondrocytes microencapsulated in alginate using a high electrostatic potential express cartilage specific mRNA and remain viable up to twelve weeks post implantation. Furthermore, microencapsulation directly affects the differentiation of the chondrocytes resulting in a hypertrophic phenotype.

CHAPTER 6

Human Articular Chondrocytes Suspended in Alginate Microbeads Demonstrate a Temporal Dependent Elevation in SOX-9 Expression

INTRODUCTION

Osteoarthritis is a debilitating disease that affects millions of people and costs the health care industry billions of dollars in treatment and disability [199]. Current treatment involves drug therapy to manage pain, reparative surgeries and eventually total joint replacement. The ultimate goal is to design a tissue engineered cartilage graft to heal the arthritic lesion before total joint arthroplasty is needed. However, the development of a tissue engineered product has proven to be difficult due to the complex biology of the chondrocyte.

SRY (sex determining region Y)-box containing gene 9, or SOX-9, is a critical transcription factor in the chondrogenic pathway. The role of SOX-9 was initially identified by its co-expression with the type II collagen gene (*COL2A1*) in cells undergoing chondrogenesis [200-202]. Additional work with *SOX-9*$^{-/-}$ knockout mice demonstrated arrestment of chondrogenesis at the mesenchymal condensation stage, indicating SOX-9 is the first transcription factor essential for cartilage-specific tissue formation [203]. SOX-9 has been shown to bind promoter regions on *COL2A1* [204] and may also directly control expression of other cartilage-specific genes like *COL9A2* and *COL11A2* [203, 205]. SOX-9 activity is regulated through Sonic hedgehog (Shh) and Indian hedgehog (Ihh) induction of the transforming growth factor beta (TGF-β) super family,

which includes bone morphogenetic proteins (BMPs) [206, 207]. Fibroblast growth factors (FGFs) and insulin-like growth factors (IGFs) have also been shown to regulate SOX-9 expression [208, 209], as has the Wnt signaling pathway via β-catenin [210].

Articular chondrocytes undergo a process known as "dedifferentiation" when cultured *in vitro* as monolayers. The lack of a three-dimensional matrix results in the chondrocytes expressing a fibroblast-like morphology and the down-regulation of cartilage-specific processes including expression of SOX-9, collagen type II and aggrecan [50, 51]. The dedifferentiation process is believed to be the result of actin stress fibers that form during attachment and spreading of the cells to a two dimensional surface [52-55].

It has been established that three-dimensional suspension of chondrocytes in hydrogels can reverse the dedifferentiation process by maintaining the rounded morphology of the cell [56, 57]. Alginate has been one of the more commonly used hydrogels for encapsulation due to its ability to rapidly cross link in the presence of divalent cations such as Ca^{2+} to form a solid gel and entrap the chondrocytes. A chelating agent can then be added to break down the alginate matrix and release the cells and extracellular matrix. Alginate suspension has been reported by several research groups to be effective at redifferentiating *in vitro* expanded human articular chondrocytes (HACs) [63, 64, 211]. Moreover, it has been shown to promote differentiation of human mesenchymal stem cells towards a chondrocytic lineage [212, 213].

High electrostatic potentials can be used to reduce alginate bead size by disrupting the surface tension of the alginate droplets [70, 75]. The microbeads produced with this technique are up to one hundred times smaller in volume than those created using other

disruption methods, and may allow minimally invasive injectable cell therapies that are capable of filling a range of articular defects. Moreover, the smaller bead size could reduce mass transfer limitations [172], a common problem among larger tissue engineered constructs that can lead to necrotic cores. Biocompatibility of alginate implants has also been shown to be improved by decreasing bead size [74, 173].

It is not known, however, what consequences the exposure to high electrostatic potential may have on chondrocyte viability and phenotypic expression. Electrostatic alginate encapsulation of cells has been limited mostly to hybridomas [174] or pancreatic islets [175-177]. Some recent work has been done with mesenchymal stem cells [178], but this study did not characterize how the high electrostatic encapsulation process impacted the phenotype of the cells; instead it focused on the effects of cell density and alginate concentration on bead morphometry. Therefore, the goal of this study was to determine if electrostatic potential could be used to produce alginate microbeads containing viable HAC, and to assess the effects microencapsulation on the phenotype of the cells.

MATERIALS AND METHODS

Human Articular Chondrocyte Source and Culture

Articular cartilage was isolated from the femoral condyles and tibial plateaus of human donors made available due to autopsy [214]. Donors had no known history of joint disease and histological analysis was performed at the time of isolation to confirm the absence of any pathologies. The articular cartilage was cut into small pieces and washed twice for 20 minutes with Hanks' balanced salt solution (HBSS) containing 1% penicillin and streptomycin. The washed cartilage was digested for 1 hour with 0.25% trypsin-1

mM ethylene diamine tetraacetic acid (EDTA), followed by treatment with 0.2% collagenase for 3 hours. All enzymes were prepared in HBSS. The digested suspension was passed though a 40 μm mesh sieve and centrifuged at 2000 rpm for 10 minutes. The supernatant was removed and the chondrocytes were resuspended in full media containing 88% Dulbecco's modified Eagle's medium (DMEM), 10% fetal bovine serum (FBS), 1% penicillin/streptomycin, and 1% L-ascorbic acid.

Isolated primary human articular chondrocytes (HACs) were plated on T75 flasks, grown to confluence, and harvested using 0.25% trypsin-1 mM EDTA. The cell suspension was centrifuged at 2000 rpm for 10 minutes, the supernatant removed, and the cells resuspended in cold DMEM, 20% FBS, 1% penicillin/streptomycin, and 5% dimethyl sulfoxide (DMSO). The chondrocytes were then frozen at –80^{o}C and shipped overnight from La Jolla, CA to Atlanta, GA. The first passage chondrocytes were thawed, centrifuged, resuspended in full media and plated on T75 flasks. The cultures were grown to confluence and passaged twice as above. Third passage HAC cells were used for all experiments.

Characterization of Cell Source

Three male and three female donors between the ages of 16-39 were used to characterize the monolayer expanded articular chondrocyte cell source. Reverse transcription polymerase chain reaction (RT-PCR) was used to assess the phenotype of the third passage HAC by measuring the mRNA expression of aggrecan, collagen type I, collagen type II, cartilage oligomeric matrix protein (COMP), and SOX-9. Total RNA was extracted from the chondrocyte cultures with Trizol reagent. Lipophilic contaminants were removed by adding chloroform and centrifuging for 25 minutes at

4700 rpm. The aqueous phase was then washed with isopropyl alcohol to precipitate the RNA, and centrifuged for 20 minutes at 4700 rpm to form a pellet. The pellet was washed with cold 70% ethanol and centrifuged for 15 minutes at 4700 rpm. The supernatant was removed and the pellet allowed to air dry. The RNA was then dissolved in diethylpyrocarbonate (DEPC) treated water and the purity and quantity was determined by UV spectrophotometry. RNA extracted from native human articular cartilage tissue or human lymphocytes was used as positive or negative controls, respectively, to verify the specificity of the aggrecan, collagen type II, COMP, and SOX-9 primers. Cultured human fibroblasts were used as a positive control from collagen type I primers, with human lymphocytes once again serving as a negative control. RT-PCR primer information is summarized in Table 6.1.

The total RNA sample from each sample was reverse transcribed using the First-strand cDNA Synthesis Kit (Amersham-Biosciences, Piscataway, NJ) and the specific anti-sense primer for each mRNA of interest. The cDNA was amplified using the Fisher PCR kit (Fisher Scientific International, Hampton, NH) and the specific sense and anti-sense primers. PCR conditions for each cycle included a 30 second denaturation at 94 ^{o}C, a 60 second annealing at 50-65 ^{o}C depending on the primer used, and a 30 second extension at 72 ^{o}C. The PCR-amplified products were run on 5% polyacrylamide gels using a buffer consisting of 0.9 M Trizma® base (tris[hydroxymethyl]aminomethane), 0.9 M boric acid, and 20 mM EDTA.

Table 6.1: RT-PCR Primers for Third Passage Human Articular Chondrocytes

	Sense Primer	Anti-Sense Primer	Anneal Temp.	Product
Aggrecan	5′-TGA GGA GGG CTG GAA CAA GTA CC-3′	5′-GGA GGT GGT AAT TGC AGG GAA CA-3′	65 °C	349 bp
Collagen 1	5′-GTC AGG CTG GTG TGA TGG GA-3′	5′-AAC CTC TCT CGC CTC TTG CT-3′	60 °C	318 bp
Collagen 2	5′-CTG CTC GTC GCC GCT GTC CTT-3′	5′-AAG GGT CCC AGG TTC TCC ATC-3′	58 °C	429 bp
COMP	5′-AGG ACA GTG ATG GCG ATG G-3′	5′-CGT GAC TTC AGC GTT CTC C-3′	58 °C	350 bp
SOX-9	5′-GGT TGT TGG AGC TTT CCT TA-3′	5′-TAG CCT CCC TCA CTC CAA GA-3′	57 °C	394 bp

Table 6.2: Real Time RT-PCR Primers for Human Articular Chondrocytes

	Sense Primer	Anti-Sense Primer	Anneal Temp.
Aggrecan	5′-TGC ATT CCA CGA AGC TAA CCT-3′	5′-CGC CTC GCC TTC TTG AAA T-3′	57 °C
SOX-9	5′-CAG TAC CCG CAC TTG CAC AA-3′	5′-CTC GTT CAG AAG TCT CCA GAG CTT-3′	61 °C
GAPDH	5′-CCA CAT CGC TCA GAC ACC AT-3′	5′-CCA GGC GCC CAA TAC-3′	54 °C

Alginate Microencapsulation

Ultrapure LVM alginate (NovaMatrix, Drammen, Norway) with a molecular weight of 130,000 g/mole and a 44% guluronate content was used to microencapsulate HACs using a Nisco Encapsulator VAR V1 LIN-0043 (Nisco Engineering AG, Zurich, Switzerland). LVM alginate has faster degradation kinetics as a result of lower molecular weight and decreased cross-linking due to low guluronate content. Chondrogenesis has been shown to be enhanced by more rapid degradation of the alginate [179, 180]. The LVM alginate powder was sterilized using UV light and dissolved in 0.9% phosphate buffered saline (PBS) to produce a 2% (w/v) alginate solution. HAC cells were suspended in a minimum volume of PBS and added to the alginate solution resulting in $6x10^6$ cells/ml (low density) or $50x10^6$ cells/ml (high density). The solution was then extruded through a 0.18mm (inner diameter) needle at 10 ml/hr into a gelation solution consisting of 50 mM $CaCl_2$ plus 150 mM glucose. A 6 kV electrostatic potential between the gelation solution and needle was used to overcome the surface tension. This encapsulation process produced spherical alginate microbeads approximately 180 μm in diameter as previously described in Chapter 5.

Viability

Viability of chondrocytes seeded at low cell density ($6x10^6$ cells/ml) and high cell density ($50x10^6$ cells/ml) in LVM alginate was measured using fluorescent confocal microscopy and a calcein/ethidium homodimer-1 stain (Molecular Probes, Eugene, OR). Alginate encapsulated chondrocytes were cultured for 0, 1, or 2 weeks in 6-well plates and media were changed at days 3, 5, 7, 10, and 12. At time of measurement, culture media were removed and the beads washed with PBS containing 1mM $CaCl_2$ to maintain

bead integrity. The samples were then incubated for 30 minutes in a PBS solution containing 1 mM $CaCl_2$, 4 μM ethidium homodimer-1, and 2 μM calcein. Images were obtained using a LSM 510 confocal microscope (Carl Zeiss MicroImaging Inc., Thornwood, NY).

In vitro Histology and Transmission Electron Microscopy

High cell density ($50x10^6$ cells/ml) LVM alginate microbeads were used for microscopy analysis to maximize the number of cells visible per section. The microbeads were cultured for 2 weeks as above, fixed with 2.5% gluteraldehyde in 0.1 M cacodylate buffer, embedded in polyacrylate resin, and sectioned. General cell appearance and matrix deposition were assessed using toluidine blue and safranin-O stained sections (Winship Cancer Institute Pathology Core Lab, Atlanta, GA). Ultrathin sections were examined by TEM to evaluate the subcellular structure of microencapsulated cells (Emory School of Medicine Microscopy Core, Atlanta, GA).

Effect of Microencapsulation on Phenotype

After 0, 1, 3, 5, 7, or 14 days in culture, low cell density LVM microbeads were washed with saline and the alginate dissolved using 75 mM sodium citrate. The samples were centrifuged to pellet the cells and the alginate removed. RNA was extracted using the Qiagen miniprep kit (Qiagen, Valencia, CA) and quantified by UV spectroscopy. RT-PCR was used to assess expression of collagen type I, collagen type II, aggrecan, COMP, and SOX-9.

HACs were either cultured as monolayers in 6-well plates or in low cell density LVM microbeads. After 0, 1, 4, or 7 days post-confluence or post-encapsulation, cells were harvested and the RNA extracted using the Qiagen miniprep kit (Qiagen, Valencia,

CA) and quantified by UV spectroscopy. Quantitative real time RT-PCR was used to measure changes in aggrecan and SOX-9 mRNA expression. Previously published real time RT-PCR primers were used [215, 216], and the information is summarized in Table 6.2. The total RNA sample from each sample was reverse transcribed as above. Real time PCR was performed on an i-cycler (Bio-Rad Laboratories, Hercules, CA) using the software I-cycler iQ, version 3.0a. The cDNA was amplified for 40 cycles in the presence of the fluorophore SYBR Green (Bio-Rad Laboratories, Hercules, CA). PCR conditions for each cycle included a 30 second denaturation at 94 ^{o}C, a 30 second annealing at 50-65 ^{o}C depending on the primer used, and a 30 second extension at 72 ^{o}C. The house keeping gene glyceraldehyde 3-phosphate dehydrogenase (GAPDH) was used to normalize the content of cDNA for each sample.

Glycosaminoglycan Quantification

The production of proteoglycans was measured in monolayer and alginate microbead cultures. HACs were either cultured as monolayers in 6-well plates or in low cell density LVM microbeads. Both monolayer and microbead samples contained approximately 500,000 cells. At 3, 5, 7, 10, 12, and 14 days post-confluence or post-encapsulation, the culture media was exchanged and the amount of free glycosaminoglcyans (GAGs) quantified using 1,9-dimethylene blue (DMMB) dye. Monolayer and microbead samples were also harvested at 1 and 2 weeks and the total accumulated GAGs quantified. Monolayer samples were harvested using trypsin and microbead samples were harvested by dissolution in 75 mM NaCitrate.

The DMMB dye solution was prepared by mixing 16 mg of DMMB with 5 ml of 100% ethanol. The dissolved DMMB was then added to a 950 ml solution containing

40.5 mM glycine and 40.5 mM NaCl. The pH was adjusted to 1.5 using 1 M HCl to reduce interference by the alginate [181], and the solution brought up to 1 liter volume using dilute HCl. The final absorbance of the solution was between 0.30 and 0.34 at 525 nm, and between 1.25 and 1.33 at 592 nm. Chondroitin sulfate diluted in the appropriate solution was used a the standard: full culture media for free GAG samples, 50% trypsin:50% full media for monolayer samples, and 75mM NaCitrate with 0.05% LVM alginate for micobead samples. Eight microliters of sample were aliquoted into 96-well plates and 200 μl of DMMB dye were added. The samples were incubated at room temperature for 5 minutes and the absorbance measured at 592 nm using a microplate reader.

Response to TGF-β1

HACs were either cultured as monolayers in 6-well plates or in low cell density LVM microbeads. At 1 week post-confluence or post-encapsulation, cells were treated with 0.2, 1.0, or 5.0 ng/ml TGF-β1 for 24 hours prior to harvest. At harvest, low cell density LVM microbeads were washed with saline and the alginate dissolved using 75 mM sodium citrate. The samples were centrifuged to pellet the cells and the alginate removed. Monolayer samples were harvested using 0.25% trypsin-1 mM EDTA. The cell suspension was centrifuged and the cell pellet washed with media and PBS. RNA was extracted from monolayer and microbeads samples using the Qiagen miniprep kit (Qiagen, Valencia, CA) and quantified by UV spectroscopy. Quantitative real time RT-PCR was used to measure changes in aggrecan and SOX-9 mRNA expression as described above.

Statistical Analysis

The results of the viability, real time PCR, and GAG quantification were calculated as the means ± SEM for each variable. The values for viability represented measurements from ten micrographs at 10x magnification. The real time PCR and GAG quantification values represent six individual cultures. The amount of total free GAG released over time was calculated by summing the values of the current and preceding time points. The variability of summed GAG time points was calculated using propagation of error. Statistical significance of viability and real time PCR samples was determined by one or two-way ANOVA followed by use of Bonferroni's modification of Student's t-test. Statistical significance of GAG quantification samples was determined by use of the Mann-Whitney rank sum test. P values ≤ 0.05 were considered significant.

RESULTS

Characterization of Cell Source

Expansion of human articular chondrocytes for three passages in monolayer culture resulted in partial loss of phenotypic expression. The chondrocytes retained their ability to express aggrecan core protein and COMP mRNA, but lost expression of collagen type II mRNA (Figure 6.1). In addition, the cells showed a strong expression collagen type I mRNA indicating a dedifferentiated phenotype. Despite loss of collagen type II expression, HAC from all six donors tested maintained expression SOX-9.

Viability of Microencapsulated HACs

Cell viability was only minimally affected during microencapsulation. The live cells appeared evenly distributed throughout the beads with an initial viability of 89% in

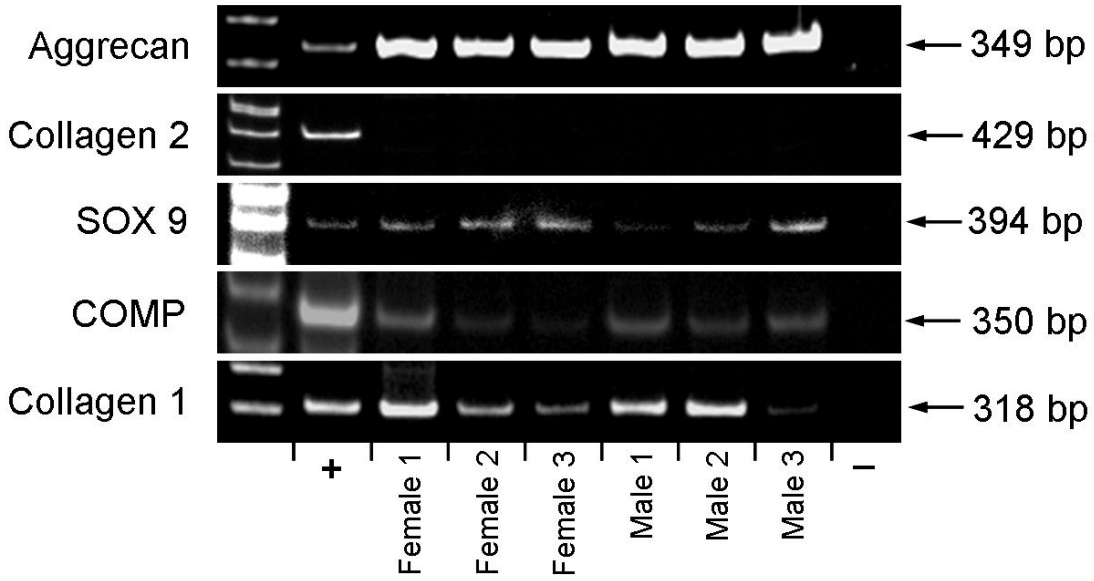

Figure 6.1: Analysis of mRNA expression of third passage human articular chondrocytes

Reverse transcription polymerase chain reaction (RT-PCR) was used to measure mRNA expression of cartilage specific genes in third passage monolayer expanded human articular chondrocytes (HACs). Cells were harvested from three male and three female donors between the ages of 16-39. RNA extracted from native human articular cartilage tissue (aggrecan, collagen type II, COMP, and SOX-9) or cultured human fibroblasts (collagen type I) were used as positive controls. Human lymphocyte RNA served as a negative control. HACs from all six donors showed a similar expression profile exhibiting a partially dedifferentiated phenotype with no detectable collagen type II expression and strong expression of collagen type I. The expanded third passage HAC maintained expression of aggrecan and COMP, and SOX-9.

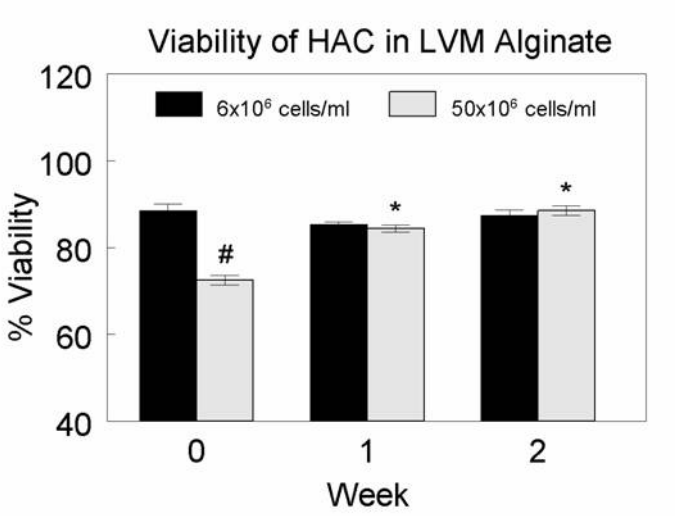

Figure 6.2: Viability of human articular chondrocytes in alginate microbeads

Third passage human articular chondrocytes (HACs) were microencapsulated in LVM alginate at low ($6x10^6$ cells/ml) and high ($50x10^6$ cells/ml) cell density. Viability was measured using calcein/ethidium homodimer-1 stain and quantified by fluorescent microscopy using ten micrographs at 10x magnification. The initial viability was greater in low cell density microbeads, but the viability of high density microbeads increased to similar levels after one week of culture. A viability of ~90% was maintained by both seeding densities during the second week of culture. *$P < 0.05$, Initial vs. End Time Point. #$P < 0.05$, Low vs. High Cell Density.

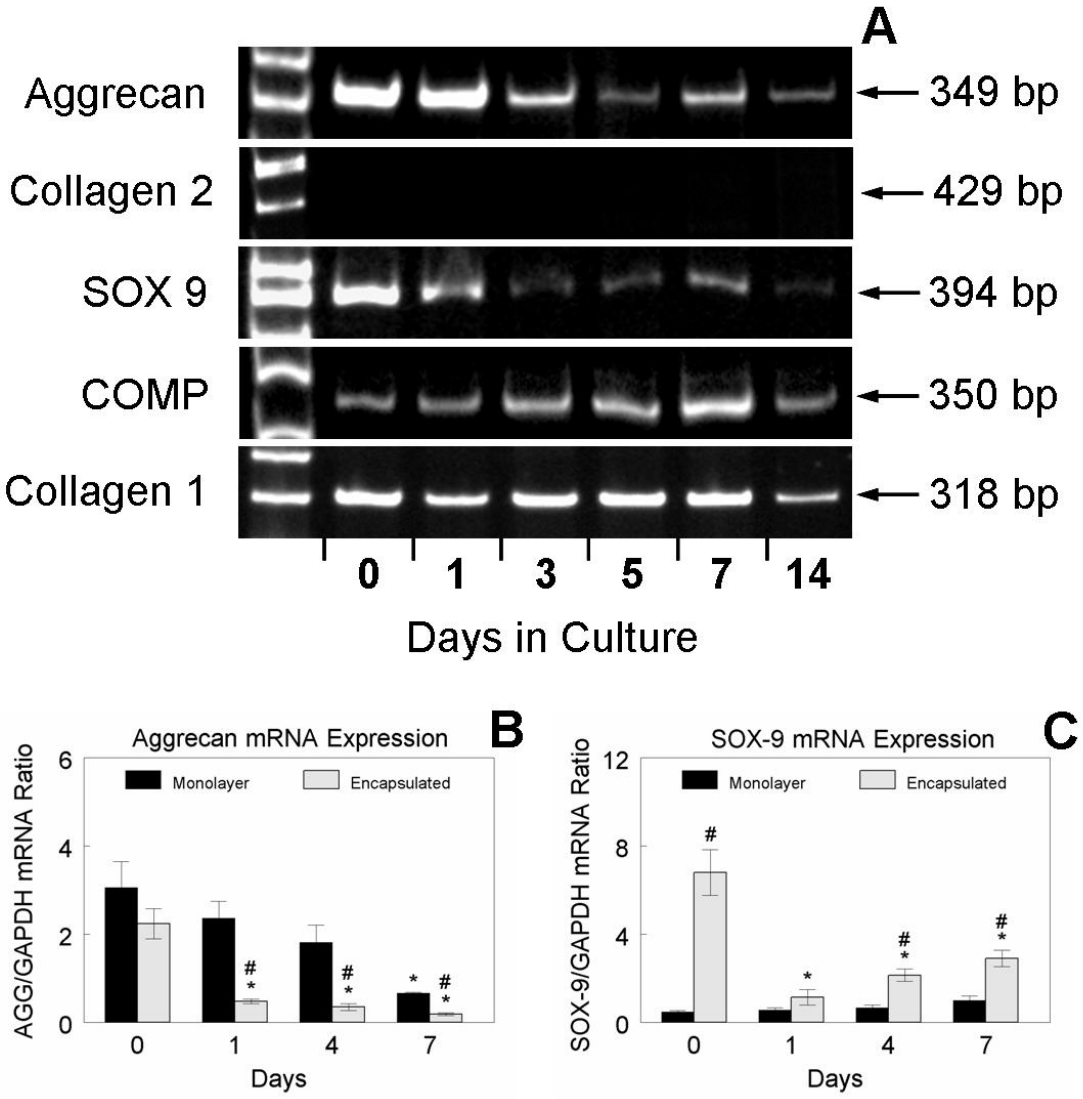

Figure 6.3: Analysis of mRNA expression of microencapsulated human articular chondrocytes

The phenotype of third passage monolayer expanded human articular chondrocytes (HACs) suspended at low density ($6x10^6$ cells/ml) in LVM alginate microbeads was assessed using reverse transcription polymerase chain reaction (RT-PCR) to measure mRNA expression of cartilage specific genes. **(A)** Samples were harvested at 0, 1, 3, 5, 7, and 14 days post-encapsulation. HACs did not redifferentiate as evidenced by the lack of collagen type II expression. Encapsulated HAC continued to express aggrecan, COMP and SOX-9 during the two week culture period. **(B)** Quantitative real time RT-PCR demonstrated a decrease in aggrecan expression in both monolayer and encapsulated cultures. Depression of aggrecan levels over time was more pronounced in alginate microbeads. **(C)** SOX-9 expression showed a biphasic response in alginate microbeads with an initial increase followed by a decrease to control levels after 24 hours. At later time points SOX-9 mRNA expression remained significantly depressed compared to the initial peak but was elevated over monolayer controls. *P < 0.05, Initial vs. End Time Point. #P < 0.05, Monolayer vs. Alginate Culture.

low cell density microbeads (Figure 6.2). Viability remained constant up to two weeks with no statistically significant differences observed. At high density, the initial viability of 73% was significantly lower compared to low density cultures. However, after one week in culture the viability increased to that of low density cultures and remained constant for up to two weeks.

Effect of Microencapsulation on Phenotype

Alginate microencapsulated HAC cells maintained the same mRNA expression profile as seen in monolayer cultures (Figure 6.3A). The encapsulated cells continued expression of aggrecan, COMP, and SOX-9 for up to 14 days in culture. Encapsulation did not reestablish collagen type II mRNA expression and there was not a significant decrease in the expression of collagen type I. In addition, there appeared to be a decrease in the expression of both aggrecan and SOX-9 mRNA, which was confirmed by quantitative real time RT-PCR. There was a significant decrease in aggrecan mRNA levels in both post-confluent monolayer cultures and alginate microbeads (Figure 6.3B). In addition, this decrease in aggrecan expression occurred earlier and was more pronounced in the microbead cultures. The mRNA levels of SOX-9 showed an initial increase immediately after encapsulation (Figure 6.3C). However, SOX-9 levels then significantly decreased after 24 hours post-encapsulation to levels similar to monolayer controls. SOX-9 mRNA expression was increased over monolayer.

Histological Analysis

Toluidine blue staining of high density ($50x10^6$ cells/ml) beads after two weeks in culture showed HAC with active formation of dark staining granules (Figure 6.4A). In

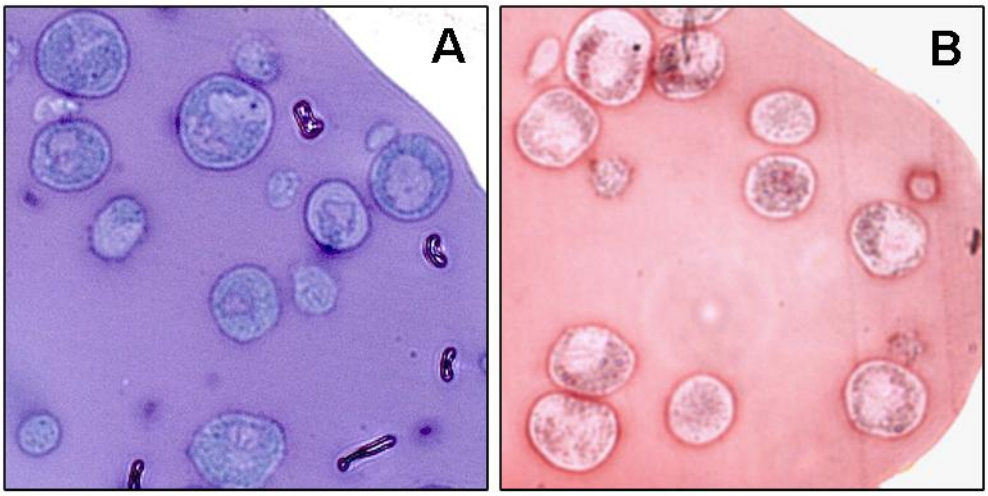

Figure 6.4: Light microscopy of microencapsulated human articular chondrocytes

Histological analysis was performed on third passage human articular chondrocytes (HACs) encapsulated at high density ($50x10^6$ cells/ml) in LVM alginate microbeads after two weeks of *in vitro* culture. **(A)** Toluidine blue staining demonstrated active living cells surrounded by a dark staining ring. **(B)** Further staining with safranin-O confirmed the presence of pericellular matrix deposition by the suspended HAC.

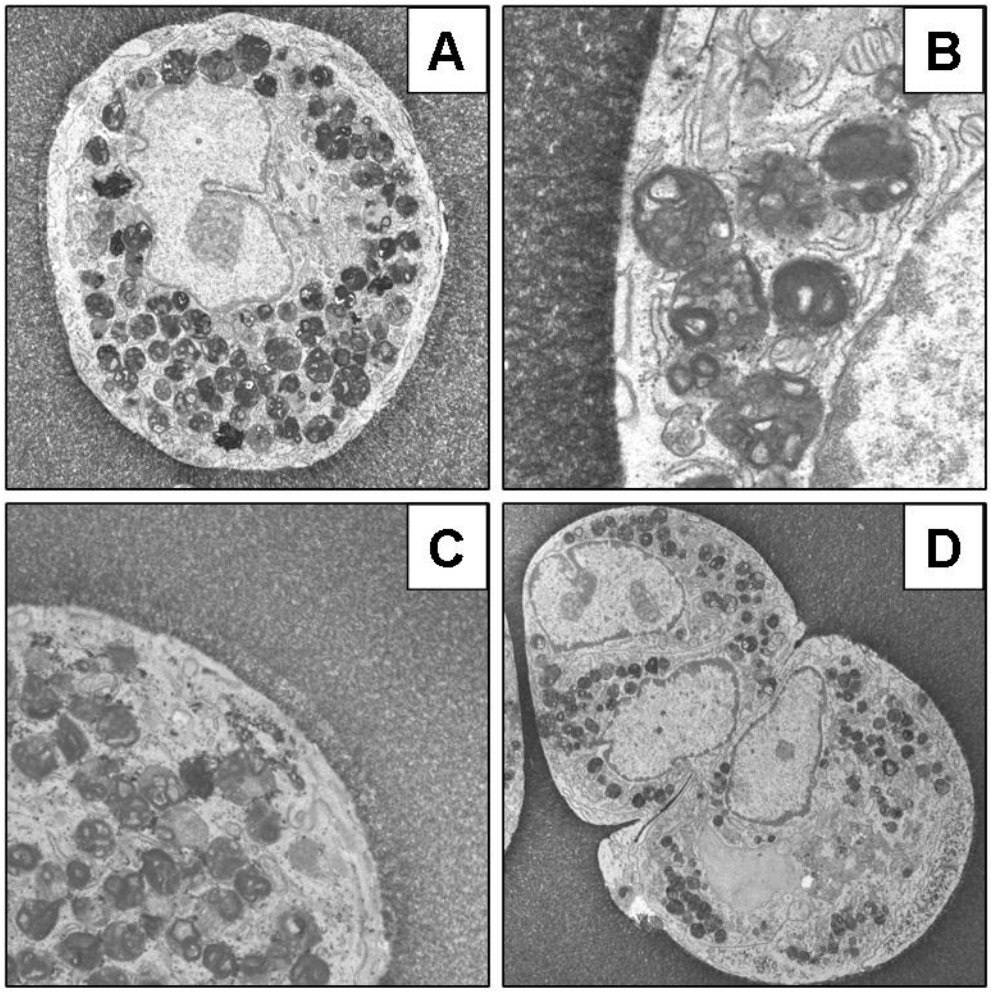

Figure 6.5: Tranmission electron microscopy of microencapsulated human articular chondrocytes

TEM was performed on third passage human articular chondrocytes (HACs) microencapsulated at high density ($50x10^6$ cells/ml) in LVM alginate following two weeks of *in vitro* culture. **(A)** HACs cells appeared intact with a distinct nucleus and highly active vesicle production in the cytoplasm. **(B)** The vesicles contained dense coiled fibers most likely composed of extracellular matrix components. In addition, the cell-alginate interface appeared denser signifying possible matrix deposition. **(C)** The presence of gaps between the cells and alginate could also indicate an attempt by the RC cells to release their matrix filled vesicles by retracting from the supporting matrix. **(D)** Minimal mitosis was observed due to the restrictive nature of the alginate which forced dividing HAC to occupy the same initial space.

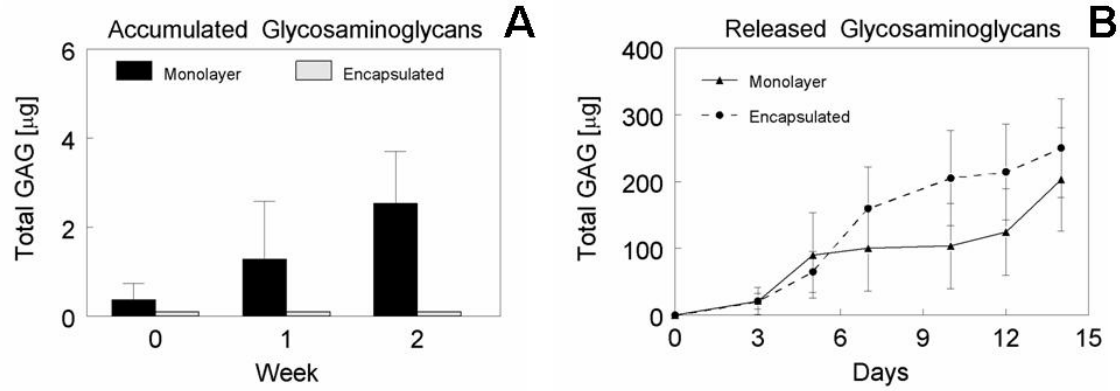

Figure 6.6: Analysis of matrix synthesis and secretion by human articular chondrocytes

Third passage human articular chondrocytes (HACs) were cultured in monolayers or low density ($6x10^6$ cells/ml) LVM microbeads, and total glycosaminoglycan (GAG) production quantified by 1,9-dimethylene blue (DMMB) dye. **(A)** Monolayer and microbead samples were harvested at 1 and 2 weeks post-confluence or post-encapsulation and the total accumulated GAGs quantified. Less than four micrograms of GAGs accumulated in monolayer HAC cultures over the two week culture period, and there were no detectable GAG levels in microbead cultures. **(B)** At 3, 5, 7, 10, 12, and 14 days post-confluence or post-encapsulation, the culture media was exchanged and the amount of free GAGs quantified. Over 200 micrograms of total GAGs were released into the culture media by both monolayer and microbead samples, indicating over fifty times more GAG was released as free GAG than was sequestered as extracellular matrix. There was no significant difference between the total GAGs released by monolayer and microbead cultures.

addition, the cells were surrounded by a dark staining ring indicating possible matrix production. Further staining with safranin-O stain suggested that the cells were producing a local matrix of proteoglycans (Figure 6.4B). A negative control of breast cancer cells encapsulated for one day did not show dark pericellular staining, signifying the observations were not an artifact of the histological processing.

TEM confirmed the histological observations in HAC cells and also showed highly active vesicle production (Figure 6.5A), containing dense coiled fibers (Figure 6.5B). Moreover, the alginate matrix in contact with HAC appeared denser, further demonstrating the deposition of pericellular matrix. The HAC did not appear to be breaking down the alginate; instead they appeared to retract from the alginate to form a gap, potentially to deposit extracellular matrix (Figure 6.5C). The HAC exhibited minimal mitosis due to the restriction of the alginate matrix and the dividing cells were forced to occupy the same space as the original cell or fill spaces vacated by dead cells (Figure 6.5D).

In vitro Matrix Production

Most of the GAG synthesized by monolayer and alginate encapsulated HAC cells was not sequestered as extracellular matrix but was instead released as free GAG into the culture media (Figure 6.6). Less than four micrograms of GAGs accumulated in post-confluent RC monolayer cultures over the two week culture period, and there were no detectable GAG levels in microbead cultures (Figure 6.6A). Over 200 micrograms of total GAGs were released into the culture media by both monolayer and microbead

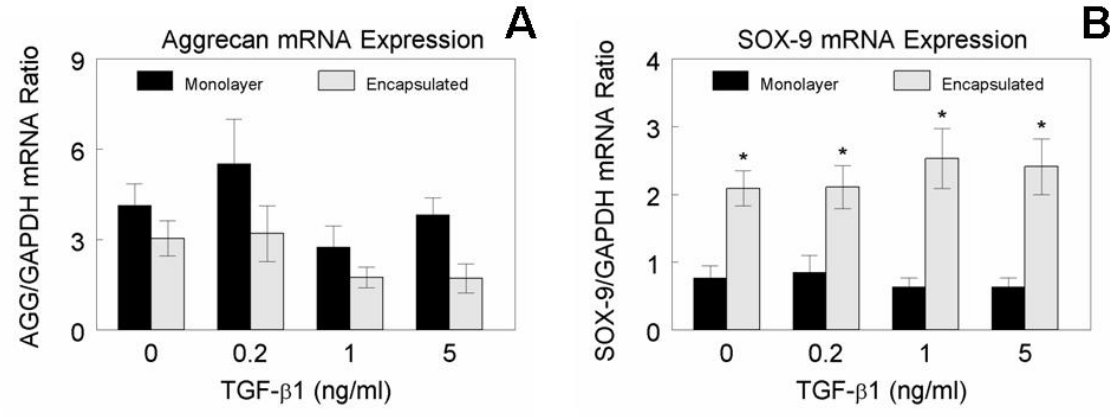

Figure 6.7: Effect of TGF-β1 on third passage human articular chondrocytes

Third passage human articular chondrocytes (HACs) suspended in LVM alginate microbeads were cultured for one week post-encapsulation before treatment with 0.2, 1.0, or 5.0 ng/ml TGF-β1 for 24 hours. Third passage HACs monolayer controls were cultured for one week post-confluence and also treated with TGF-β1. RNA was extracted and real time reverse transcription PCR (real time RT-PCR) was performed. All samples were negative for collagen type II expression. **(A)** Aggrecan expression was not significantly affected by alginate encapsulation or TGF-β1 treatment. **(B)** SOX-9 expression was not affected by TGF-β1 treatment but was significantly elevated compared to monolayer controls. *$P < 0.05$, Monolayer vs. Alginate Culture.

samples during the same two week incubation time (Figure 6.6B). There was no significant difference between the total GAGs released by monolayer or microbead cultures.

Response to TGF-β1

Treatment with TGF-β1 did not have a significant effect on redifferentiating the encapsulated HAC at any of the dosages tested. Collagen type II mRNA was not detected after treatment with TGF-β1 nor was there any effect on aggrecan or SOX-9 expression (Figure 6.7A and 6.7B). However, SOX-9 expression was significantly elevated in encapsulated cells compared to monolayer controls (Figure 6.7B).

DISCUSSION

Alginate microencapsulation using an electrostatic potential was not able to reestablish a collagen type II expressing phenotype of third passage HAC after two weeks of *in vitro* culture. Although a majority of studies using alginate encapsulation of human articular chondrocytes have reported redifferentiation, it has also been shown that three dimensional encapsulation can be insufficient. Alginate encapsulation alone was unable to redifferentiate human septal chondrocytes expanded beyond first passage [217] or HAC expanded to third passage [218]. Several factors have been identified that may account for this variation.

The serum conditions used for *in vitro* culture of chondrocytes have been shown to be critical for phenotype development. The expression of collagen type II by alginate suspended second passage HAC was shown to be highly dependent upon the lot of FBS used to culture the cells [219]. Moreover, it has been established that the use human serum

is more beneficial than FBS for promoting a chondrocytic phenotype in human chondrocytes [196, 220]. Serum-free culture of chondrocytes has also been investigated to simulate the avascular environment of cartilage tissue. Chondrogenesis of human mesenchymal stem cells was shown to be enhanced under serum-free conditions [221]. In addition, the use of serum-free media supplemented with specific chondrogenic factors like IGF-1, FGF-2, and TGF-β2 was superior to FBS for supporting redifferentiation of expanded human auricular chondrocytes [208, 222].

Cartilage tissue has a low oxygen tension due to its lack of vasculature, and it is well-known that using a more physiologic oxygen tension when culturing chondrocytes improves the expression of cartilage specific genes [168, 218]. The smaller size of the microbeads results in a more uniform gradient of nutrient diffusion throughout the construct [70]. This would be beneficial for most types of tissue by reducing mass transfer limitations and decreasing the development of necrotic cores. However, this may have been counter productive for promoting a chondrocytic phenotype, which favors a nutrient poor environment. This hypothesis is further supported by the fact that increasing chondrocyte seeding density of alginate constructs, and therefore the competition for nutrients, leads to improved cartilage tissue formation [67]. The mRNA expression profile of high cell density and low cell density microbeads could be significantly different based on these previous studies and should be investigated. Moreover, the possible temporal changes observed in aggrecan and SOX-9 expression may in part be due to an initial hypoxia or lack of nutrients during the encapsulation process.

Despite the lack of collagen type II expression, the HAC suspended in alginate microbeads maintained strong levels of aggrecan and COMP, and also showed increased

levels of SOX-9 compared to confluent monolayer controls. It has been well established that alginate suspension increases SOX-9 levels [208, 223, 224], but it has also been reported that a high expression of SOX-9 does not necessarily correlate to an increase in collagen type II expression [225]. Recent work has suggested that SOX-9 exerts a bi-functional effect on *COL2A1* that is dependent on the differentiation state of the chondrocyte [204]. Low levels of SOX-9 overexpression enhanced *COL2A1* gene transcription of both primary and second passage rabbit articular chondrocytes, but high levels of SOX-9 overexpression were inhibitory. Further dedifferentiation of the chondrocytes to fifth passage resulted in depressed *COL2A1* transcriptional activity that was independent of SOX-9 levels. Moreover, osteoarthritic chondrocytes, which exhibit similar cellular biology to dedifferentiated chondrocytes, have an up-regulation of *COL2A1* despite a decrease in SOX-9 levels [226].

Supplementation of the growth media with various chondrogenic factors has demonstrated the ability to enhance redifferentiation of expanded human articular chondrocytes [194, 219, 227, 228]. TGF-β1 plays a role in early chondrogenesis [229] and has been shown to be important in the differentiation of mesenchymal stem cells toward a chondrogenic lineage [212, 230]. In addition, TGF-β1 is responsible for preventing terminal differentiation of chondrocytes towards a hypertrophic and apoptotic pathway [231, 232]. In the present study, however, TGF-β1 treatment did not have any effect on aggrecan, collagen type II, or SOX-9 levels in HACs suspended in alginate microbeads. TGF-β1 was selected based on our previous work with rat growth plate chondrocytes which showed enhanced differentiation via interacting PKC and PKA mediated mechanisms [89, 233, 234]. Improved redifferentiation of alginate suspended HAC has been demonstrated

using TGF-β1 [219, 235], but it has also been reported that TGF-β1 can be ineffective and even inhibitory [236, 237]. These varying observations may be due to the precise state of dedifferentiation of the chondrocytes based on species, passage number and culture conditions.

The formation of microbeads has many applications for tissue engineering and biotechnology. The small size allows for minimally invasive injectable therapies where the cells are protected by the hydrogel matrix, while also being large enough to easily manipulate and permit precise control over the number, type, and distribution of cells implanted. The electrostatic encapsulation process was well tolerated by the HACs as signified by their viability and expression of cartilage specific molecules. However, the HACs did not redifferentiate when suspended in the microbeads. Further studies are needed to determine what biological effects the alteration in mass transport had on the microbead system.

CHAPTER 7

Conclusions and Future Perspectives

This work has established that 17β-estradiol (E_2) plays a significant role in orthopaedic tissue engineering and regenerative medicine. We have shown that E_2 has an important sex-specific function in regulating the phenotype of human articular chondrocytes. Moreover, the osteoinductive properties of demineralized bone matrix (DBM) are inhibited in an estrogen deficient environment. However, there are still numerous unanswered questions regarding sexual dimorphism and cartilage regeneration.

The most important next step is identifying what receptor protein is mediating the rapid membrane-associated effects of E_2. This would allow further characterization and understanding of this non-traditional steroid signaling mechanism. Furthermore, it may lead to the discovering of other steroid membrane receptors including membrane receptors for androgens. It would also be of interest to investigate if this sex-specific E_2 membrane effect was present in all tissues including other types of cartilage like elastic auricular tissue or intervertebral discs. Perhaps different tissues express variable concentrations and isoforms of sex steroid membrane receptors that control their sexual dimorphism. If this is the case, then the development of drugs that are more beneficial for only men or women may be a reality in the future. Moreover, it may be possible to design compounds that only activate the membrane steroid receptors and not the traditional cytoplasmic receptors. This could be very beneficial for the treatment of post-menopausal osteoarthritis and osteoporosis while not increasing the risks commonly

associated with hormone replacement therapy like increased incidence of breast and ovarian cancers.

We were unable to produce a tissue engineered cartilage implant to determine what role E_2 could have on *in vivo* tissue formation. However, we did uncover many interesting differences between human articular chondrocytes (HAC) and rat costochondral resting zone growth plate chondrocytes (RCs) and their response to alginate microencapsulation. First, RC cells did not express SOX-9 but still showed expression of collagen type II, while HAC had the opposite expression profile. This lack of correlation between collagen type II and SOX-9 expression accentuates the complexity of chondrocyte biology. Further study is needed to determine what effects species, cartilage type, and monolayer expansion have on the activity of SOX-9. Second, HACs had a significantly better survival rate at high cell densities than RC cells. This is not completely unexpected as the resting zone of the growth plate is accustomed to receiving more nutrients than articular cartilage due to the vasculature of the surrounding bone. However, this difference highlights that there are important biological differences between the resting zone growth plate and articular cartilage even though they both are hyaline cartilage. Third, HAC produced significantly more glycosaminoglcyans (GAGs) compared to RC cells. However, the retention of secreted GAGs was minimal in both cell types.

Previous studies have also reported this lack of GAG accumulation in alginate suspended chondrocyte cultures [189, 190]. One possible explanation is that the chondrocytes are not generating or correctly assembling the necessary hyaluronic acid (HA) backbone to aggregate the proteoglycans produced. Moreover, there could be a deficiency in link

proteins that are necessary for binding of the proteoglycans to HA. The collagen scaffold is also important for the accumulation of GAGs via the anchoring of HA. The lack of collagen type II expression by HACs could have partially been responsible for our observations. In addition, we did not measure the expression of other cartilage specific collagens like type VI, type IX, and type XI. The RCs could have been deficient in these collagens even though they showed expression of collagen type II and thereby potentially explain their inability to aggregate proteoglycans. It is also possible that the inability to sequester GAGs was the result of increased activity of degradation enzymes like matrix metalloproteinases (MMPs) and aggrecanases. This theory is further supported by the fact that chondrocytes isolated from arthritic cartilage have an increased expression of degradation enzymes, and dedifferentiated chondrocytes have been shown to exhibit similar biochemistry to osteoarthritic chondrocytes. The composition of the surrounding extracellular matrix is critical for chondrogenesis [191], and the addition of extracellular matrix molecules like fibronectin or collagen to the alginate gel can significantly alter the phenotype of chondrocytes [192].

Alginate microencapsulation was not able to redifferentiate second or third passage HACs using our culture conditions. As previously mentioned in Chapter 6, there are many possible modifications that could be investigated to enhance chondrogenesis of the alginate microbeads. One of the more important parameters appears to be the culture serum. Screening different lots of fetal bovine serum for redifferentiation potential may be required to maximize the chondrocytic phenotype of suspended HACs. In addition, it would of interest to study the effects of human serum, especially if there are sex-specific effects that are dependent on serum donor sex. Serum-free conditions that simulate the

avascularity of cartilage have also been shown to enhance redifferentiation, especially when supplement with growth factors. Speaking of which, we could examine the effects of other growth factors besides TGF-β1 like BMP-2, TGF-β2, IGF-1, and FGF-2 either alone or in combinations. Finally, there is the application of reduced oxygen tension to further mimic the normal physiologic cartilage environment. This requires the development of a specialized incubation chamber, but oxygen tension has been well established as a major component affecting chondrogenesis *in vitro* and should be explored with respect to our microbead system.

There has been minimal experimentation on the how alginate composition affects encapsulated cells. Our studies did not detect any differences based on composition, but we limited our measurements to viability. Although there have not been any reports of cells interacting biologically with alginate, the composition of alginate does determine the pore size of the matrix. This is very important in determining how much space the cells have to deposit matrix, as well as for defining the diffusivity of large molecules like growth factors and matrix components into and out of the microbeads. The addition of other matrix molecules to the alginate suspension could also assist in further simulating a normal environment for the chondrocytes. This is especially relevant for pericellular components like fibronectin and collagen type VI, which would aid in the reestablishment of biochemical and biomechanical signals between the chondrocytes and extracellular matrix.

The chondrocytes encapsulated within alginate microbeads were unable to form hyaline cartilage tissue when implanted into athymic mice. There are several possible reasons to explain these results as well as alternative approaches that could improve

chondrogenesis in the microbead system. The RCs demonstrated they were capable of forming cartilage nodules at the implantation site when not suspended in alginate. This suggests the lack of chondrogenesis is the result of the alginate restricting cell proliferation and matrix synthesis. This hypothesis could be tested by modifying the microbead system to degrade faster. Possible methods to achieve this include using a lower concentration of alginate, gamma irradiating the alginate to reduce the molecular weight, and mixing in other substances into the alginate like gelatin that will degrade more rapidly.

Reducing the total amount of alginate by increasing the cell density would also decrease the degradation time. In addition, our results and previous studies have shown that cell seeding density is important in regulating the phenotype of chondrocytes [67, 238]. It is unknown why chondrocytes require a high cell density to maintain a differentiated state. One possible explanation is that a critical threshold of autocrine or paracrine factors must be produced locally by the chondrocytes. It is known chondrocytes are capable of producing several factors locally, including steroid hormones like estrogen. Cell-matrix interactions are also very important for maintaining a chondrocytic phenotype. A greater number of chondrocytes would produce more extracellular matrix and therefore facilitate these interactions. Lastly, chondrocytes may also require cell-cell interactions similar to osteocytes. These cell-cell connections could provide another avenue for information to pass between cells via receptor mediated pathways or junctions.

Our choice of implantation site also could have influenced the ability of the microbeads to form cartilaginous tissue. As previously discussed, cartilage is an

avascular tissue and therefore the normal physiologic environment is poor in oxygen and serum components. The intramuscular implant site was chosen because induced endochondral ossification by demineralized bone matrix (DBM) has been shown to be optimal in this location. A different implant site, however, may be preferable for forming cartilage with our microbead system. The most obvious choice is to use a cartilage defect model. This has the advantage of mimicking the eventual clinical scenario, but a cartilage site also has several disadvantages as well. The size of the implant is restricted by the joint which can be significantly limiting in the case of rodents. In addition, articular sites introduce mechanical forces which can dislodge and damage the implant, as well as provide an uncontrolled variable to the system. Non-load bearing sites like the xiphoid could be used to circumvent this issue. Another commonly used implant site is the skin. A subcutaneous pouch is more nutrient poor compared to muscle and alginate constructs have been shown to be form cartilage-like tissue in such models [238].

The minimal degradation we observed in our system could have also been the result of the animal model chosen. The athymic mice have an impaired immune system which is beneficial for the implanted xenogeneic cells, but this could have reduced the enzymatic degradation of the alginate [238]. This problem could potentially be circumvented by using allogeneic cells of inbred rodent strains, thereby eliminating the need for athymic animals. However, the use of allogeneic mature chondrocytes would still require the expansion of cells over multiple passages to provide a sufficient cell number capable of repairing a cartilage defect. As previously discussed, monolayer expansion negatively impacts the phenotype of chondrocytes. One possible solution would be to use adult stem cells derived from mesenchymal tissues including bone

marrow stroma, muscle, and fat. Mesenchymal stem cells (MSCs) have the benefit of being able to divide indefinitely allowing substantial expansion of the cell source. The MSCs could then be differentiated towards a chondrogenic phenotype using various growth factor protocols previously discussed. Moreover, the use three dimensional suspension culture has been shown to enhance the differentiation of MSCs towards a chondrogenic phenotype.

The microbead technology has other possible applications in tissue engineering besides the use as a culture system. The microbeads also provide the potential for double encapsulation procedures. The small size of the microbeads would allow them to be suspended in a second alginate and cell solution. This solution could then be extruded through a larger bore needle to form constructs with islands of microbeads. Different combinations of cells could be used to form heterogeneous tissue arrangements. Examples include the mixture of mature osteoblasts or chondrocytes with mesenchymal stem cells, or the use of microbeads with vascular progenitor cells to form vascularized tissues like bone, liver, or spleen. Microbeads with cells genetically engineered to express specific growth factors could also be used in this system to provide a more uniform gradient compared to diffusion of factors from the bulk fluid.

Finally, further investigation between the interaction of hormones and hydrogel suspension should be investigated. As previous mentioned, E_2 and alginate encapsulation have been shown to activate the same protein kinase C (PKC) isoform. It is unknown whether this could result in a synergistic increase in chondrogenesis, or have a negative effect due to over-stimulation. Moreover, it has been shown that estrogen treatment can increase SOX-9 expression in chondrocytes. This study and others have shown alginate

suspension increases SOX-9 expression, further supporting a possible interaction. A thorough understanding of the complex interactions between cells, scaffolds and environment is needed before a successful strategy for cartilage tissue engineering and regeneration can be developed.

REFERENCES

1. Sadler T.W. Skeletal System. In: Sun B., eds. Langman's Medical Embryology, 9th Ed. Philadelphia, PA: Lippincott Williams & Wilkins 2004: pg. 171-98

2. Goldring M.B., Tsuchimochi K. and Ijiri K. The control of chondrogenesis. J Cell Biochem 2006; 97: 33-44

3. Goldring S.R. and Goldring M.B. Biology of the Normal Joint. In: Harris E.D., Budd R.C., Genovese M.C., Firestein G.S., Sargent J.S. and Sledge C.B., eds. Kelley's Textbook of Rheumatology, 7th Ed. Philadelphia, PA: Elsevier Saunders 2005: pg. 1-37

4. Lin Z., Willers C., Xu J. and Zheng M.H. The chondrocyte: biology and clinical application. Tissue Eng 2006; 12: 1971-84

5. Buckwalter J.A. Articular Cartilage: Overview. In: Goldberg V.M. and Caplan A.I., eds. Orthopedic Tissue Engineering: Basic Science and Practice, Ed. New York, NY: Marcel Dekker, Inc. 2004: pg. 179-200

6. Gupta R., Caiozzo V.J. and Skinner H.B. Basic Science in Orthopedic Surgery. In: Skinner H.B., eds. Current Diagnosis & Treatment in Orthopedics, 4th Ed. Columbus, OH: The McGraw-Hill Companies, Inc. 2006: pg. 1-63

7. Buckwalter J.A. and Mow V.C. Basic Science and Injury of Articular Cartilage, Menisci, and Bone: Section A. In: Delee J.C. and Drez D., eds. DeLee & Drez's Orthopaedic Sports Medicine, 2nd Ed. Philadelphia, PA Elsevier Saunders 2003: pg. 67-86

8. Guilak F., Alexopoulos L.G., Upton M.L., Youn I., Choi J.B., Cao L., Setton L.A. and Haider M.A. The pericellular matrix as a transducer of biomechanical and biochemical signals in articular cartilage. Ann N Y Acad Sci 2006; 1068: 498-512

9. Koelling S., Clauditz T.S., Kaste M. and Miosge N. Cartilage oligomeric matrix protein is involved in human limb development and in the pathogenesis of osteoarthritis. Arthritis Res Ther 2006; 8: R56

10. Merritt T.M., Alcorn J.L., Haynes R. and Hecht J.T. Expression of mutant cartilage oligomeric matrix protein in human chondrocytes induces the pseudoachondroplasia phenotype. J Orthop Res 2006; 24: 700-7

11. Rosenstrauch D., Kadipasaoglu K., Shelat H., Zoldhelyi P. and Frazier O.H. Auricular Cartilage Tissue Engineering. In: Yaszemski M.J., Trantolo D.J.,

Lewandrowski K., Hasirci A., Altobelle D.E. and Wise D.L., eds. Tissue Engineering and Novel Delivery Systems, Ed. New York, NY: Marcel Dekker, Inc. 2004: pg. 253-64

12. Goldring M.B. Chondrocytes. In: Harris E.D., Budd R.C., Genovese M.C., Firestein G.S., Sargent J.S. and Sledge C.B., eds. Kelley's Textbook of Rheumatology, 7th Ed. Philadelphia, PA: Elsevier Saunders 2005: pg. 203-34

13. Young B. and Heath J.W. Skeletal Tissues. In: eds. Wheater's Functional Histology, 4th Ed. London, England: Harcourt Publishers Limited 2000: pg. 172-92

14. Rosenberg A. Bones, Joints, and Soft Tissue Tumors. In: Cotran R.S., Kumar V. and Collins T., eds. Robbins Pathologic Basis of Disease, 6th Ed. Philadelphia, PA: W.B. Saunders Company 1999: pg.

15. Kinner B. and Spector M. Cartilage: Current Applications. In: Goldberg V.M. and Caplan A.I., eds. Orthopedic Tissue Engineering: Basic Science and Practice, Ed. New York, NY: Marcel Dekker, Inc. 2004: pg. 210-36

16. Tuan R.S. Experimental Principles and Future Perspectives of Skeletal Tissue Engineering. In: Sandell L.J. and Grodzinsky A.J., eds. Tissue Engineering in Musculoskeletal Clinical Practice, Ed. Rosemont, IL: American Academy of Orthopaedic Surgeons 2004: pg.

17. Namba R.S., Skinner H.B. and Gupta R. Adult Reconstructive Surgery. In: Skinner H.B., eds. Current Diagnosis & Treatment in Orthopedics, 4th Ed. Columbus, OH: The McGraw-Hill Companies, Inc. 2006: pg. 381-423

18. Stryer L. Biosynthesis of Membrane Lipids and Steroids. In: Stryer L., eds. Biochemistry, 4th Ed. New York, NY: W.H. Freeman and Company 1995: pg. 685-712

19. Guyton A.C. and Hall J.E. Female Physiology Before Pregnancy; and the Female Hormones. In: Guyton A.C. and Hall J.E., eds. Textbook of Medical Physiology, 9th Ed. Philadelphia, PA: W.B. Saunders Company 1996: pg. 1017-32

20. Guyton A.C. and Hall J.E. Introduction to Endocrinology. In: Guyton A.C. and Hall J.E., eds. Textbook of Medical Physiology, 9th Ed. Philadelphia, PA: W.B. Saunders Company 1996: pg. 925-32

21. Boyan B.D. and Schwartz Z. Rapid vitamin D-dependent PKC signaling shares features with estrogen-dependent PKC signaling in cartilage and bone. Steroids 2004; 69: 591-7

22. van der Eerden B.C., Karperien M. and Wit J.M. The estrogen receptor in the growth plate: implications for pubertal growth. J Pediatr Endocrinol Metab 2001; 14 Suppl 6: 1527-33

23. Grumbach M.M. Estrogen, bone, growth and sex: a sea change in conventional wisdom. J Pediatr Endocrinol Metab 2000; 13 Suppl 6: 1439-55

24. Juul A. The effects of oestrogens on linear bone growth. Hum Reprod Update 2001; 7: 303-13

25. Tosi L.L., Boyan B.D. and Boskey A.L. Does sex matter in musculoskeletal health? The influence of sex and gender on musculoskeletal health. J Bone Joint Surg Am 2005; 87: 1631-47

26. Tosi L.L., Boyan B.D. and Boskey A.L. Does sex matter in musculoskeletal health? A workshop report. Orthop Clin North Am 2006; 37: 523-9

27. Cecil R.L. and Archer B. Athritis of the menopause. J Am Med Assoc 1925; 84: 75-9

28. Felson D.T. and Nevitt M.C. The effects of estrogen on osteoarthritis. Curr Opin Rheumatol 1998; 10: 269-72

29. Richette P., Corvol M. and Bardin T. Estrogens, cartilage, and osteoarthritis. Joint Bone Spine 2003; 70: 257-62

30. Wluka A.E., Cicuttini F.M. and Spector T.D. Menopause, oestrogens and arthritis. Maturitas 2000; 35: 183-99

31. Rosner I.A., Manni A., Malemud C.J., Boja B. and Moskowitz R.W. Estradiol receptors in articular chondrocytes. Biochem Biophys Res Commun 1982; 106: 1378-82

32. Young P.C. and Stack M.T. Estrogen and glucocorticoid receptors in adult canine articular cartilage. Arthritis Rheum 1982; 25: 568-73

33. Ushiyama T., Ueyama H., Inoue K., Ohkubo I. and Hukuda S. Expression of genes for estrogen receptors alpha and beta in human articular chondrocytes. Osteoarthritis Cartilage 1999; 7: 560-6

34. Claassen H., Hassenpflug J., Schunke M., Sierralta W., Thole H. and Kurz B. Immunohistochemical detection of estrogen receptor alpha in articular chondrocytes from cows, pigs and humans: in situ and in vitro results. Ann Anat 2001; 183: 223-7

35. Nasatzky E., Schwartz Z., Soskolne W.A., Brooks B.P., Dean D.D., Boyan B.D. and Ornoy A. Evidence for receptors specific for 17 beta-estradiol and testosterone in chondrocyte cultures. Connect Tissue Res 1994; 30: 277-94

36. Felson D.T. and Nevitt M.C. Estrogen and osteoarthritis: how do we explain conflicting study results? Prev Med 1999; 28: 445-8; discussion 9-50

37. Reginster J.Y., Kvasz A., Bruyere O. and Henrotin Y. Is there any rationale for prescribing hormone replacement therapy (HRT) to prevent or to treat osteoarthritis? Osteoarthritis Cartilage 2003; 11: 87-91

38. Wluka A.E., Davis S.R., Bailey M., Stuckey S.L. and Cicuttini F.M. Users of oestrogen replacement therapy have more knee cartilage than non-users. Ann Rheum Dis 2001; 60: 332-6

39. Rosner I.A., Goldberg V.M., Getzy L. and Moskowitz R.W. Effects of estrogen on cartilage and experimentally induced osteoarthritis. Arthritis Rheum 1979; 22: 52-8

40. Rosner I.A., Goldberg V.M. and Moskowitz R.W. Estrogens and osteoarthritis. Clin Orthop Relat Res 1986; 77-83

41. Tsai C.L. and Liu T.K. Estradiol-induced knee osteoarthrosis in ovariectomized rabbits. Clin Orthop Relat Res 1993; 295-302

42. Turner A.S., Athanasiou K.A., Zhu C.F., Alvis M.R. and Bryant H.U. Biochemical effects of estrogen on articular cartilage in ovariectomized sheep. Osteoarthritis Cartilage 1997; 5: 63-9

43. Ham K.D., Loeser R.F., Lindgren B.R. and Carlson C.S. Effects of long-term estrogen replacement therapy on osteoarthritis severity in cynomolgus monkeys. Arthritis Rheum 2002; 46: 1956-64

44. Nasatzky E., Schwartz Z., Boyan B.D., Soskolne W.A. and Ornoy A. Sex-dependent effects of 17-beta-estradiol on chondrocyte differentiation in culture. J Cell Physiol 1993; 154: 359-67

45. Sylvia V.L., Hughes T., Dean D.D., Boyan B.D. and Schwartz Z. 17beta-estradiol regulation of protein kinase C activity in chondrocytes is sex-dependent and involves nongenomic mechanisms. J Cell Physiol 1998; 176: 435-44

46. Sylvia V.L., Boyan B.D., Dean D.D. and Schwartz Z. The membrane effects of 17beta-estradiol on chondrocyte phenotypic expression are mediated by activation of protein kinase C through phospholipase C and G-proteins. J Steroid Biochem Mol Biol 2000; 73: 211-24

47. Sylvia V.L., Walton J., Lopez D., Dean D.D., Boyan B.D. and Schwartz Z. 17 beta-estradiol-BSA conjugates and 17 beta-estradiol regulate growth plate chondrocytes by common membrane associated mechanisms involving PKC dependent and independent signal transduction. J Cell Biochem 2001; 81: 413-29

48. Schwartz Z., Sylvia V.L., Guinee T., Dean D.D. and Boyan B.D. Tamoxifen elicits its anti-estrogen effects in growth plate chondrocytes by inhibiting protein kinase C. J Steroid Biochem Mol Biol 2002; 80: 401-10

49. McMillan J., Fatehi-Sedeh S., Sylvia V.L., Bingham V., Zhong M., Boyan B.D. and Schwartz Z. Sex-specific regulation of growth plate chondrocytes by estrogen is via multiple MAP kinase signaling pathways. Biochim Biophys Acta 2006; 1763: 381-92

50. Mayne R., Vail M.S., Mayne P.M. and Miller E.J. Changes in type of collagen synthesized as clones of chick chondrocytes grow and eventually lose division capacity. Proc Natl Acad Sci U S A 1976; 73: 1674-8

51. Darling E.M. and Athanasiou K.A. Rapid phenotypic changes in passaged articular chondrocyte subpopulations. J Orthop Res 2005; 23: 425-32

52. Benya P.D. Modulation and reexpression of the chondrocyte phenotype; mediation by cell shape and microfilament modification. Pathol Immunopathol Res 1988; 7: 51-4

53. Loty S., Forest N., Boulekbache H. and Sautier J.M. Cytochalasin D induces changes in cell shape and promotes in vitro chondrogenesis: a morphological study. Biol Cell 1995; 83: 149-61

54. Newman P. and Watt F.M. Influence of cytochalasin D-induced changes in cell shape on proteoglycan synthesis by cultured articular chondrocytes. Exp Cell Res 1988; 178: 199-210

55. Takigawa M., Takano T., Shirai E. and Suzuki F. Cytoskeleton and differentiation: effects of cytochalasin B and colchicine on expression of the differentiated phenotype of rabbit costal chondrocytes in culture. Cell Differ 1984; 14: 197-204

56. Benya P.D. and Shaffer J.D. Dedifferentiated chondrocytes reexpress the differentiated collagen phenotype when cultured in agarose gels. Cell 1982; 30: 215-24

57. Guo J.F., Jourdian G.W. and MacCallum D.K. Culture and growth characteristics of chondrocytes encapsulated in alginate beads. Connect Tissue Res 1989; 19: 277-97

58. Smidsrod O. and Skjak-Braek G. Alginate as immobilization matrix for cells. Trends Biotechnol 1990; 8: 71-8

59. Hauselmann H.J., Aydelotte M.B., Schumacher B.L., Kuettner K.E., Gitelis S.H. and Thonar E.J. Synthesis and turnover of proteoglycans by human and bovine adult articular chondrocytes cultured in alginate beads. Matrix 1992; 12: 116-29

60. Lee D.A., Reisler T. and Bader D.L. Expansion of chondrocytes for tissue engineering in alginate beads enhances chondrocytic phenotype compared to conventional monolayer techniques. Acta Orthop Scand 2003; 74: 6-15

61. Tamponnet C., Ramdi H., Guyot J.B. and Lievremont M. Rabbit articular chondrocytes in alginate gel: characterisation of immobilized preparations and potential applications. Appl Microbiol Biotechnol 1992; 37: 311-5

62. Yoon Y.M., Kim S.J., Oh C.D., Ju J.W., Song W.K., Yoo Y.J., Huh T.L. and Chun J.S. Maintenance of differentiated phenotype of articular chondrocytes by protein kinase C and extracellular signal-regulated protein kinase. J Biol Chem 2002; 277: 8412-20

63. Bonaventure J., Kadhom N., Cohen-Solal L., Ng K.H., Bourguignon J., Lasselin C. and Freisinger P. Reexpression of cartilage-specific genes by dedifferentiated human articular chondrocytes cultured in alginate beads. Exp Cell Res 1994; 212: 97-104

64. Hauselmann H.J., Masuda K., Hunziker E.B., Neidhart M., Mok S.S., Michel B.A. and Thonar E.J. Adult human chondrocytes cultured in alginate form a matrix similar to native human articular cartilage. Am J Physiol 1996; 271: C742-52

65. Schulze-Tanzil G., de Souza P., Villegas Castrejon H., John T., Merker H.J., Scheid A. and Shakibaei M. Redifferentiation of dedifferentiated human chondrocytes in high-density cultures. Cell Tissue Res 2002; 308: 371-9

66. Loty S., Sautier J.M., Loty C., Boulekbache H., Kokubo T. and Forest N. Cartilage formation by fetal rat chondrocytes cultured in alginate beads: a proposed model for investigating tissue-biomaterial interactions. J Biomed Mater Res 1998; 42: 213-22

67. Chang S.C., Rowley J.A., Tobias G., Genes N.G., Roy A.K., Mooney D.J., Vacanti C.A. and Bonassar L.J. Injection molding of chondrocyte/alginate constructs in the shape of facial implants. J Biomed Mater Res 2001; 55: 503-11

68. Lim F. and Sun A.M. Microencapsulated islets as bioartificial endocrine pancreas. Science 1980; 210: 908-10

69. Reis C.P., Neufeld R.J., Vilela S., Ribeiro A.J. and Veiga F. Review and current status of emulsion/dispersion technology using an internal gelation process for the design of alginate particles. J Microencapsul 2006; 23: 245-57

70. Goosen M.F. Physico-chemical and mass transfer considerations in microencapsulation. Ann N Y Acad Sci 1999; 875: 84-104

71. Colton C.K. Engineering challenges in cell-encapsulation technology. Trends Biotechnol 1996; 14: 158-62

72. Smith M.K. and Mooney D.J. Hypoxia leads to necrotic hepatocyte death. J Biomed Mater Res A 2007; 80: 520-9

73. Stabler C., Wilks K., Sambanis A. and Constantinidis I. The effects of alginate composition on encapsulated betaTC3 cells. Biomaterials 2001; 22: 1301-10

74. Robitaille R., Pariseau J.F., Leblond F.A., Lamoureux M., Lepage Y. and Halle J.P. Studies on small (<350 microm) alginate-poly-L-lysine microcapsules. III. Biocompatibility Of smaller versus standard microcapsules. J Biomed Mater Res 1999; 44: 116-20

75. Klokk T.I. and Melvik J.E. Controlling the size of alginate gel beads by use of a high electrostatic potential. J Microencapsul 2002; 19: 415-24

76. van der Kraan P.M., Buma P., van Kuppevelt T. and van den Berg W.B. Interaction of chondrocytes, extracellular matrix and growth factors: relevance for articular cartilage tissue engineering. Osteoarthritis Cartilage 2002; 10: 631-7

77. Schwartz Z., Soskolne W.A., Neubauer T., Goldstein M., Adi S. and Ornoy A. Direct and sex-specific enhancement of bone formation and calcification by sex steroids in fetal mice long bone in vitro (biochemical and morphometric study. Endocrinology 1991; 129: 1167-74

78. Schwartz Z., Gates P.A., Nasatzky E., Sylvia V.L., Mendez J., Dean D.D. and Boyan B.D. Effect of 17 beta-estradiol on chondrocyte membrane fluidity and phospholipid metabolism is membrane-specific, sex-specific, and cell maturation-dependent. Biochim Biophys Acta 1996; 1282: 1-10

79. Harvey B.J., Doolan C.M., Condliffe S.B., Renard C., Alzamora R. and Urbach V. Non-genomic convergent and divergent signalling of rapid responses to aldosterone and estradiol in mammalian colon. Steroids 2002; 67: 483-91

80. Doolan C.M. and Harvey B.J. A Galphas protein-coupled membrane receptor, distinct from the classical oestrogen receptor, transduces rapid effects of oestradiol on [Ca2+]i in female rat distal colon. Mol Cell Endocrinol 2003; 199: 87-103

81. Boyan B.D., Schwartz Z., Swain L.D., Carnes D.L., Jr. and Zislis T. Differential expression of phenotype by resting zone and growth region costochondral chondrocytes in vitro. Bone 1988; 9: 185-94

82. Schnabel M., Marlovits S., Eckhoff G., Fichtel I., Gotzen L., Vecsei V. and Schlegel J. Dedifferentiation-associated changes in morphology and gene expression in primary human articular chondrocytes in cell culture. Osteoarthritis Cartilage 2002; 10: 62-70

83. Schwartz Z., Schlader D.L., Ramirez V., Kennedy M.B. and Boyan B.D. Effects of vitamin D metabolites on collagen production and cell proliferation of growth zone and resting zone cartilage cells in vitro. J Bone Miner Res 1989; 4: 199-207

84. Hale L.V., Kemick M.L. and Wuthier R.E. Effect of vitamin D metabolites on the expression of alkaline phosphatase activity by epiphyseal hypertrophic chondrocytes in primary cell culture. J Bone Miner Res 1986; 1: 489-95

85. O'Keefe R.J., Puzas J.E., Brand J.S. and Rosier R.N. Effects of transforming growth factor-beta on matrix synthesis by chick growth plate chondrocytes. Endocrinology 1988; 122: 2953-61

86. Herbert J.M., Augereau J.M., Gleye J. and Maffrand J.P. Chelerythrine is a potent and specific inhibitor of protein kinase C. Biochem Biophys Res Commun 1990; 172: 993-9

87. Jarvis W.D., Turner A.J., Povirk L.F., Traylor R.S. and Grant S. Induction of apoptotic DNA fragmentation and cell death in HL-60 human promyelocytic leukemia cells by pharmacological inhibitors of protein kinase C. Cancer Res 1994; 54: 1707-14

88. Kandasamy R.A., Yu F.H., Harris R., Boucher A., Hanrahan J.W. and Orlowski J. Plasma membrane Na+/H+ exchanger isoforms (NHE-1, -2, and -3) are differentially responsive to second messenger agonists of the protein kinase A and C pathways. J Biol Chem 1995; 270: 29209-16

89. Sylvia V.L., Schwartz Z., Dean D.D. and Boyan B.D. Transforming growth factor-beta1 regulation of resting zone chondrocytes is mediated by two separate but interacting pathways. Biochim Biophys Acta 2000; 1496: 311-24

90. Benya P.D., Padilla S.R. and Nimni M.E. Independent regulation of collagen types by chondrocytes during the loss of differentiated function in culture. Cell 1978; 15: 1313-21

91. Lagumdzija A., Bucht E., Stark A., Hulting A.L. and Petersson M. Arg-vasopressin increases proliferation of human osteoblast-like cells and decreases

production of interleukin-6 and macrophage colony-stimulating factor. Regul Pept 2004; 121: 41-8

92. Valhmu W.B. and Raia F.J. myo-Inositol 1,4,5-trisphosphate and Ca(2+)/calmodulin-dependent factors mediate transduction of compression-induced signals in bovine articular chondrocytes. Biochem J 2002; 361: 689-96

93. Zagar Y., Chaumaz G. and Lieberherr M. Signaling cross-talk from Gbeta4 subunit to Elk-1 in the rapid action of androgens. J Biol Chem 2004; 279: 2403-13

94. Wang Y., Schattenberg J.M., Rigoli R.M., Storz P. and Czaja M.J. Hepatocyte resistance to oxidative stress is dependent on protein kinase C-mediated down-regulation of c-Jun/AP-1. J Biol Chem 2004; 279: 31089-97

95. Yu R., Mandlekar S., Tan T.H. and Kong A.N. Activation of p38 and c-Jun N-terminal kinase pathways and induction of apoptosis by chelerythrine do not require inhibition of protein kinase C. J Biol Chem 2000; 275: 9612-9

96. Lee S.K., Qing W.G., Mar W., Luyengi L., Mehta R.G., Kawanishi K., Fong H.H., Beecher C.W., Kinghorn A.D. and Pezzuto J.M. Angoline and chelerythrine, benzophenanthridine alkaloids that do not inhibit protein kinase C. J Biol Chem 1998; 273: 19829-33

97. Chaban V.V., Lakhter A.J. and Micevych P. A membrane estrogen receptor mediates intracellular calcium release in astrocytes. Endocrinology 2004; 145: 3788-95

98. Arvanitis D.N., Wang H., Bagshaw R.D., Callahan J.W. and Boggs J.M. Membrane-associated estrogen receptor and caveolin-1 are present in central nervous system myelin and oligodendrocyte plasma membranes. J Neurosci Res 2004; 75: 603-13

99. Kousteni S., Bellido T., Plotkin L.I., O'Brien C.A., Bodenner D.L., Han L., Han K., DiGregorio G.B., Katzenellenbogen J.A., Katzenellenbogen B.S., Roberson P.K., Weinstein R.S., Jilka R.L. and Manolagas S.C. Nongenotropic, sex-nonspecific signaling through the estrogen or androgen receptors: dissociation from transcriptional activity. Cell 2001; 104: 719-30

100. Oz O.K., Millsaps R., Welch R., Birch J. and Zerwekh J.E. Expression of aromatase in the human growth plate. J Mol Endocrinol 2001; 27: 249-53

101. Audi L., Carrascosa A. and Ballabriga A. Androgen metabolism by human fetal epiphyseal cartilage and its chondrocytes in primary culture. J Clin Endocrinol Metab 1984; 58: 819-25

102. Raz P., Nasatzky E., Boyan B.D., Ornoy A. and Schwartz Z. Sexual dimorphism of growth plate prehypertrophic and hypertrophic chondrocytes in response to testosterone requires metabolism to dihydrotestosterone (DHT) by steroid 5-alpha reductase type 1. J Cell Biochem 2005; 95: 108-19

103. Sylvia V.L., Gay I., Hardin R., Dean D.D., Boyan B.D. and Schwartz Z. Rat costochondral chondrocytes produce 17beta-estradiol and regulate its production by 1alpha,25(OH)(2)D(3). Bone 2002; 30: 57-63

104. Cornell C.N., Lane J.M. and Poynton A.R. Orthopedic management of vertebral and long bone fractures in patients with osteoporosis. Clin Geriatr Med 2003; 19: 433-55

105. Price C.T., Connolly J.F., Carantzas A.C. and Ilyas I. Comparison of bone grafts for posterior spinal fusion in adolescent idiopathic scoliosis. Spine 2003; 28: 793-8

106. Tiedeman J.J., Garvin K.L., Kile T.A. and Connolly J.F. The role of a composite, demineralized bone matrix and bone marrow in the treatment of osseous defects. Orthopedics 1995; 18: 1153-8

107. Urist M.R. Bone: formation by autoinduction. Science 1965; 150: 893-9

108. Van de Putte K.A. and Urist M.R. Osteogenesis in the interior of intramuscular implants of decalcified bone matrix. Clin Orthop Relat Res 1965; 43: 257-70

109. McCarthy K.F., Wientroub S., Hale M. and Reddi A.H. Establishment of the hematopoietic microenvironment in the marrow of matrix-induced endochondral bone. Exp Hematol 1984; 12: 131-8

110. Honsawek S., Powers R.M. and Wolfinbarger L. Extractable bone morphogenetic protein and correlation with induced new bone formation in an in vivo assay in the athymic mouse model. Cell Tissue Bank 2005; 6: 13-23

111. Becker W., Urist M.R., Tucker L.M., Becker B.E. and Ochsenbein C. Human demineralized freeze-dried bone: inadequate induced bone formation in athymic mice. A preliminary report. J Periodontol 1995; 66: 822-8

112. Block J.E. and Poser J. Does xenogeneic demineralized bone matrix have clinical utility as a bone graft substitute? Med Hypotheses 1995; 45: 27-32

113. Chesmel K.D., Branger J., Wertheim H. and Scarborough N. Healing response to various forms of human demineralized bone matrix in athymic rat cranial defects. J Oral Maxillofac Surg 1998; 56: 857-63; discussion 64-5

114. Nathan R.M., Bentz H., Armstrong R.M., Piez K.A., Smestad T.L., Ellingsworth L.R., McPherson J.M. and Seyedin S.M. Osteogenesis in rats with an inductive bovine composite. J Orthop Res 1988; 6: 324-34

115. Ripamonti U., Magan A., Ma S., van den Heever B., Moehl T. and Reddi A.H. Xenogeneic osteogenin, a bone morphogenetic protein, and demineralized bone matrices, including human, induce bone differentiation in athymic rats and baboons. Matrix 1991; 11: 404-11

116. Torricelli P., Fini M., Rocca M., Giavaresi G. and Giardino R. Xenogenic demineralized bone matrix: osteoinduction and influence of associated skeletal defects in heterotopic bone formation in rats. Int Orthop 1999; 23: 178-81

117. Liang G., Yang Y., Oh S., Ong J.L., Zheng C., Ran J., Yin G. and Zhou D. Ectopic osteoinduction and early degradation of recombinant human bone morphogenetic protein-2-loaded porous beta-tricalcium phosphate in mice. Biomaterials 2005; 26: 4265-71

118. Pekkarinen T., Lindholm T.S., Hietala O. and Jalovaara P. The effect of different mineral frames on ectopic bone formation in mouse hind leg muscles induced by native reindeer bone morphogenetic protein. Arch Orthop Trauma Surg 2005; 125: 10-5

119. Ranly D.M., McMillan J., Keller T., Lohmann C.H., Meunch T., Cochran D.L., Schwartz Z. and Boyan B.D. Platelet-derived growth factor inhibits demineralized bone matrix-induced intramuscular cartilage and bone formation. A study of immunocompromised mice. J Bone Joint Surg Am 2005; 87: 2052-64

120. Schwartz Z., Weesner T., van Dijk S., Cochran D.L., Mellonig J.T., Lohmann C.H., Carnes D.L., Goldstein M., Dean D.D. and Boyan B.D. Ability of deproteinized cancellous bovine bone to induce new bone formation. J Periodontol 2000; 71: 1258-69

121. Zhang M., Powers R.M., Jr. and Wolfinbarger L., Jr. A quantitative assessment of osteoinductivity of human demineralized bone matrix. J Periodontol 1997; 68: 1076-84

122. Han B., Yang Z. and Nimni M. Effects of moisture and temperature on the osteoinductivity of demineralized bone matrix. J Orthop Res 2005; 23: 855-61

123. Lohmann C.H., Andreacchio D., Koster G., Carnes D.L., Jr., Cochran D.L., Dean D.D., Boyan B.D. and Schwartz Z. Tissue response and osteoinduction of human bone grafts in vivo. Arch Orthop Trauma Surg 2001; 121: 583-90

124. McCauley L.K., Rosol T.J., Capen C.C. and Horton J.E. A comparison of bone turnover in athymic (nude) and euthymic mice: biochemical, histomorphometric, bone ash and in vitro studies. Bone 1989; 10: 29-34

125. Bessho K. and Iizuka T. Changes in bone inducing activity of bone morphogenetic protein with aging. Ann Chir Gynaecol Suppl 1993; 207: 49-53

126. Nishimoto S.K., Chang C.H., Gendler E., Stryker W.F. and Nimni M.E. The effect of aging on bone formation in rats: biochemical and histological evidence for decreased bone formation capacity. Calcif Tissue Int 1985; 37: 617-24

127. Strates B.S., Stock A.J. and Connolly J.F. Skeletal repair in the aged: a preliminary study in rabbits. Am J Med Sci 1988; 296: 266-9

128. Syftestad G.T. and Urist M.R. Bone aging. Clin Orthop Relat Res 1982; 288-97

129. Torricelli P., Fini M., Giavaresi G., Rimondini L. and Giardino R. Characterization of bone defect repair in young and aged rat femur induced by xenogenic demineralized bone matrix. J Periodontol 2002; 73: 1003-9

130. Capanna R., Donati D., Masetti C., Manfrini M., Panozzo A., Cadossi R. and Campanacci M. Effect of electromagnetic fields on patients undergoing massive bone graft following bone tumor resection. A double blind study. Clin Orthop Relat Res 1994; 213-21

131. Ciombor D.M., Lester G., Aaron R.K., Neame P. and Caterson B. Low frequency EMF regulates chondrocyte differentiation and expression of matrix proteins. J Orthop Res 2002; 20: 40-50

132. Torricelli P., Fini M., Giavaresi G. and Giardino R. In vitro osteoinduction of demineralized bone. Artif Cells Blood Substit Immobil Biotechnol 1998; 26: 309-15

133. Davis M.E., Lanzl L.H. and Strandjord N.M. Estrogens and the aging process. The detection, prevention, and retardation of osteoporosis. Jama 1966; 196: 219-24

134. Lafferty F.W., Spencer G.E., Jr. and Pearson O.H. Effects of Androgens, Estrogens and High Calcium Intakes on Bone Formation and Resorption in Osteoporosis. Am J Med 1964; 36: 514-28

135. Lohmann C.H., Tandy E.M., Sylvia V.L., Hell-Vocke A.K., Cochran D.L., Dean D.D., Boyan B.D. and Schwartz Z. Response of normal female human osteoblasts (NHOst) to 17beta-estradiol is modulated by implant surface morphology. J Biomed Mater Res 2002; 62: 204-13

136. Nilsson A., Ohlsson C., Isaksson O.G., Lindahl A. and Isgaard J. Hormonal regulation of longitudinal bone growth. Eur J Clin Nutr 1994; 48 Suppl 1: S150-8; discussion S8-60

137. Gao Y., Qian W.P., Dark K., Toraldo G., Lin A.S., Guldberg R.E., Flavell R.A., Weitzmann M.N. and Pacifici R. Estrogen prevents bone loss through transforming growth factor beta signaling in T cells. Proc Natl Acad Sci U S A 2004; 101: 16618-23

138. Roggia C., Gao Y., Cenci S., Weitzmann M.N., Toraldo G., Isaia G. and Pacifici R. Up-regulation of TNF-producing T cells in the bone marrow: a key mechanism by which estrogen deficiency induces bone loss in vivo. Proc Natl Acad Sci U S A 2001; 98: 13960-5

139. Hughes D.E., Dai A., Tiffee J.C., Li H.H., Mundy G.R. and Boyce B.F. Estrogen promotes apoptosis of murine osteoclasts mediated by TGF-beta. Nat Med 1996; 2: 1132-6

140. Manolagas S.C., Bellido T. and Jilka R.L. Sex steroids, cytokines and the bone marrow: new concepts on the pathogenesis of osteoporosis. Ciba Found Symp 1995; 191: 187-96; discussion 97-202

141. Pacifici R. Estrogen, cytokines, and pathogenesis of postmenopausal osteoporosis. J Bone Miner Res 1996; 11: 1043-51

142. Edwards J.T., Diegmann M.H. and Scarborough N.L. Osteoinduction of human demineralized bone: characterization in a rat model. Clin Orthop Relat Res 1998; 219-28

143. Schwartz Z., Somers A., Mellonig J.T., Carnes D.L., Jr., Dean D.D., Cochran D.L. and Boyan B.D. Ability of commercial demineralized freeze-dried bone allograft to induce new bone formation is dependent on donor age but not gender. J Periodontol 1998; 69: 470-8

144. Traianedes K., Russell J.L., Edwards J.T., Stubbs H.A., Shanahan I.R. and Knaack D. Donor age and gender effects on osteoinductivity of demineralized bone matrix. J Biomed Mater Res B Appl Biomater 2004; 70: 21-9

145. Roggia C., Tamone C., Cenci S., Pacifici R. and Isaia G.C. Role of TNF-alpha producing T-cells in bone loss induced by estrogen deficiency. Minerva Med 2004; 95: 125-32

146. Vaessen L.M., Broekhuizen R., Rozing J., Vos J.G. and Schuurman H.J. T-cell development during ageing in congenitally athymic (nude) rats. Scand J Immunol 1986; 24: 223-35

147. Sass D.A., Liss T., Bowman A.R., Rucinski B., Popoff S.N., Pan Z., Ma Y.F. and Epstein S. The role of the T-lymphocyte in estrogen deficiency osteopenia. J Bone Miner Res 1997; 12: 479-86

148. Wlodarski K.H. and Reddi A.H. Importance of skeletal muscle environment for ectopic bone induction in mice. Folia Biol (Krakow) 1986; 34: 425-34

149. Kimble R.B., Bain S. and Pacifici R. The functional block of TNF but not of IL-6 prevents bone loss in ovariectomized mice. J Bone Miner Res 1997; 12: 935-41

150. Kitazawa R., Kimble R.B., Vannice J.L., Kung V.T. and Pacifici R. Interleukin-1 receptor antagonist and tumor necrosis factor binding protein decrease osteoclast formation and bone resorption in ovariectomized mice. J Clin Invest 1994; 94: 2397-406

151. Boskey A.L., Rimnac C.M., Bansal M., Federman M., Lian J. and Boyan B.D. Effect of short-term hypomagnesemia on the chemical and mechanical properties of rat bone. J Orthop Res 1992; 10: 774-83

152. Ornoy A., Giron S., Aner R., Goldstein M., Boyan B.D. and Schwartz Z. Gender dependent effects of testosterone and 17 beta-estradiol on bone growth and modelling in young mice. Bone Miner 1994; 24: 43-58

153. Boyan B.D., Lohmann C.H., Somers A., Niederauer G.G., Wozney J.M., Dean D.D., Carnes D.L., Jr. and Schwartz Z. Potential of porous poly-D,L-lactide-co-glycolide particles as a carrier for recombinant human bone morphogenetic protein-2 during osteoinduction in vivo. J Biomed Mater Res 1999; 46: 51-9

154. Schwartz Z., Somers A., Mellonig J.T., Carnes D.L., Jr., Wozney J.M., Dean D.D., Cochran D.L. and Boyan B.D. Addition of human recombinant bone morphogenetic protein-2 to inactive commercial human demineralized freeze-dried bone allograft makes an effective composite bone inductive implant material. J Periodontol 1998; 69: 1337-45

155. Cesnjaj M., Stavljenic A. and Vukicevic S. Decreased osteoinductive potential of bone matrix from ovariectomized rats. Acta Orthop Scand 1991; 62: 471-5

156. Nasatzky E., Grinfeld D., Boyan B.D., Dean D.D., Ornoy A. and Schwartz Z. Transforming growth factor-beta1 modulates chondrocyte responsiveness to 17beta-estradiol. Endocrine 1999; 11: 241-9

157. Ornoy A. Transplacental effects of estrogen on osteogenesis in rat foetuses. Pathology 1973; 5: 183-8

158. Schwartz Z., Finer Y., Nasatzky E., Soskolne W.A., Dean D.D., Boyan B.D. and Ornoy A. The effects of 17 beta-estradiol on chondrocyte differentiation are modulated by vitamin D3 metabolites. Endocrine 1997; 7: 209-18

159. Movsowitz C., Epstein S., Fallon M., Ismail F. and Thomas S. Cyclosporin-A in vivo produces severe osteopenia in the rat: effect of dose and duration of administration. Endocrinology 1988; 123: 2571-7

160. Boyan B.D. and Schwartz Z. Consideration of systemic hormone status when treating patients with osteopenia. J Periodontol 2003; 74: 1692-3

161. Duarte P.M., Cesar-Neto J.B., Sallum A.W., Sallum E.A. and Nociti F.H., Jr. Effect of estrogen and calcitonin therapies on bone density in a lateral area adjacent to implants placed in the tibiae of ovariectomized rats. J Periodontol 2003; 74: 1618-24

162. Finkelman R.D. Re: Effect of estrogen and calcitonin therapies on bone density in a lateral area adjacent to implants placed in the tibiae of ovariectomized rats. Duarte PM, Cesar-Neto JB, Sallum AW, Sallum EA, Nociti FH Jr (2003;74:1618-1624). Re: Guest editorial. Consideration of systemic hormone status when treating patients with osteopenia. Boyan BD, Schwartz Z (2003;74:1692-1693). J Periodontol 2004; 75: 1742-3

163. Hart E.S., Albright M.B., Rebello G.N. and Grottkau B.E. Broken bones: common pediatric fractures--part I. Orthop Nurs 2006; 25: 251-6

164. Perron A.D., Miller M.D. and Brady W.J. Orthopedic pitfalls in the ED: pediatric growth plate injuries. Am J Emerg Med 2002; 20: 50-4

165. Mizuta T., Benson W.M., Foster B.K., Paterson D.C. and Morris L.L. Statistical analysis of the incidence of physeal injuries. J Pediatr Orthop 1987; 7: 518-23

166. von der Mark K., Gauss V., von der Mark H. and Muller P. Relationship between cell shape and type of collagen synthesised as chondrocytes lose their cartilage phenotype in culture. Nature 1977; 267: 531-2

167. Boyan B.D., Schwartz Z., Howell D.S., Naski M., Ranly D.M., Sylvia V.L. and Dean D.D. The biology, chemistry, and biochemistry of the mammalian growth plate. In: Coe F. and Favus M., eds. Disorders of Bone and Mineral Metabolism, 2nd Edition Ed. Philapdelphia, PA: Lippincott Williams & Wilkins 2002: pg. 255-314

168. Murphy C.L. and Sambanis A. Effect of oxygen tension and alginate encapsulation on restoration of the differentiated phenotype of passaged chondrocytes. Tissue Eng 2001; 7: 791-803

169. Duke J., Montufar-Solis D., Underwood S., Lalani Z. and Hecht J.T. Apoptosis staining in cultured pseudoachondroplasia chondrocytes. Apoptosis 2003; 8: 191-7

170. Olney R.C., Smith R.L., Kee Y. and Wilson D.M. Production and hormonal regulation of insulin-like growth factor binding proteins in bovine chondrocytes. Endocrinology 1993; 133: 563-70

171. Aydelotte M.B., Thonar E.J., Mollenhauer J. and Flechtenmacher J. Culture of chondrocytes in alginate gel: variations in conditions of gelation influence the structure of the alginate gel, and the arrangement and morphology of proliferating chondrocytes. In Vitro Cell Dev Biol Anim 1998; 34: 123-30

172. Halle J.P., Leblond F.A., Pariseau J.F., Jutras P., Brabant M.J. and Lepage Y. Studies on small (< 300 microns) microcapsules: II--Parameters governing the production of alginate beads by high voltage electrostatic pulses. Cell Transplant 1994; 3: 365-72

173. Lum Z.P., Krestow M., Tai I.T., Vacek I. and Sun A.M. Xenografts of rat islets into diabetic mice. An evaluation of new smaller capsules. Transplantation 1992; 53: 1180-3

174. Arus L., Orive G., Hernandez R., Rodriguez A., Rojas A. and Pedraz J.L. The influence of cellular seeding density in the microencapsulation of hybridoma cells. J Biomater Sci Polym Ed 2005; 16: 521-9

175. King A., Sandler S., Andersson A., Hellerstrom C., Kulseng B. and Skjak-Braek G. Glucose metabolism in vitro of cultured and transplanted mouse pancreatic islets microencapsulated by means of a high-voltage electrostatic field. Diabetes Care 1999; 22 Suppl 2: B121-6

176. Sun Y.L., Ma X., Zhou D., Vacek I. and Sun A.M. Porcine pancreatic islets: isolation, microencapsulation, and xenotransplantation. Artif Organs 1993; 17: 727-33

177. Woods E.J., Liu J., Zieger M.A., Lakey J.R. and Critser J.K. The effects of microencapsulation on pancreatic islet osmotically induced volumetric response. Cell Transplant 1999; 8: 699-708

178. Rong L., Baoguo L., Huifeng D. and Tingting T. Factors Influencing the Formation of MSCs APA Microcapsules. Conf Proc IEEE Eng Med Biol Soc 2005; 5: 4900-3

179. Alsberg E., Kong H.J., Hirano Y., Smith M.K., Albeiruti A. and Mooney D.J. Regulating bone formation via controlled scaffold degradation. J Dent Res 2003; 82: 903-8

180. Kong H.J., Kaigler D., Kim K. and Mooney D.J. Controlling rigidity and degradation of alginate hydrogels via molecular weight distribution. Biomacromolecules 2004; 5: 1720-7

181. Enobakhare B.O., Bader D.L. and Lee D.A. Quantification of sulfated glycosaminoglycans in chondrocyte/alginate cultures, by use of 1,9-dimethylmethylene blue. Anal Biochem 1996; 243: 189-91

182. Domm C., Schunke M., Steinhagen J., Freitag S. and Kurz B. Influence of various alginate brands on the redifferentiation of dedifferentiated bovine articular chondrocytes in alginate bead culture under high and low oxygen tension. Tissue Eng 2004; 10: 1796-805

183. Stabler C.L., Sambanis A. and Constantinidis I. Effects of alginate composition on the growth and overall metabolic activity of betaTC3 cells. Ann N Y Acad Sci 2002; 961: 130-3

184. Pound J.C., Green D.W., Chaudhuri J.B., Mann S., Roach H.I. and Oreffo R.O. Strategies to promote chondrogenesis and osteogenesis from human bone marrow cells and articular chondrocytes encapsulated in polysaccharide templates. Tissue Eng 2006; 12: 2789-99

185. Rowley J.A. and Mooney D.J. Alginate type and RGD density control myoblast phenotype. J Biomed Mater Res 2002; 60: 217-23

186. Bouhadir K.H., Lee K.Y., Alsberg E., Damm K.L., Anderson K.W. and Mooney D.J. Degradation of partially oxidized alginate and its potential application for tissue engineering. Biotechnol Prog 2001; 17: 945-50

187. Wang L., Shelton R.M., Cooper P.R., Lawson M., Triffitt J.T. and Barralet J.E. Evaluation of sodium alginate for bone marrow cell tissue engineering. Biomaterials 2003; 24: 3475-81

188. Boontheekul T., Hill E.E., Kong H.J. and Mooney D.J. Regulating myoblast phenotype through controlled gel stiffness and degradation. Tissue Eng 2007; 13: 1431-42

189. Lindenhayn K., Perka C., Spitzer R., Heilmann H., Pommerening K., Mennicke J. and Sittinger M. Retention of hyaluronic acid in alginate beads: aspects for in vitro cartilage engineering. J Biomed Mater Res 1999; 44: 149-55

190. Loeser R.F., Todd M.D. and Seely B.L. Prolonged treatment of human osteoarthritic chondrocytes with insulin-like growth factor-I stimulates proteoglycan synthesis but not proteoglycan matrix accumulation in alginate cultures. J Rheumatol 2003; 30: 1565-70

191. Mouw J.K., Case N.D., Guldberg R.E., Plaas A.H. and Levenston M.E. Variations in matrix composition and GAG fine structure among scaffolds for cartilage tissue engineering. Osteoarthritis Cartilage 2005; 13: 828-36

192. Ramdi H., Legay C. and Lievremont M. Influence of matricial molecules on growth and differentiation of entrapped chondrocytes. Exp Cell Res 1993; 207: 449-54

193. Jenniskens Y.M., Koevoet W., de Bart A.C., Weinans H., Jahr H., Verhaar J.A., DeGroot J. and van Osch G.J. Biochemical and functional modulation of the cartilage collagen network by IGF1, TGFbeta2 and FGF2. Osteoarthritis Cartilage 2006; 14: 1136-46

194. Grunder T., Gaissmaier C., Fritz J., Stoop R., Hortschansky P., Mollenhauer J. and Aicher W.K. Bone morphogenetic protein (BMP)-2 enhances the expression of type II collagen and aggrecan in chondrocytes embedded in alginate beads. Osteoarthritis Cartilage 2004; 12: 559-67

195. Akeda K., An H.S., Okuma M., Attawia M., Miyamoto K., Thonar E.J., Lenz M.E., Sah R.L. and Masuda K. Platelet-rich plasma stimulates porcine articular chondrocyte proliferation and matrix biosynthesis. Osteoarthritis Cartilage 2006; 14: 1272-80

196. Tallheden T., van der Lee J., Brantsing C., Mansson J.E., Sjogren-Jansson E. and Lindahl A. Human serum for culture of articular chondrocytes. Cell Transplant 2005; 14: 469-79

197. Tallheden T., Karlsson C., Brunner A., Van Der Lee J., Hagg R., Tommasini R. and Lindahl A. Gene expression during redifferentiation of human articular chondrocytes. Osteoarthritis Cartilage 2004; 12: 525-35

198. Heywood H.K., Sembi P.K., Lee D.A. and Bader D.L. Cellular utilization determines viability and matrix distribution profiles in chondrocyte-seeded alginate constructs. Tissue Eng 2004; 10: 1467-79

199. Woolf A.D. and Pfleger B. Burden of major musculoskeletal conditions. Bull World Health Organ 2003; 81: 646-56

200. Ng L.J., Wheatley S., Muscat G.E., Conway-Campbell J., Bowles J., Wright E., Bell D.M., Tam P.P., Cheah K.S. and Koopman P. SOX9 binds DNA, activates transcription, and coexpresses with type II collagen during chondrogenesis in the mouse. Dev Biol 1997; 183: 108-21

201. Wright E., Hargrave M.R., Christiansen J., Cooper L., Kun J., Evans T., Gangadharan U., Greenfield A. and Koopman P. The Sry-related gene Sox9 is expressed during chondrogenesis in mouse embryos. Nat Genet 1995; 9: 15-20

202. Zhao Q., Eberspaecher H., Lefebvre V. and De Crombrugghe B. Parallel expression of Sox9 and Col2a1 in cells undergoing chondrogenesis. Dev Dyn 1997; 209: 377-86

203. Bi W., Deng J.M., Zhang Z., Behringer R.R. and de Crombrugghe B. Sox9 is required for cartilage formation. Nat Genet 1999; 22: 85-9

204. Kypriotou M., Fossard-Demoor M., Chadjichristos C., Ghayor C., de Crombrugghe B., Pujol J.P. and Galera P. SOX9 exerts a bifunctional effect on type II collagen gene (COL2A1) expression in chondrocytes depending on the differentiation state. DNA Cell Biol 2003; 22: 119-29

205. Bridgewater L.C., Lefebvre V. and de Crombrugghe B. Chondrocyte-specific enhancer elements in the Col11a2 gene resemble the Col2a1 tissue-specific enhancer. J Biol Chem 1998; 273: 14998-5006

206. Tavella S., Biticchi R., Schito A., Minina E., Di Martino D., Pagano A., Vortkamp A., Horton W.A., Cancedda R. and Garofalo S. Targeted expression of SHH affects chondrocyte differentiation, growth plate organization, and Sox9 expression. J Bone Miner Res 2004; 19: 1678-88

207. Zehentner B.K., Dony C. and Burtscher H. The transcription factor Sox9 is involved in BMP-2 signaling. J Bone Miner Res 1999; 14: 1734-41

208. Mandl E.W., Jahr H., Koevoet J.L., van Leeuwen J.P., Weinans H., Verhaar J.A. and van Osch G.J. Fibroblast growth factor-2 in serum-free medium is a potent mitogen and reduces dedifferentiation of human ear chondrocytes in monolayer culture. Matrix Biol 2004; 23: 231-41

209. Shakibaei M., Seifarth C., John T., Rahmanzadeh M. and Mobasheri A. Igf-I extends the chondrogenic potential of human articular chondrocytes in vitro: molecular association between Sox9 and Erk1/2. Biochem Pharmacol 2006; 72: 1382-95

210. Akiyama H., Lyons J.P., Mori-Akiyama Y., Yang X., Zhang R., Zhang Z., Deng J.M., Taketo M.M., Nakamura T., Behringer R.R., McCrea P.D. and de Crombrugghe B. Interactions between Sox9 and beta-catenin control chondrocyte differentiation. Genes Dev 2004; 18: 1072-87

211. Liu H., Lee Y.W. and Dean M.F. Re-expression of differentiated proteoglycan phenotype by dedifferentiated human chondrocytes during culture in alginate beads. Biochim Biophys Acta 1998; 1425: 505-15

212. Ma H.L., Hung S.C., Lin S.Y., Chen Y.L. and Lo W.H. Chondrogenesis of human mesenchymal stem cells encapsulated in alginate beads. J Biomed Mater Res A 2003; 64: 273-81

213. Yang I.H., Kim S.H., Kim Y.H., Sun H.J., Kim S.J. and Lee J.W. Comparison of phenotypic characterization between "alginate bead" and "pellet" culture systems as chondrogenic differentiation models for human mesenchymal stem cells. Yonsei Med J 2004; 45: 891-900

214. Kinney R.C., Schwartz Z., Week K., Lotz M.K. and Boyan B.D. Human articular chondrocytes exhibit sexual dimorphism in their responses to 17beta-estradiol. Osteoarthritis Cartilage 2005; 13: 330-7

215. Wang L., Zhao G., Olivares-Navarrete R., Bell B.F., Wieland M., Cochran D.L., Schwartz Z. and Boyan B.D. Integrin beta1 silencing in osteoblasts alters substrate-dependent responses to 1,25-dihydroxy vitamin D3. Biomaterials 2006; 27: 3716-25

216. Yagi R., McBurney D., Laverty D., Weiner S. and Horton W.E., Jr. Intrajoint comparisons of gene expression patterns in human osteoarthritis suggest a change in chondrocyte phenotype. J Orthop Res 2005; 23: 1128-38

217. Chia S.H., Homicz M.R., Schumacher B.L., Thonar E.J., Masuda K., Sah R.L. and Watson D. Characterization of human nasal septal chondrocytes cultured in alginate. J Am Coll Surg 2005; 200: 691-704

218. Murphy C.L. and Polak J.M. Control of human articular chondrocyte differentiation by reduced oxygen tension. J Cell Physiol 2004; 199: 451-9

219. Yaeger P.C., Masi T.L., de Ortiz J.L., Binette F., Tubo R. and McPherson J.M. Synergistic action of transforming growth factor-beta and insulin-like growth factor-I induces expression of type II collagen and aggrecan genes in adult human articular chondrocytes. Exp Cell Res 1997; 237: 318-25

220. Alexander T.H., Sage A.B., Schumacher B.L., Sah R.L. and Watson D. Human serum for tissue engineering of human nasal septal cartilage. Otolaryngol Head Neck Surg 2006; 135: 397-403

221. Kurth T., Hedbom E., Shintani N., Sugimoto M., Chen F.H., Haspl M., Martinovic S. and Hunziker E.B. Chondrogenic potential of human synovial mesenchymal stem cells in alginate. Osteoarthritis Cartilage 2007;

222. Mandl E.W., van der Veen S.W., Verhaar J.A. and van Osch G.J. Serum-free medium supplemented with high-concentration FGF2 for cell expansion culture

of human ear chondrocytes promotes redifferentiation capacity. Tissue Eng 2002; 8: 573-80

223. Saas J., Lindauer K., Bau B., Takigawa M. and Aigner T. Molecular phenotyping of HCS-2/8 cells as an in vitro model of human chondrocytes. Osteoarthritis Cartilage 2004; 12: 924-34

224. Tew S.R. and Hardingham T.E. Regulation of SOX9 mRNA in human articular chondrocytes involving p38 MAPK activation and mRNA stabilization. J Biol Chem 2006; 281: 39471-9

225. Aigner T., Gebhard P.M., Schmid E., Bau B., Harley V. and Poschl E. SOX9 expression does not correlate with type II collagen expression in adult articular chondrocytes. Matrix Biol 2003; 22: 363-72

226. Aigner T., Stoss H., Weseloh G., Zeiler G. and von der Mark K. Activation of collagen type II expression in osteoarthritic and rheumatoid cartilage. Virchows Arch B Cell Pathol Incl Mol Pathol 1992; 62: 337-45

227. Chubinskaya S., Hakimiyan A., Pacione C., Yanke A., Rappoport L., Aigner T., Rueger D.C. and Loeser R.F. Synergistic effect of IGF-1 and OP-1 on matrix formation by normal and OA chondrocytes cultured in alginate beads. Osteoarthritis Cartilage 2007; 15: 421-30

228. Loeser R.F., Pacione C.A. and Chubinskaya S. The combination of insulin-like growth factor 1 and osteogenic protein 1 promotes increased survival of and matrix synthesis by normal and osteoarthritic human articular chondrocytes. Arthritis Rheum 2003; 48: 2188-96

229. Origuchi N., Ishidou Y., Nagamine T., Onishi T., Matsunaga S., Yoshida H. and Sakou T. The spatial and temporal immunolocalization of TGF-beta 1 and bone morphogenetic protein-2/-4 in phallic bone formation in inbred Sprague Dawley male rats. In Vivo 1998; 12: 473-80

230. Johnstone B., Hering T.M., Caplan A.I., Goldberg V.M. and Yoo J.U. In vitro chondrogenesis of bone marrow-derived mesenchymal progenitor cells. Exp Cell Res 1998; 238: 265-72

231. Ballock R.T., Heydemann A., Wakefield L.M., Flanders K.C., Roberts A.B. and Sporn M.B. TGF-beta 1 prevents hypertrophy of epiphyseal chondrocytes: regulation of gene expression for cartilage matrix proteins and metalloproteases. Dev Biol 1993; 158: 414-29

232. Mello M.A. and Tuan R.S. Effects of TGF-beta1 and triiodothyronine on cartilage maturation: in vitro analysis using long-term high-density micromass

cultures of chick embryonic limb mesenchymal cells. J Orthop Res 2006; 24: 2095-105

233. Schwartz Z., Bonewald L.F., Caulfield K., Brooks B. and Boyan B.D. Direct effects of transforming growth factor-beta on chondrocytes are modulated by vitamin D metabolites in a cell maturation-specific manner. Endocrinology 1993; 132: 1544-52

234. Sylvia V.L., Mackey S., Schwartz Z., Schuman L., Gomez R. and Boyan B.D. Regulation of protein kinase C by transforming growth factor beta 1 in rat costochondral chondrocyte cultures. J Bone Miner Res 1994; 9: 1477-87

235. Jakob M., Demarteau O., Schafer D., Hintermann B., Dick W., Heberer M. and Martin I. Specific growth factors during the expansion and redifferentiation of adult human articular chondrocytes enhance chondrogenesis and cartilaginous tissue formation in vitro. J Cell Biochem 2001; 81: 368-77

236. Chadjichristos C., Ghayor C., Herrouin J.F., Ala-Kokko L., Suske G., Pujol J.P. and Galera P. Down-regulation of human type II collagen gene expression by transforming growth factor-beta 1 (TGF-beta 1) in articular chondrocytes involves SP3/SP1 ratio. J Biol Chem 2002; 277: 43903-17

237. Galera P., Redini F., Vivien D., Bonaventure J., Penfornis H., Loyau G. and Pujol J.P. Effect of transforming growth factor-beta 1 (TGF-beta 1) on matrix synthesis by monolayer cultures of rabbit articular chondrocytes during the dedifferentiation process. Exp Cell Res 1992; 200: 379-92

238. Paige K.T., Cima L.G., Yaremchuk M.J., Schloo B.L., Vacanti J.P. and Vacanti C.A. De novo cartilage generation using calcium alginate-chondrocyte constructs. Plast Reconstr Surg 1996; 97: 168-78; discussion 79-80